BRITISH COLUMBIA HYDRO AND POWER AUTHORITY

HAT CREEK PROJECT

Environmental Research and Technology Inc. - Air Quality and Climatic Effects of the Proposed Hat Creek Project Report - Appendix D - Assessment of Atmospheric Effects and Drift Deposition due to Alternate Cooling Tower Designs - April 1978.

ENVIRONMENTAL IMPACT STATEMENT REFERENCE NUMBER: 14e

Document P-5074-F-D
April 1978

Prepared for
British Columbia Hydro and Power Authority

Air quality and climatic effects of the proposed Hat Creek project

Appendix D
Assessment of atmospheric effects and drift deposition due to alternate cooling tower designs

2030 Alameda Padre Serra
Santa Barbara, California 93103

ENVIRONMENTAL RESEARCH & TECHNOLOGY, INC.
CONCORD, MASS. • LOS ANGELES • ATLANTA • SAN JUAN, P.R.
FORT COLLINS, CO. • WASHINGTON, D.C. • HOUSTON • CHICAGO

PRINTED IN U.S.A.

TABLE OF CONTENTS

LIST OF FIGURES

LIST OF FIGURES (Continued)

LIST OF FIGURES (Continued)

LIST OF TABLES

APPENDIX D

D1.0 INTRODUCTION

D1.1 SCOPE OF STUDY

Environmental Research & Technology, Inc. (ERT) has completed an analysis of the potential atmospheric effects of emissions from the operation of four alternate closed-cycle cooling tower systems at the proposed 2,000 Mw Hat Creek Thermal Generating Station. This report documents work performed in fulfillment of requirements specified in Appendix D2 of the Terms of Reference for Detailed Environmental Studies for the Hat Creek Project.

The following cooling tower designs were considered:

- a line of four rectangular mechanical draft cooling towers (a total of 36 fans);
- four round mechanical draft cooling towers (a total of 36 fans) in a box configuration;
- two natural draft cooling towers; and
- four natural draft cooling towers in a box configuration.

Figures D1-1 through D1-5 indicate the relative locations of the various cooling tower systems assumed in the present analysis. The deployments and orientations of the towers depicted in these figures reflect an effort to minimize potentially adverse effects associated with each design. A major concern in this regard is avoidance of undesirable plume interference at other power plant facilities. For example, the placement of towers southeast of the switchyard is intended to take advantage of the relatively infrequent occurrence of winds from this direction during the winter and thereby decrease the likelihood of icing at that location.

Rectangular mechanical draft towers are oriented with their long axes parallel to the prevailing (westerly) winds, since average plume rise is enhanced and ground-level plume downwash frequency is minimized with this

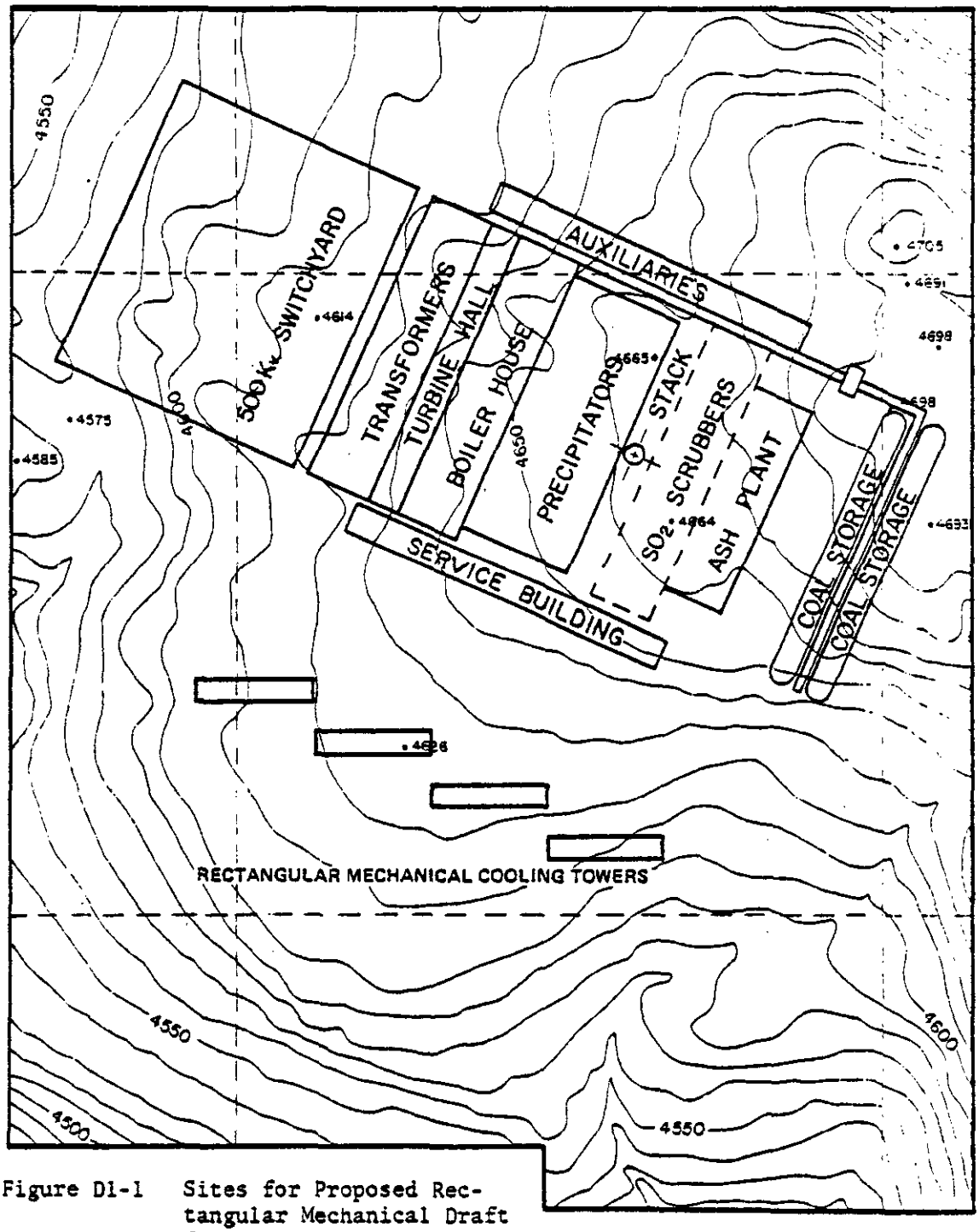

Figure D1-1 Sites for Proposed Rectangular Mechanical Draft Cooling Towers Relative to Other Power Plant Installations

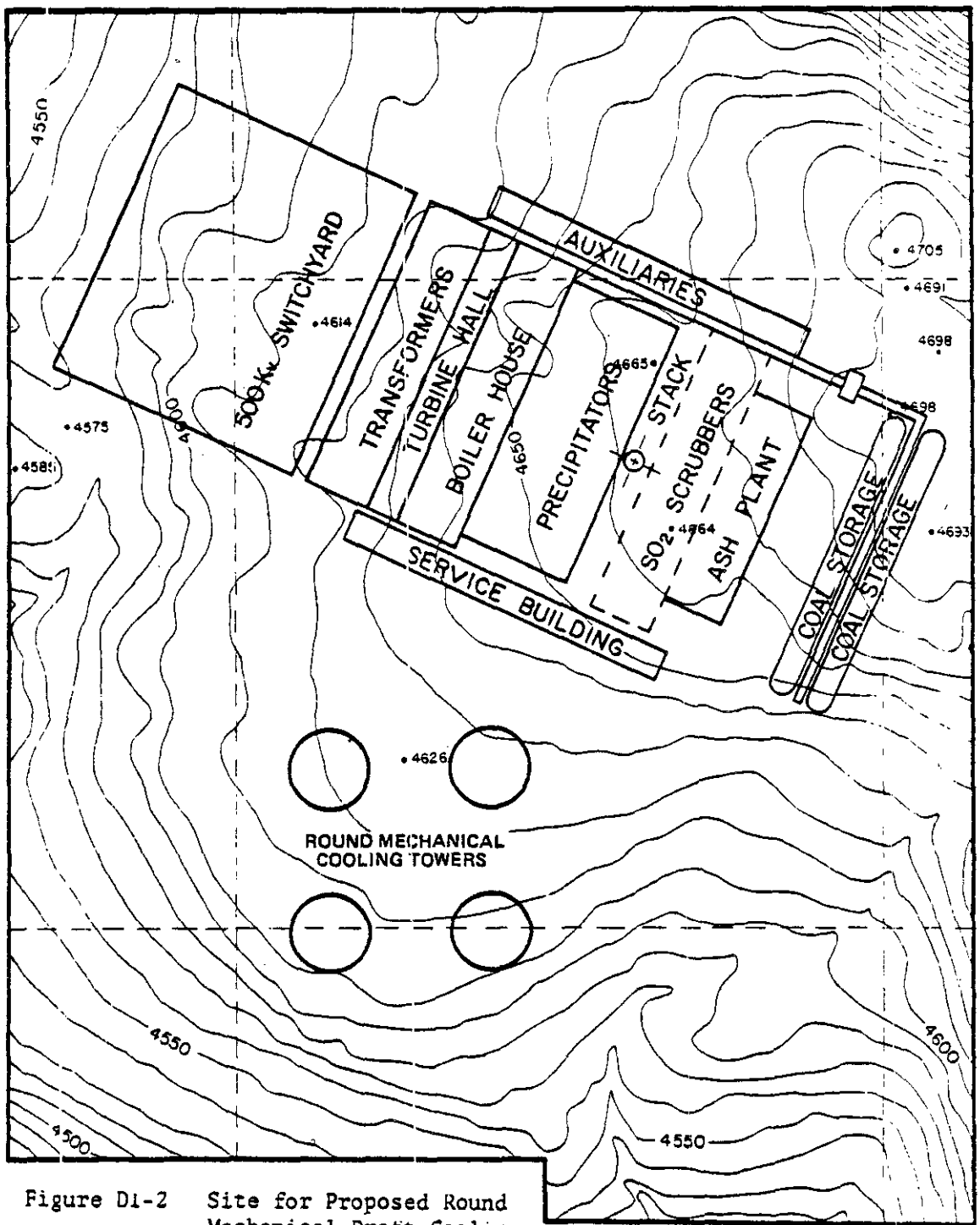

Figure D1-2 Site for Proposed Round Mechanical Draft Cooling Towers Relative to Other Power Plant Installations

804253

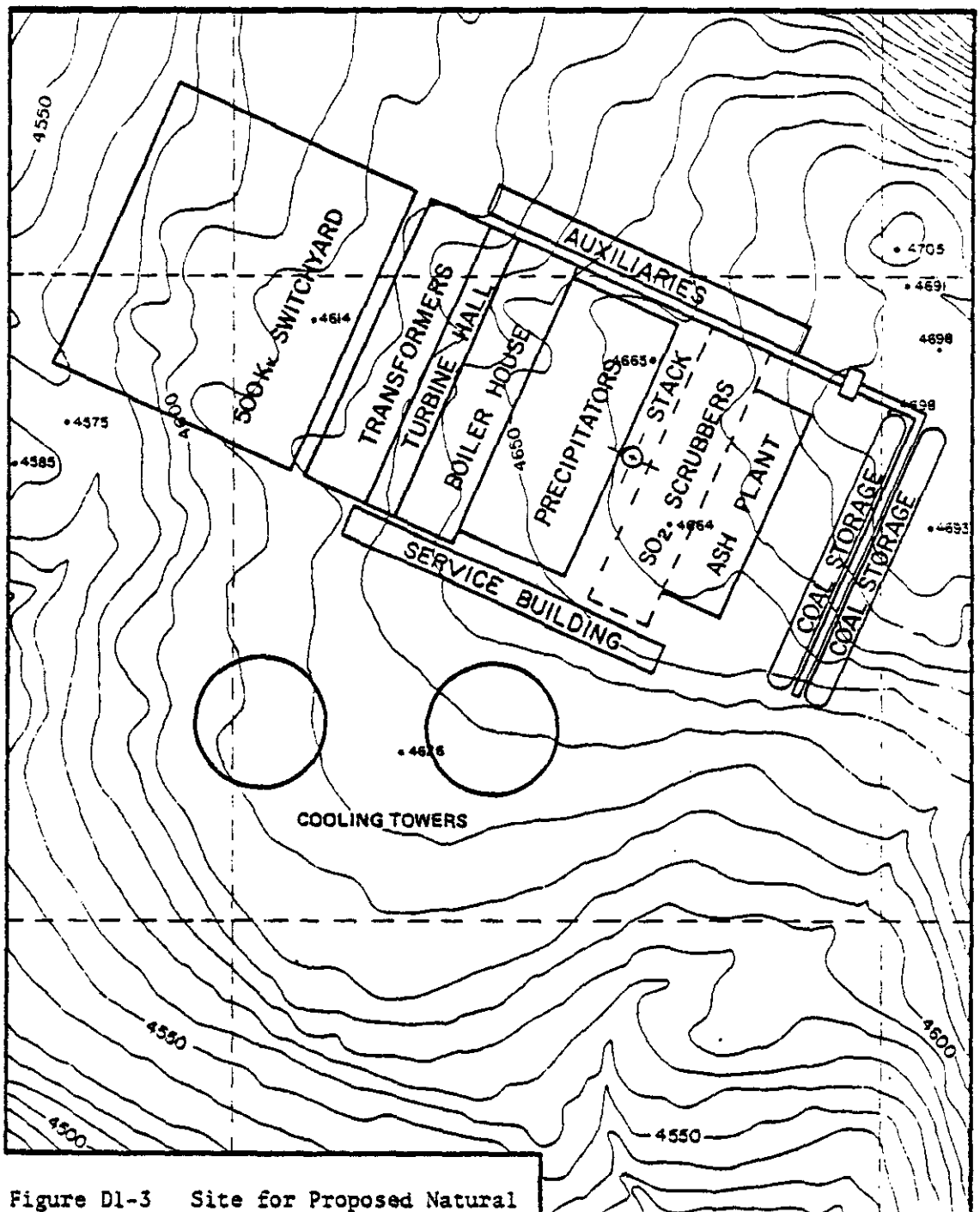

Figure D1-3 Site for Proposed Natural Draft Cooling Towers (Two Towers) Relative to Other Power Plant Installations

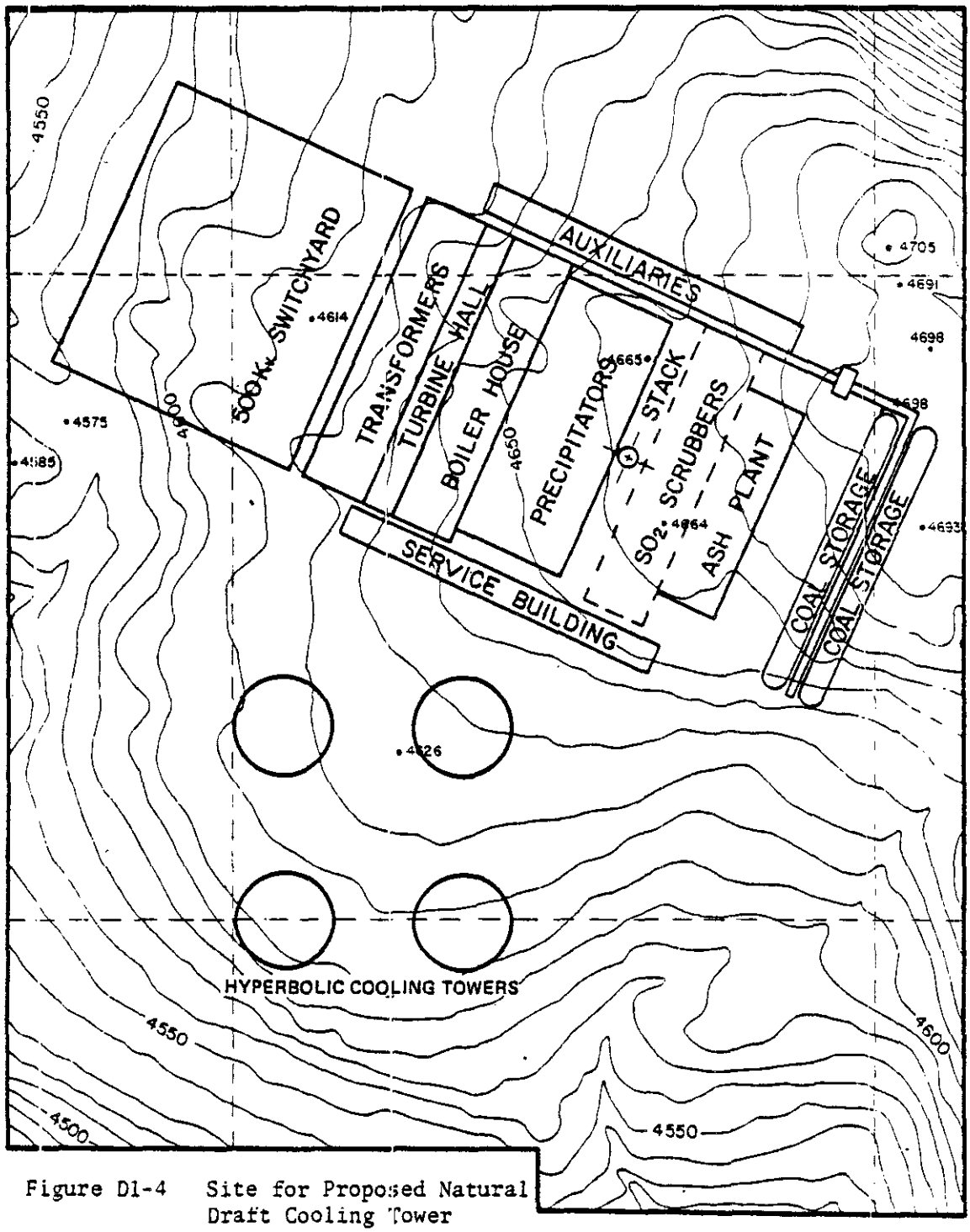

Figure D1-4 Site for Proposed Natural Draft Cooling Tower (Four Towers) Relative to Other Power Plant Installations

configuration. The separation distances between these towers were chosen to reduce problems of plume recirculation, i.e., entrainment of plumes from windward towers through the intakes of downwind towers. For the other designs (round mechanical draft and natural draft), downwash and recirculation are less important. The box configurations recommended for these systems ensures maximum aggregate plume rise with minimum dependence on wind direction.

Physical dimensions and operating characteristics for each cooling tower design are presented in Tables D1-1 and D1-2. The tabulated emission parameters correspond to full-load operation of the power plant year-round operation at maximum generating capacity was assumed in this analysis, ensuring that the magnitude and frequency of calculated effects will be conservative estimates.* Scheduled and unscheduled unit outages were not considered in this study.

Advanced mathematical modeling techniques were employed to estimate the following specific effects for each cooling tower option:

- surface icing and fogging due to cooling tower operation - seasonal and annual frequencies as functions of distance and direction from the towers;
- visible plume lengths - seasonal and annual distributions; and
- drift deposition - seasonal and annual deposition patterns.

D1.2 POTENTIAL ENVIRONMENTAL IMPACTS OF THE FOUR ALTERNATE COOLING TOWER DESIGNS

The potential impacts of natural and mechanical draft towers differ substantially. The shape of a rectangular mechanical draft tower presents a significant obstacle to the local airflow. During periods of moderate to strong winds, the potential for plume downwash and recirculation is greatest for this design. Due to the relatively

*The current operating schedule for the power plant indicates a lifetime average capacity factor of 60%.

TABLE D1-1

ENGINEERING DATA FOR MECHANICAL DRAFT COOLING TOWERS[1]

A. Design Conditions (Rectangular and Round)

Ambient Wet Bulb Temperature	13.9°C
Approach	12.8°C
Range	18.7°C
Circulating Water Flow Rate/Tower	10,112 liters/sec

B. Physical Dimensions

	Rectangular	Round
Number of Towers	4	4
Tower Length and Width	110m x 23m	-
Tower Diameter	-	76m
Number of Fans per Tower	9	9
Effluent Release Height	20m	21m
Effluent Discharge Area per Fan	$75m^2$	$84m^2$

C. Effluent Properties (Rectangular and Round)

Dry Bulb Temperature (°C)	Wet Bulb Temperature (°C)	Airflow Rate per Fan (m^3/sec)	Wet Bulb Temperature Out (°C)
-15.0	-16.3	800.56	26.7
-15.0	-15.0	800.56	27.8
10.0	3.3	800.56	33.3
10.0	10.0	800.56	37.2
32.2	23.9	800.56	41.1

D. Drift Properties (Rectangular and Round)

Percent of Circulating Water Escaping as Drift	0.008%
Recirculation Buildup Factor	14
Salt Drift Emission Rate per Tower	1.23 g/sec

[1]Data provided by INTEG/EBASCO.

TABLE D1-2[1]

ENGINEERING DATA FOR NATURAL DRAFT COOLING TOWERS

A. Design Conditions

	2 Towers	4 Towers
Ambient Wet Bulb Temperature	13.9°C	13.9°C
Approach	12.8°C	12.8°C
Range	18.7°C	18.7°C
Circulating Water Flow Rate/ Tower	20,224 liters/sec	10,112 liters/sec

B. Physical Dimensions

	2 Towers	4 Towers
Tower Diameter at Top	67.1m	49.1m
Effluent Release Height	116.4m	91.4m

C. Effluent Properties

Dry Bulb Temperature (°C)	Wet Bulb Temperature (°C)	Wet Bulb Temperature Out (°C)	Air Flow Rate Per Tower (m^3/sec) 2 Towers	4 Towers
-15.0	-16.3	28.9	13,470	6,735
-15.0	-15.0	29.4	13,508	6,754
10.0	3.3	36.7	12,393	6,196
10.0	10.0	36.7	12,393	6,196
32.2	23.9	42.2	12,006	6,003

D. Drift Properties

	2 Towers	4 Towers
Percent of Circulating Water Escaping as Drift	0.008%	0.008%
Recirculation Buildup Factor	14	14
Salt Drift Emission Rate Per Tower	2.46 g/sec	1.23 g/sec

[1]Data provided by INTEG/EBASCO.

low plume release height, ground-level impact (for example, fogging) is expected whenever high wind speeds occur. The ambient temperature accompanying such winds determines whether the intersection of the plume with the ground also results in the formation of ice at the surface. The severity of downwash depends on the angle of the wind relative to the tower. The greatest ground-level impact is expected when the wind is perpendicular to the line of cells; conversely, maximum plume rise and the least ground-level impact should occur with winds parallel to the tower's long dimension.

In contrast, round mechanical draft and natural draft towers, as a result of their shape, present less of an obstruction to the wind field. This reduces the frequency of downwash. In addition, the behavior of effluent from each tower is independent of wind direction. Due to the low release height of round mechanical draft towers (21 meters or approximately 65 feet), fogging and/or icing due to downwash does occur under conditions of high wind speeds. However, ground-level impacts will be much less frequent than with the rectangular towers. Unlike the mechanical draft towers, large natural draft towers typically discharge their effluents from heights of 90 to 150m (300 to 500 feet) above grade. In general, observations in the vicinity of such towers indicate that visible plumes do not extend to the ground in regions of relatively flat terrain. Incremental icing and fogging due to natural draft towers are, therefore, not normally impacts of concern.

In addition to fogging and icing due to downwash, it is possible that the elevated plumes will impact upon elevated terrain downwind of the cooling towers. Another important consideration in the case of mechanical draft towers is the potential for plume impacts (in particular, icing) at specific locations, such as the switchyard, located on the plant site itself.

All the cooling tower designs under consideration will lead to extended visible plumes during situations of light wind and high relative humidity. Thus, some obscuration due to elevated cooling tower plumes is unavoidable. However, the extent of the obscuration is a function of the type of cooling towers and their relative placement. For a row of towers, for instance, the angle of the wind with respect to the center-to-center axis is important in determining the degree of enhancement of plume rise and length due to plume interaction. In contrast, a box layout of cooling towers will create a much more uniform enhancement of rise resulting from plume merging. The observed plume lengths in this case will be less dependent on wind direction, other meteorological conditions being the same, than those from a line of towers.

The rate of drift deposition at any point in the vicinity of evaporative cooling towers is also a function of the type of cooling towers and their relative deployment. The low release height and susceptibility to downwash which characterize the mechanical draft towers tend to produce patterns of drift deposition that are chiefly concentrated in the area near the tower structure. Drift from the hyperbolic (natural draft) design is dispersed over a larger area than that from mechanical draft towers, resulting in less concentrated deposition patterns. The deployment of multiple-tower cooling systems is important because drift patterns from individual towers can overlap, increasing the total mass deposition rate at points near the towers.

D2.0 SUMMARY AND CONCLUSIONS

Results of the model simulation analyses performed to evaluate visible plume and drift effects due to the four alternate cooling tower designs at the Hat Creek Generating Plant are summarized below. It should be mentioned that, while the study provides realistic estimates of the magnitude of such effects, the results obtained are based on meteorological data collected over just one year (1975), and, thus, may not be representative of a "typical" annual cycle. In particular, the available relative humidity record from measurements at the B.C. Hydro Harry Lake mechanical weather station includes only 47 hours with recorded relative humidity greater than 90%. This is believed to be an unrealistically low frequency of high-humidity conditions, although observations at the nearest full-time weather stations tend to confirm that southcentral British Columbia was dryer (and slightly cooler) than normal during 1975 (see Appendix E, Climatic Assessment). As a result, it is probable that frequencies of fogging, icing, and extended visible plumes presented here are somewhat underestimated. However, the relative effects of the various tower designs are believed to be accurately stated. With this qualification, the major conclusions of our analyses are as follows.

- Ground-level impacts of visible plumes due to downwash are predicted to occur frequently (915 hours of fogging per year and 170 hours of icing per year) with the rectangular mechanical draft towers. Even though such effects will be limited to within 600 meters from the towers, fogging is expected to reach other power plant installations up to 200 hours during the year with associated ice formation up to 80 hours per year (40 hours in the switchyard).
- Ground-level fogging from round mechanical draft towers will occur only infrequently (about 30 hours per year). Elevated plumes from these towers would intercept switchyard equipment more often, possibly producing icing up to 100 hours per year.
- No localized fogging or icing are predicted for either of the two natural draft tower designs examined in this study.

- For all tower designs, elevated plumes with visible extent greater than 5 km are expected to occur relatively rarely. Plume lengths exceeding 15 km will occur several hours per year during periods of high relative humidity accompanied by low wind speed. Visible plumes are expected to pass above the Indian Reserve 2 km northwest of the plant site about 40 hours per year. Plume impacts on the elevated terrain in the Cornwall Hills are predicted to occur about 5 hours during the year.
- The greatest drift deposition rate is predicted for the round mechanical draft towers. On an annual basis, these towers will have a maximum deposition rate of about 51,000 kg/km^2/year. The rectangular mechanical draft towers will also produce relatively deposition rates (maximum = 24,000 kg/km^2/year), while both natural draft designs will result in much lower maxima but wider patterns of distribution. For all tower options, maximum annual deposition rates decrease to about 560 kg/km^2/year (5 lb/acre/year) within 3 km from the towers.

Based on the conclusions stated above, the following ranking (most desirable to least desirable) can be inferred:

1) two natural draft towers (most desirable);

2) four natural draft towers; and

3) four round or rectangular mechanical draft towers (least desirable).

This ranking reflects only consideration of potential environmental effects associated with these tower designs. Other factors that must ultimately be weighed in the selection of a cooling system for the proposed power plant (e.g., engineering and cost aspects) were not considered in this study.

D3.0 ATMOSPHERIC EFFECTS

By means of the COOLTOWR model (see Addendum A), the behavior of saturated plumes from the cooling towers, for a representative subset of meteorological conditions, was determined. Hourly observations compiled over a period of one year at the B.C. Hydro mechanical weather station near Harry Lake were incorporated to predict the frequencies of occurrence of visible plume lengths and the incremental effects produced by the towers upon local patterns of ground-level icing and fogging. A complete description of meteorological data used in this study is provided in Addendum C. The calculations were performed for each month of the year. To avoid unnecessary repetition, however, detailed analyses of cooling tower impacts are presented only for the annual period and for selected seasons.

D3.1 GROUND-LEVEL FOGGING AND ICING

The occurrence of ground-level fogging and/or icing due to cooling tower plumes is chiefly a by-product of aerodynamic downwash. The meteorological condition associated with downwash is high wind speed. Under this condition, the presence of the tower structure in the ambient flow field results in the formation of a low-pressure wake in the lee of the towers. Plume rise is inhibited in such circumstances, and part or all of the tower effluent may be temporarily deflected into this wake region. At sufficient downwind distances, the reserve buoyancy of the plume allows it to escape the lee cavity; therefore, ground-level impact is restricted to the region adjacent to the cooling towers.

The cooling tower plume model incorporates schemes to simulate aerodynamic effects associated with each tower design. For rectangular mechanical draft towers, downwash of the plume is assumed to occur when the ratio of tower exit velocity to the wind speed at tower height falls below a critical value, which is a function of the plume exit radius, tower height, and the angle between the wind vector and the long axis of the tower. The scheme used is a modified form of one originally suggested by Briggs[1]

and found to be valid for rectangular mechanical draft cooling towers by Hanna.[2] For the rectangular towers studied here, the critical wind speed for downwash varied from 4.7 m/s for winds perpendicular to the tower's long axis to 9.7 m/s for winds parallel to the tower's long axis.

On the basis of numerical modeling results, the occurrence of tower-related ground-level fogging and/or icing associated with the four rectangular mechanical draft cooling towers is expected to be frequent. In all, fogging is predicted for 915 hours during the year or more than 10% of the time. This result is reasonable since the frequency of occurrence of tower-related fogging around rectangular mechanical draft towers has been observed to be extensive.[2] However, no more than about 200 hours of fogging are expected at any one point.

The results of the analyses for annual and worst-season (autumn*) frequencies of ground-level fogging due to the four rectangular mechanical draft cooling towers are illustrated in Figures D3-1 and D3-2 respectively. In addition, Table D3-1 lists the predicted hours of fogging by month. The patterns depicted in the figures illustrate the asymmetrical distribution of fogging associated with these towers and the contributions from individual towers. The annual fogging frequencies indicate that the majority of fogging cases occur with a south-southwest wind, resulting in fogging north-northeast of the towers. The power plant installations north of the towers will receive up to 200 hours of fogging during the year. Portions of the switchyard and most of the other plant structures could have as many as 100 hours of fogging during the annual period, as could most of the other plant installations.

*Autumn is defined as the months of September, October, and November. The other seasons follow from this definition. See Addendum C for details.

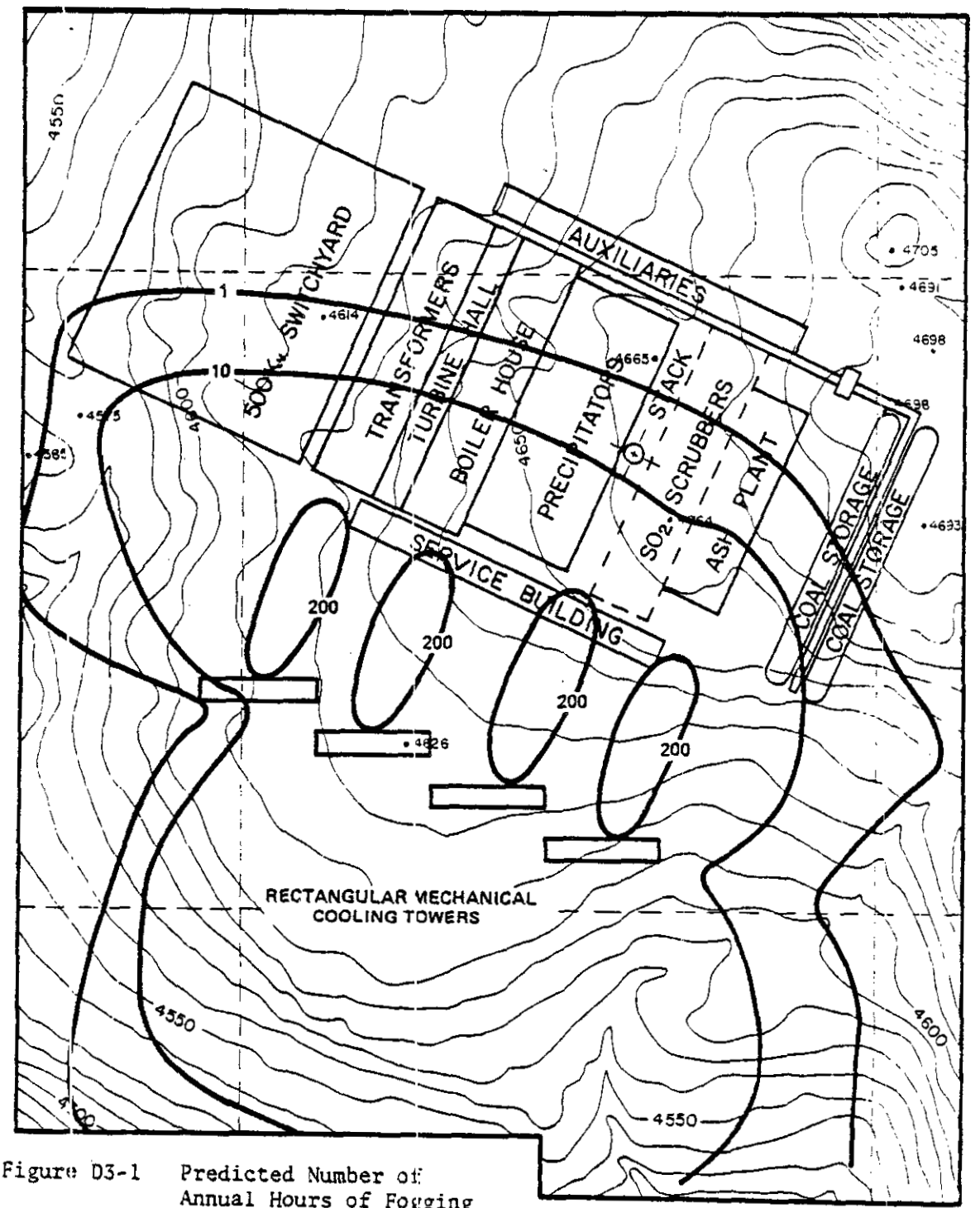

Figure D3-1 Predicted Number of Annual Hours of Fogging Induced by Proposed Rectangular Mechanical Draft Cooling Towers

TABLE D3-1

HOURS OF INCREMENTAL FOGGING AND ICING BY MONTH*
FOR MECHANICAL DRAFT COOLING TOWERS

Month	Fogging		Icing**
	Rectangular	Round	Rectangular
January	27 SSE	0	17 SSE
February	15 SSE	0	12 SSE
March	64 SSE	1 S	25 SSE
April	37 SSE	1 E	0
May	29 SSE	0	0
June	20 SSE	0	0
July	34 SSW	0	0
August	85 NNE	0	0
September	97 SSE	0	0
October	270 NNE	6 NNE	4 NNE
November	185 NNE	20 NNE	91 NNE
December	52 NNE	1 NNE	21 SE
Annual	915 NNE	29 NNE	170 NNE

*The direction (relative to the towers) coresponding to the maximum fogging and icing frequency for each month is given next to the number of hours.

**No ground-level icing is predicted for the round mechanical draft towers.

The highest seasonal frequency of fogging (552 hours) is expected during the autumn, which has the greatest number of high wind-speed cases (see Appendix E, Climatic Assessment). As can be seen in Figure D3-2, the pattern of fogging for autumn is very similar to the annual pattern. The greatest predicted impact is again to the north of the towers with as many as 60 hours of fog reaching other power plant installations. The predicted frequencies of fogging during the other seasons are significantly less, with the lowest frequency (94 hours) predicted for winter. In contrast with the results for autumn, the maximum occurrence for fogging during the other seasons is predicted to be to the south-southeast, away from the other plant installations.

The criteria for determining an occurrence of icing attributable to the cooling tower vapor plumes are similar to those used in the identification of fogging, with the exception that the liquid content of a plume intersecting the surface is assumed to freeze upon impact whenever the ambient temperature is at or below 0°C. Fogging just above the ground is assumed to accompany each incidence of icing; thus, the frequency of occurrence of icing and fogging may be nearly identical during the coldest months of the year.

Figure D3-3 illustrates predicted annual frequencies of ground-level icing produced by the four rectangular mechanical draft cooling towers. In all, a total of 170 hours of icing is predicted. As might be expected, the spatial distribution of icing shown in the figures is similar to the predicted spatial distribution of fogging. Maximum icing (about 40 hours) is predicted to occur north of the towers. There will be instances of low-level icing on the power plant installations. Nearly 40 hours of icing are predicted for portions of the service buildings with 20 hours of icing reaching the switchyard.

Seasonally, the greatest frequency of icing is predicted during the fall, especially in November (see Table D3-1). This result again reflects the fact that the greatest percentage of high wind speed cases occurs during the latter portion of the year. No icing is predicted for the months May through September.

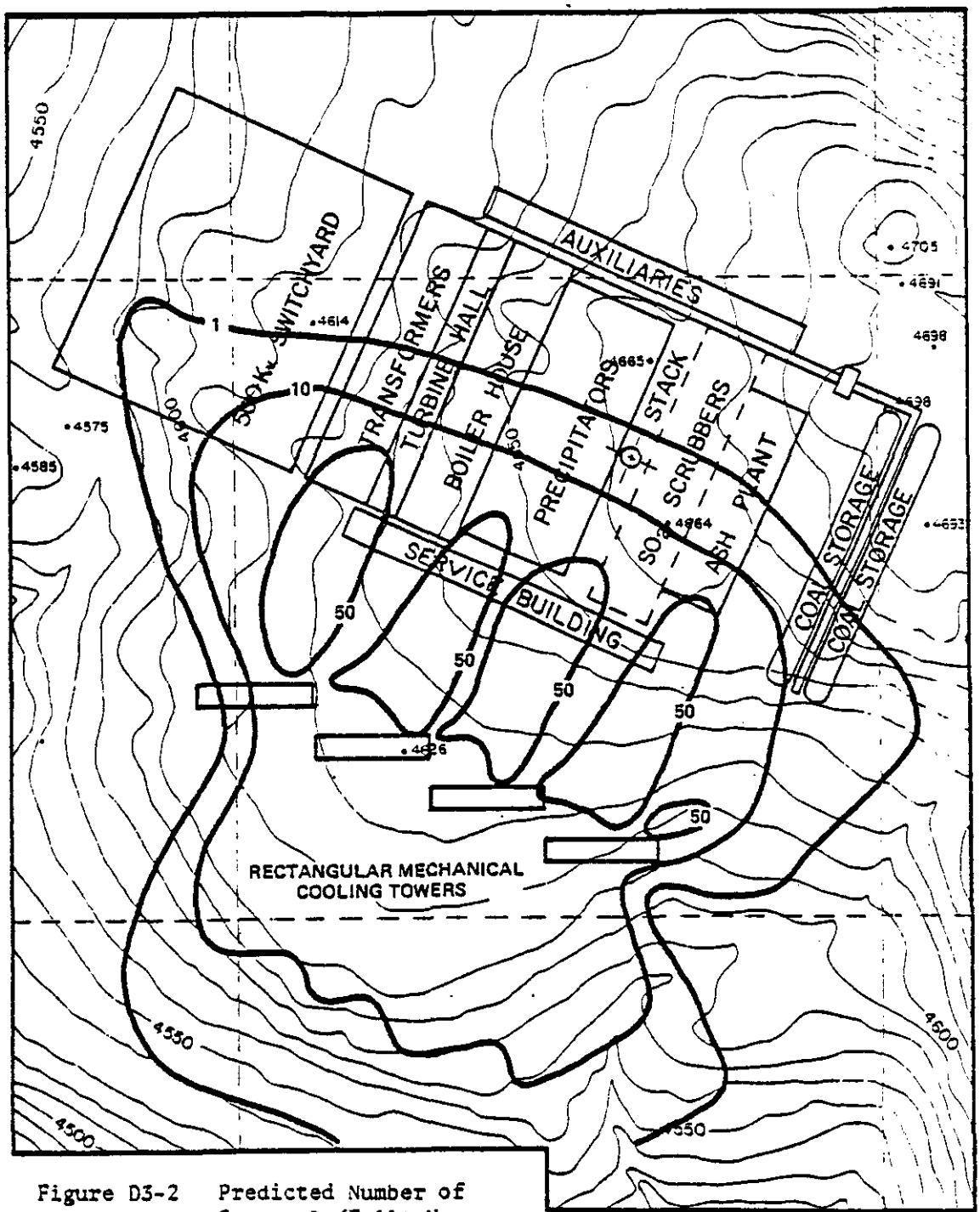

Figure D3-2 Predicted Number of Seasonal (Fall) Hours of Fogging Induced by Proposed Rectangular Mechanical Draft Cooling Towers

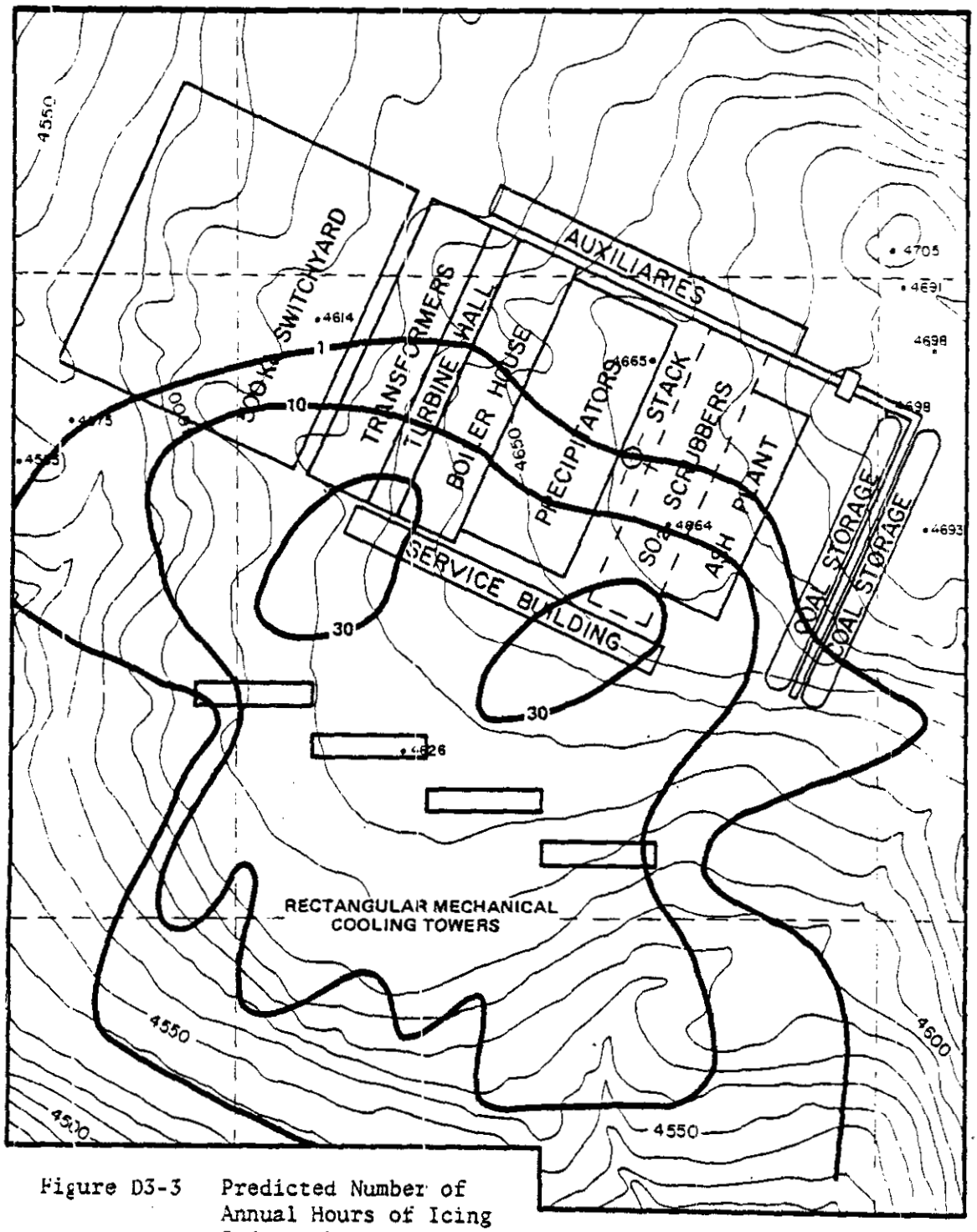

Figure D3-3 Predicted Number of Annual Hours of Icing Induced by Proposed Rectangular Mechanical Draft Cooling Towers

The isopleths in Figure D3-3 represent hours of potential initiation of tower-induced icing. They do not reflect the total number of hours when ice attributable to the towers may exist on the ground. Again, only the high wind speed cases with plume aerodynamic downwash are expected to produce ground-level impact. The accumulation of ice deposited on the ground in the vicinity of the towers by downwash is chiefly dependent upon the persistence of the meteorological conditions giving rise to such icing. In particular, the persistence over an extended period of strong winds from a particular direction may possibly produce a thin layer of ice during prolonged subfreezing ambient conditions. The region affected by plume impact is then usually restricted to the first 500 meters from the towers, since aerodynamic downwash is the major mechanism by which visible plumes are brought to the surface.

A different downwash criterion is used when considering ground-level fogging and icing due to round mechanical draft towers and natural draft towers. This criterion, which is explained in Addendum A, results in a significantly higher critical wind speed (11 m/s) for round mechanical draft towers than for rectangular mechanical draft towers. Therefore, less downwash and fogging/icing are predicted with the round design. This is reasonable, since round structures do not affect the local air flow as much as rectangular structures.

On the basis of the numerical simulations, ground-level fogging is predicted only 29 hours during the year for the round mechanical draft towers. Again, the majority of the fogging cases are expected in autumn (see Table D3-1). It is expected that the fogging induced by these towers will only rarely reach other power plant installations. In addition, no ground-level icing is predicted for these towers. Neither of the natural draft tower configurations is expected to produce ground-level fogging or icing within the first several kilometers. This result is in agreement with observations of plume behavior at operational natural draft tower sites.[3]

A final point must be made concerning the results presented above. In developing meteorological frequency distributions, it was not possible

tc eliminate cases of natural fog from consideration because on-site observations of fog were not available. Therefore, it is possible that some of the predicted tower-induced fogging cases will occur during conditions of natural obscuration.

D3.2 ICING DUE TO COOLING TOWER DRIFT DROPLETS

Since not all the water escaping the cooling towers is in the form of plume condensate, it is of interest to investigate the possibility of adverse effects, in particular, icing, due to impingement by drift droplets. However, a simple calculation serves to demonstrate that the extent of such icing must be negligible in comparison with that which can occur due to plume downwash for mechanical draft towers.

Current drift eliminator design specifications (see Table D1-1) indicate that the emission of drift will be restricted to 0.008% of the circulating water flow rate (40,448 liters/sec). Total water escaping as drift is then about 3.24 liters/sec. During the winter, the water emission rate associated with evaporative cooling tower plumes is 800 to 900 liters/sec. Inasmuch as wintertime conditions that would cause drift to reach the switchyard (or any other area) would also transport the condensate plume in the same direction, the above comparison is a strong indication that the potential severity of icing due to drift droplets is substantially less than that associated with plume impact. The following illustrates this conclusively.

- Assume that all drift water droplets reach the switchyard area without evaporation for a period of one hour.
- Assume the point of emission is in the center of the mechanical draft tower cluster (see Figure D1-1). A 22.5° sector emanating from this point would intercept the switchyard area between the downwind distances of approximately 365m and 730m. Assume all drift water falls within this portion of the sector (area about 78,800m^2).
- During an hour the total drift water emitted is about 11,664 liters of approximately 12m^3.
- If the water is evenly distributed over the calculated area, the equivalent depth of such water (ice) during one hour is 0.015cm.

While this calculation is quite crude, it does demonstrate the point that icing due to drift water is relatively unimportant. The potential for icing due to plume impact is much greater, but only if mechanical draft towers are used. No significant icing of any kind is anticipated for natural draft towers.

D3.3 VISIBLE PLUME LENGTH

Model sensitivity tests indicate that over a wide range of temperatures and regardless of stability category, the cases of light winds accompanied by high relative humidity are those producing the longest plumes. The climatology of the Hat Creek Valley Region indicates a pronounced winter maximum of ambient relative humidity (see Appendix E). On this basis, one might expect the greatest frequency of long plumes during the winter season. This is not reflected in the model calculation results. Although the average relative humidity is greater in winter, there are a small number of synoptic situations which produce very high relative humidity with light winds in the Hat Creek Region during the summer season. It is during these periods of high relative humidity that the longest plumes are predicted. The extent of these long plumes is illustrated in Figures D3-4 through D3-7 which show the annual plume length frequencies for each tower configuration.

While cooling tower plumes with lengths exceeding 10 km can occur, it is felt that one assumption incorporated by the model; namely, constant relative humidity in the plume rise layer, is responsible for overpredicting the frequency of long plumes for cases with light winds and high humidity near the surface. In nature, such conditions normally occur under specific circumstances. Light winds and high relative humidities near the ground are typical of early morning inversions with clear skies. Normally, these conditions prevail through only a shallow layer, the region above which is characterized by a rapid decrease in humidity. The assumption of uniformly high relative humidity with height is overly conservative in such cases, the more so since the depth of the plume rise layer itself is greatest with light winds. In addition, the model does not consider the possibility that decks of stratus clouds can occur well within the plume rise layer predicted for low wind cases. Under

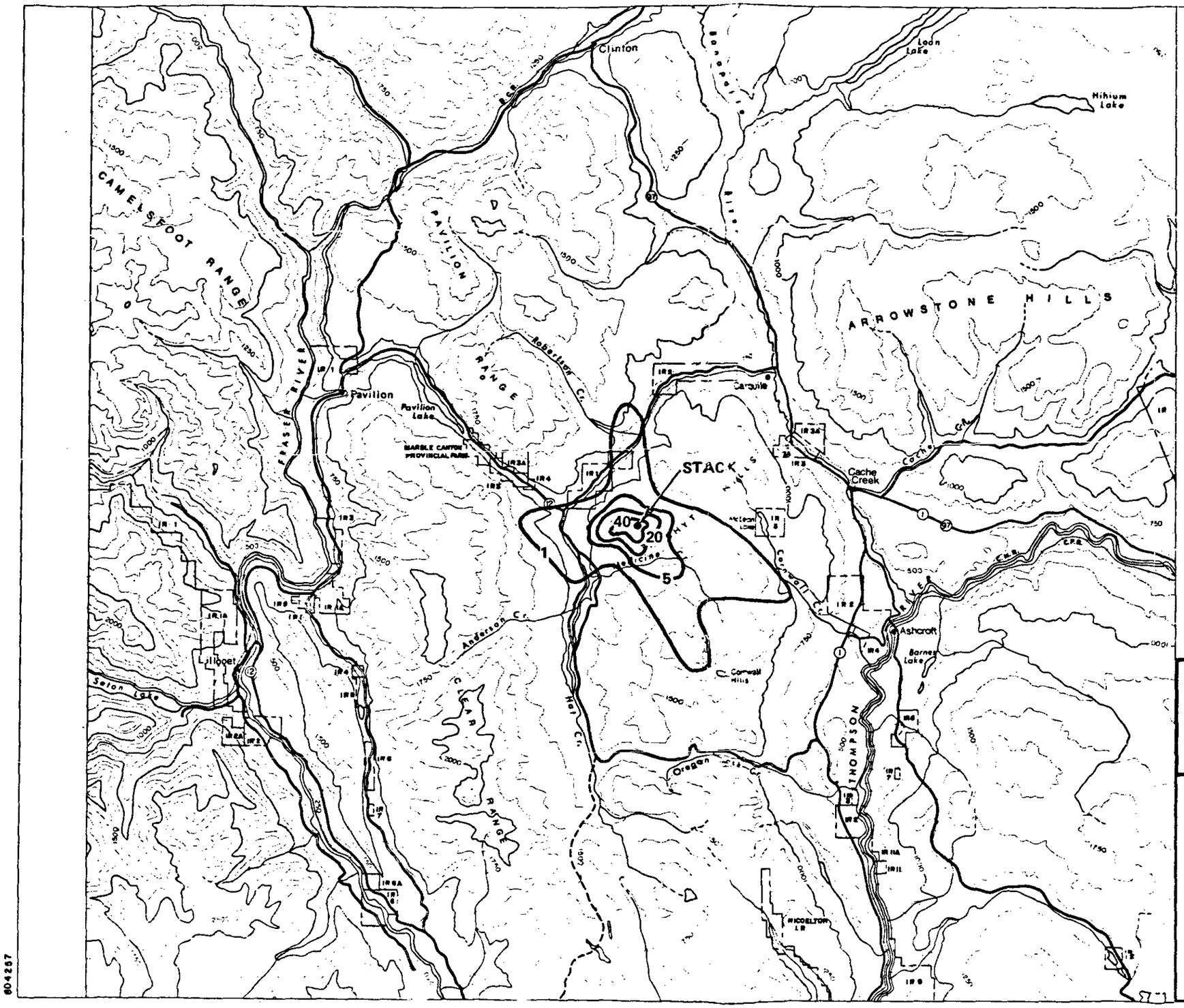

BRITISH COLUMBIA HYDRO AND POWER AUTHORITY
HAT CREEK PROJECT

DETAILED ENVIRONMENTAL STUDIES

Figure D3-4 Predicted Number of Annual Hours of Visible Plumes from Proposed Rectangular Mechanical Draft Cooling Towers

604267

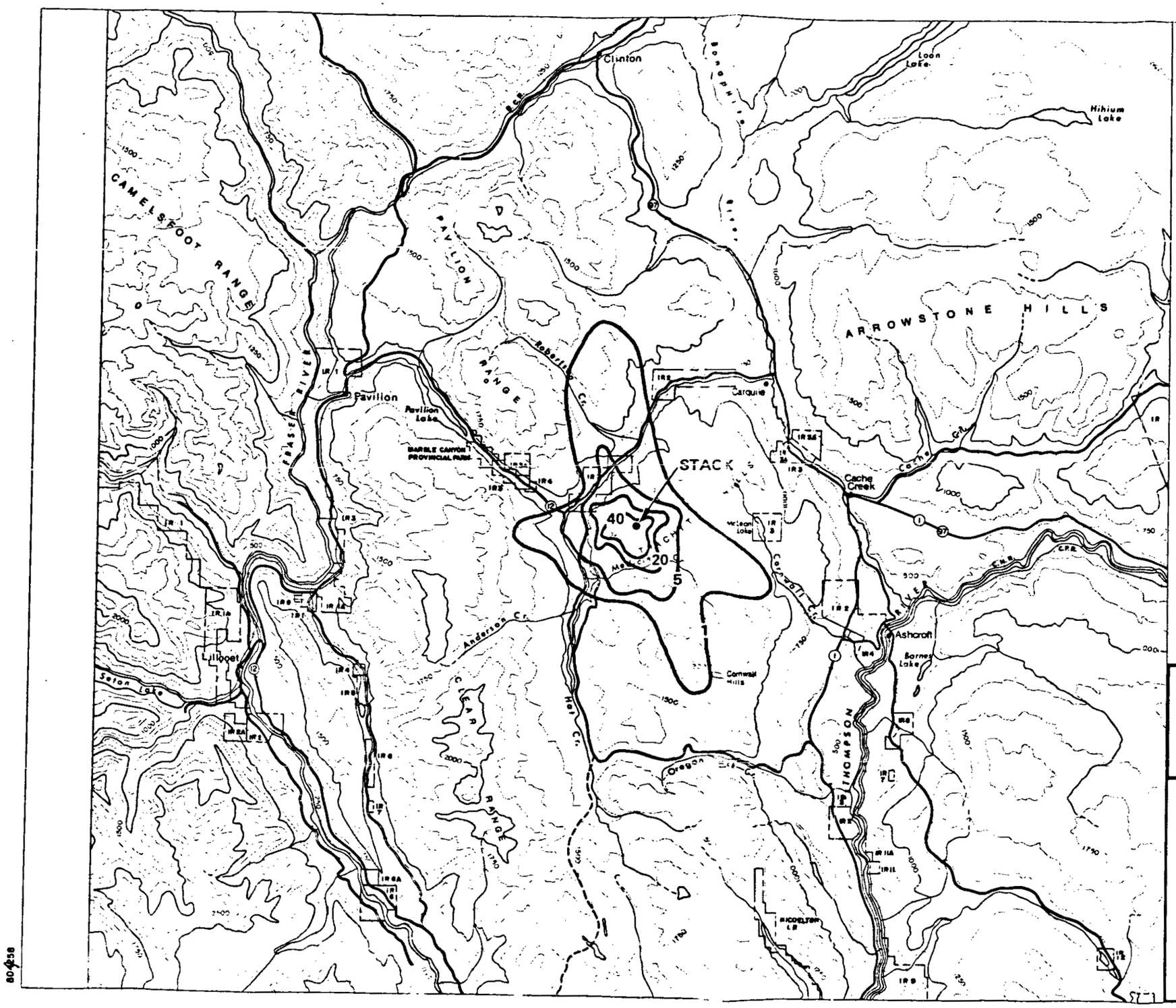

X=maximum=953 hours

SCALE - 1:250,000

0 Kilometres 5 10 15

CONTOUR INTERVAL - 250 METRES

BRITISH COLUMBIA HYDRO AND POWER AUTHORITY
HAT CREEK PROJECT

DETAILED ENVIRONMENTAL STUDIES

Figure D3-5 Predicted Number of Annual Hours of Visible Plumes from Proposed Round Mechnical Draft Cooling Towers

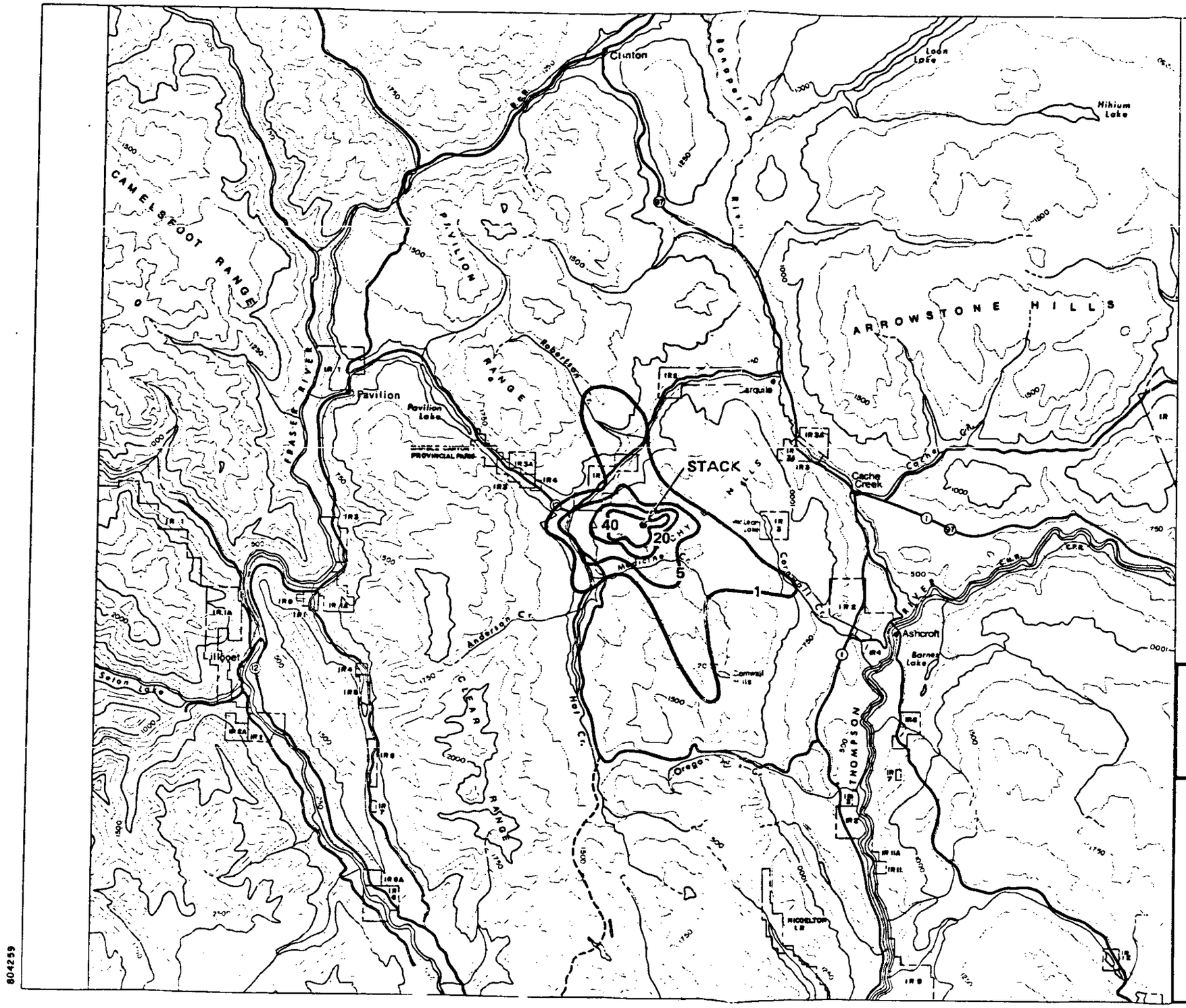

X=maximum=1100 hours

SCALE - 1:250,000

5 0 Kilometres 5 10 15

CONTOUR INTERVAL - 250 METRES

BRITISH COLUMBIA HYDRO AND POWER AUTHORITY
HAT CREEK PROJECT

DETAILED ENVIRONMENTAL STUDIES

Figure D3-6 Predicted Number of Annual Hours of Visible Plumes from Proposed (Two) Natural Draft Cooling Towers

804259

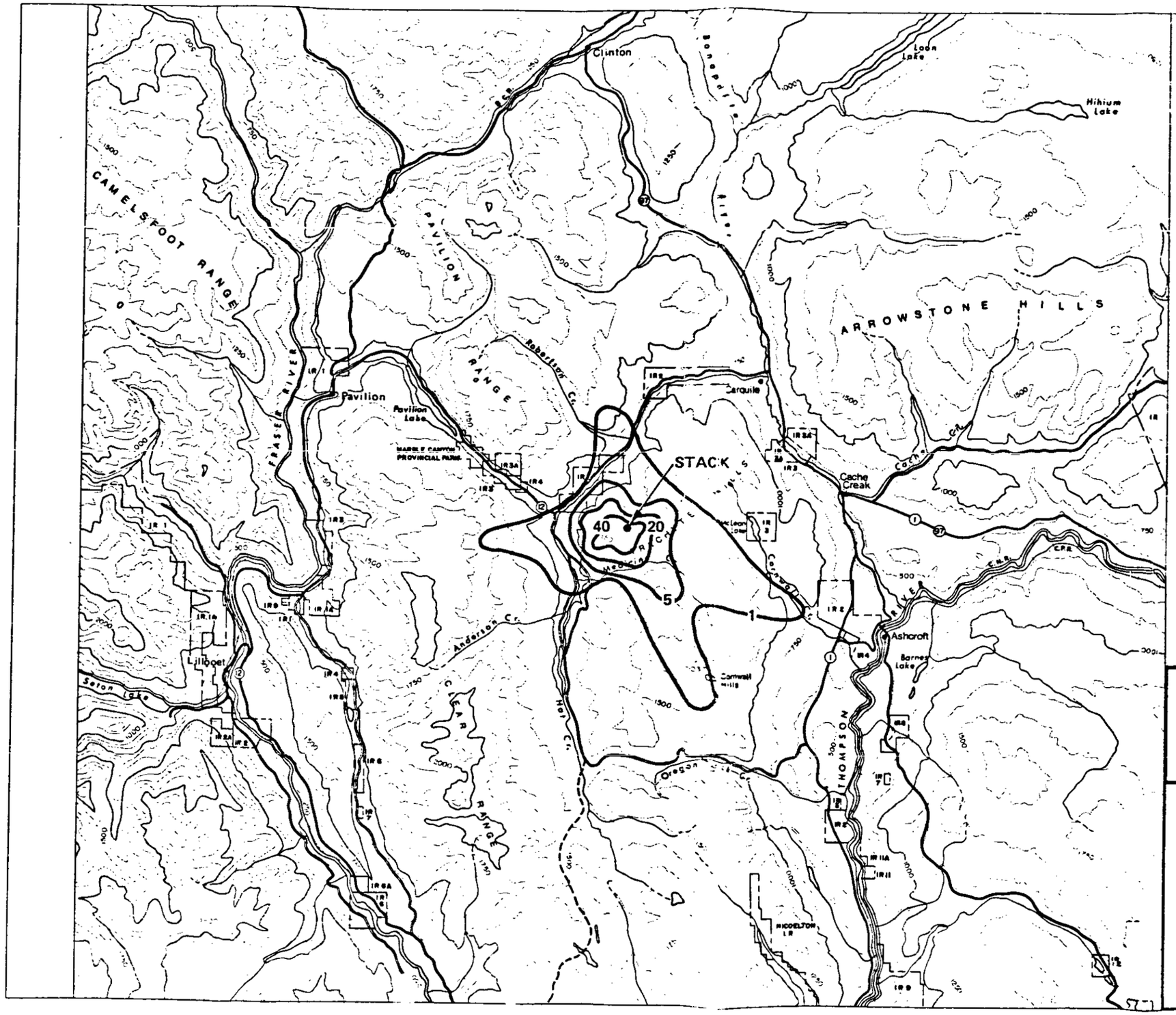

X=maximum=1100 hours

SCALE - 1:250,000

0 Kilometres 5 10 15

CONTOUR INTERVAL - 250 METRES

BRITISH COLUMBIA HYDRO AND POWER AUTHORITY
HAT CREEK PROJECT

DETAILED ENVIRONMENTAL STUDIES

Figure D3-7 Predicted Number of Annual Hours of Visible Plumes from Proposed (Four) Natural Draft Cooling Towers

6U4260

such circumstances, the plume would be merged with the natural clouds and have no practical significance. For these reasons, the predicted frequencies of plume lengths greater than about 10 to 12 km are probably overestimates.

The annual patterns of plume frequencies predicted for the four tower designs are similar, which is not surprising since the results in each case were derived from the same meteorological data. However, the rectangular mechanical draft plumes dissipate before the plumes from the other tower designs. Longer plumes occur with natural draft towers because their plumes have smaller surface-to-volume ratio which results in less rapid entrainment. The box configuration of round mechanical draft towers produces quick plume merging, which again reduces entrainment because of the smaller surface-to-volume ratio of the aggregate plume and, therefore, results in longer plumes.

The pronounced lobes observed on the visible plume frequency isopleths may in part reflect the use of only one year of meteorological data in the modeling analysis. It is probable that, if climatological data representing a period of, for example, ten years were available, some smoothing of the isopleth patterns would result. The figures show isopleths representing the highest frequencies skewed toward the west. This appears to be a real effect, despite the dominant westerly winds. On-site data reveal that higher relative humidities, which would produce longer plumes, occur more often with easterly winds. The mountain ranges to the west of the proposed site effectively shield that location from a moist westerly flow of air. Downslope flow from the Coast Range would cause warming and drying of the air. An easterly (upslope) wind would experience cooling, resulting in a higher relative humidity at the site with this direction.

The season corresponding to shortest plume lengths is autumn, when visible plumes reaching further than 4 km from the towers. are predicted. The greatest number of medium-length plumes (1 to 5 km) is expected during winter (December, January, and February). For comparison, the winter season visible plume frequencies for each tower design are presented in Figures D3-8 through D3-11.

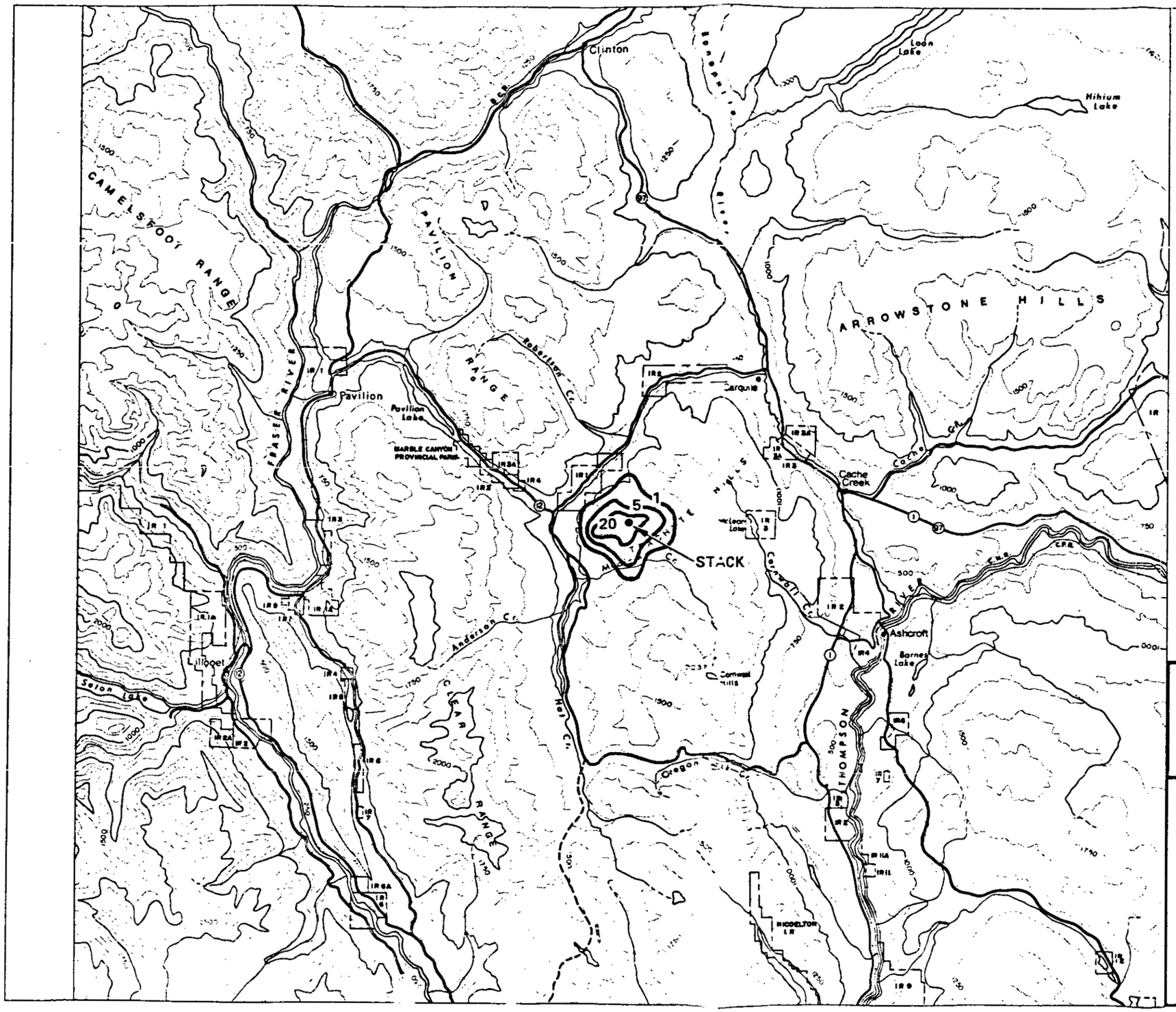

X=maximum=271 hours

SCALE - 1:250,000

0 Kilometres 5 10 15

CONTOUR INTERVAL - 250 METRES

BRITISH COLUMBIA HYDRO AND POWER AUTHORITY HAT CREEK PROJECT

DETAILED ENVIRONMENTAL STUDIES

Figure D3-8 Predicted Number of Seasonal (Winter) Hours of Visible Plumes from Proposed Rectangular Mechnical Draft Cooling Towers

804261

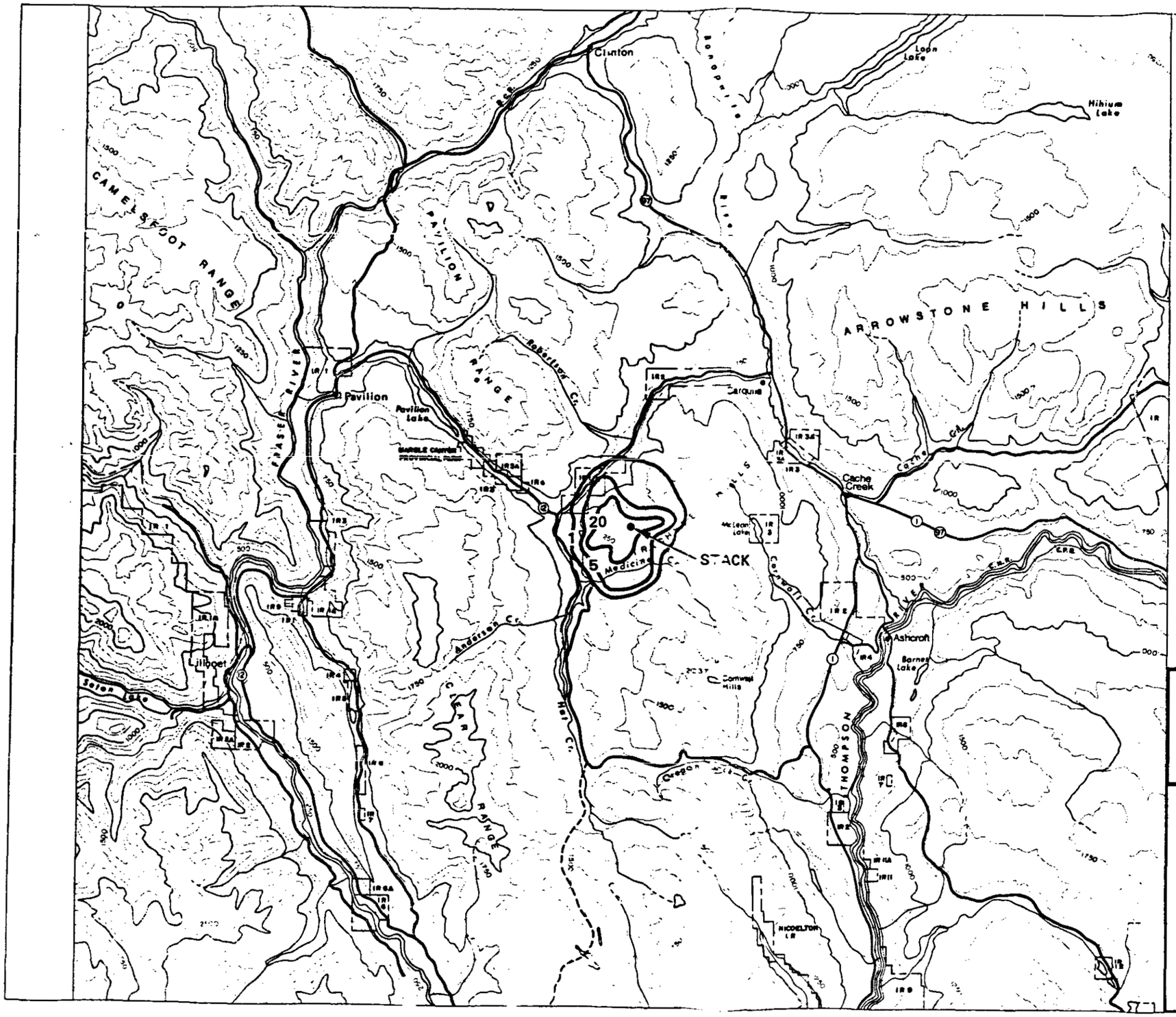

X=maximum=271 hours

SCALE - 1:250,000

0 Kilometres 5 10 15

CONTOUR INTERVAL - 250 METRES

BRITISH COLUMBIA HYDRO AND POWER AUTHORITY
HAT CREEK PROJECT

DETAILED ENVIRONMENTAL STUDIES

Figure D3-9 Predicted Number of Seasonal (Winter) Hours of Visible Plumes from Proposed Round Mechanical Draft Cooling Towers

804262

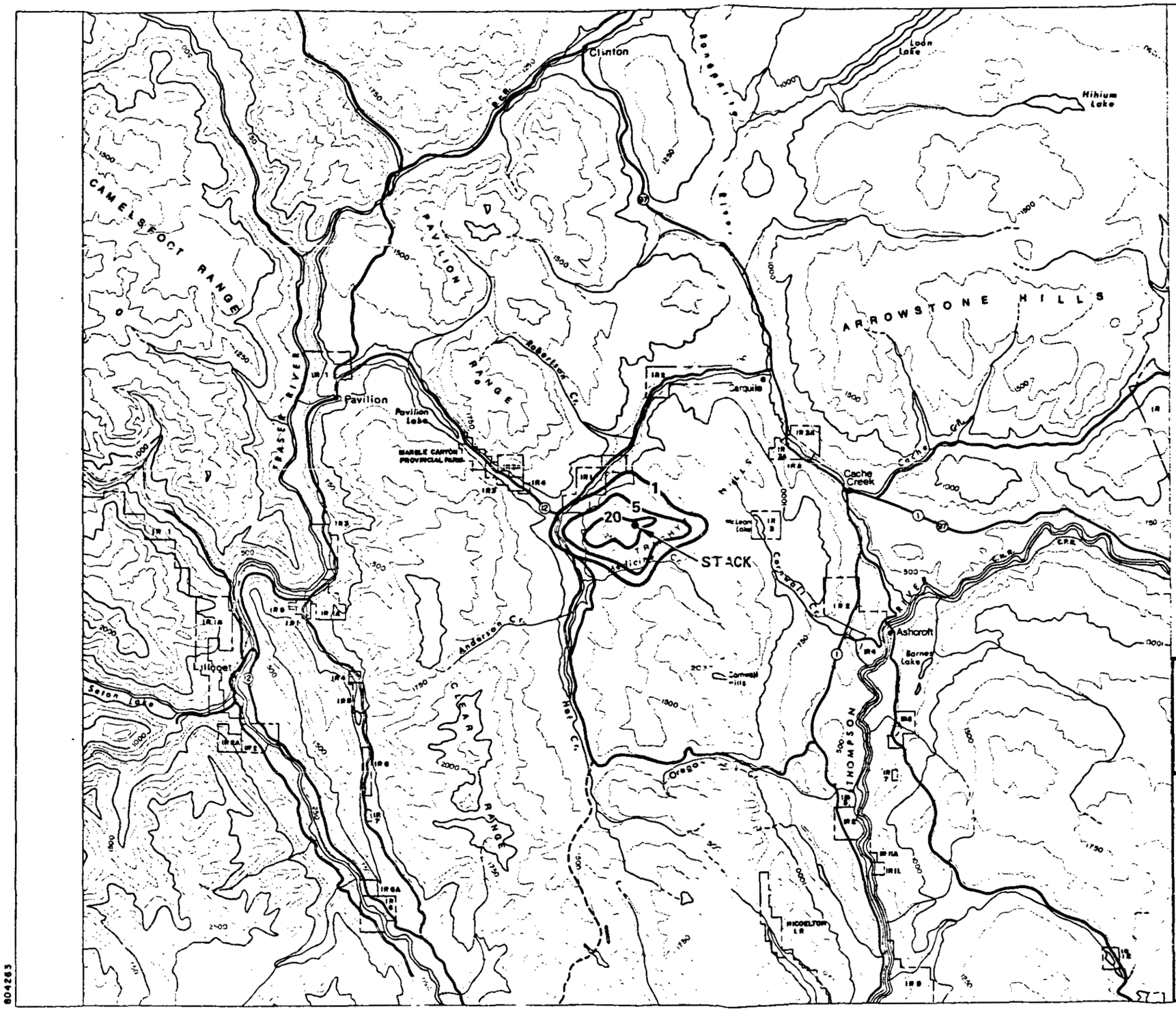

X=maximum=271 hours

SCALE - 1:250,000

0 Kilometres 5 10 15

CONTOUR INTERVAL - 250 METRES

BRITISH COLUMBIA HYDRO AND POWER AUTHORITY
HAT CREEK PROJECT

DETAILED ENVIRONMENTAL STUDIES

Figure D3-10 Predicted Number of Seasonal (Winter) Hours of Visible Plumes from Proposed (Two) Natural Draft Cooling Towers

804263

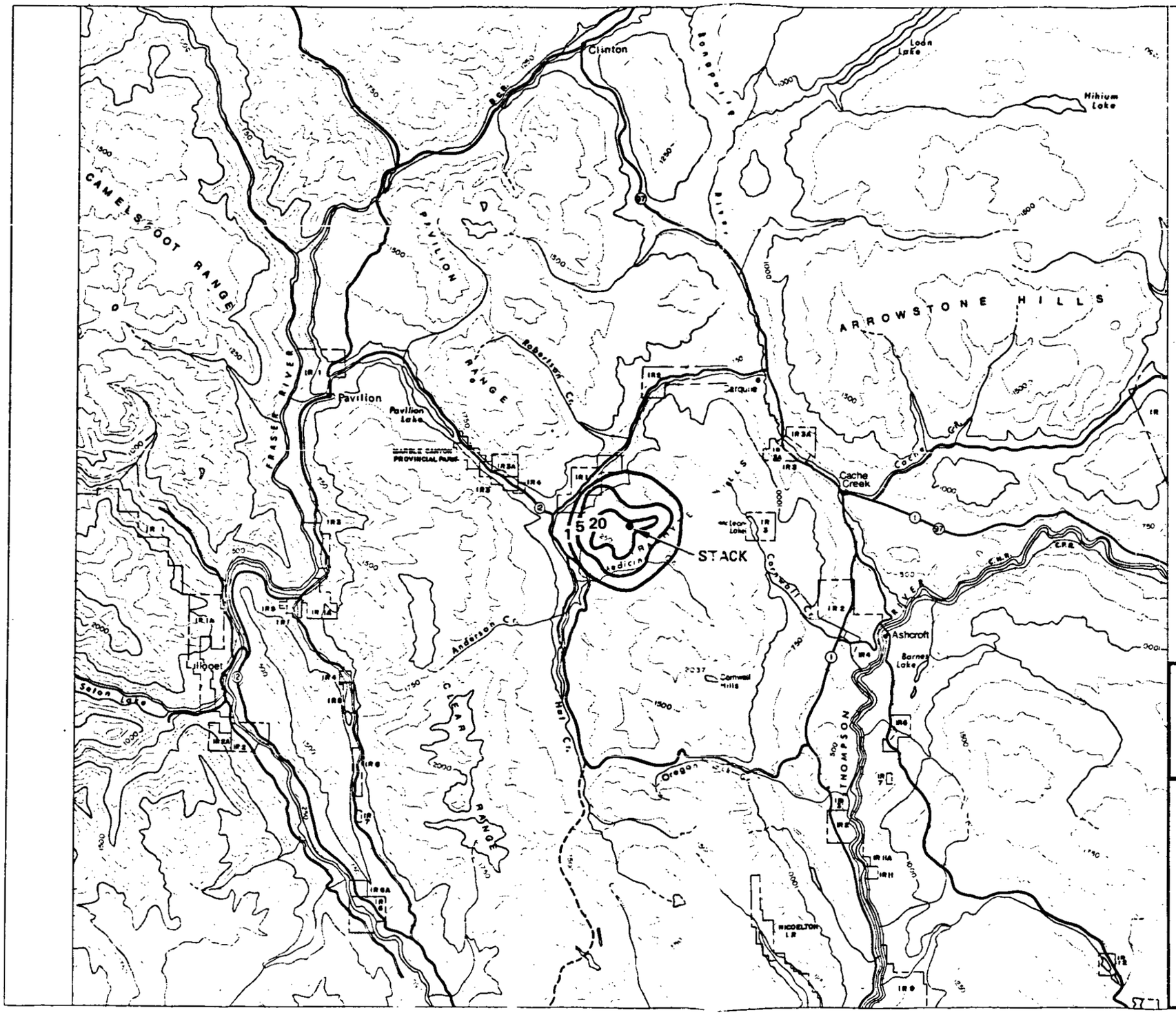

BRITISH COLUMBIA HYDRO AND POWER AUTHORITY
HAT CREEK PROJECT

DETAILED ENVIRONMENTAL STUDIES

Figure D3-11 Predicted Number of Seasonal (Winter) Hours of Visible Plumes from Proposed (Four) Natural Draft Cooling Towers

804264

As indicated by the figures presented in this section, the frequency of plume lengths greater than 5 km will be very small. The calculations that produced these results incorporate the assumption of flat terrain. The rugged topography in the vicinity of the proposed site will normally tend to increase turbulence, leading to greater mixing with ambient air, and, therefore, shorter plume lengths. Thus, the results presented are conservative estimates of visible plume length.

D3.4 ATMOSPHERIC EFFECTS AT SPECIFIC RECEPTORS

It has already been shown that, during downwash conditions, rectangular mechanical draft towers will produce a significant number of hours of ground-level fogging and icing which will reach other power plant installations (see Section D3.1). However, elevated plumes with low release heights can also impact on power plant installations. Under freezing conditions, significant icing could occur and pose a hazard or nuisance to power plant operation. Figures D3-12 and D3-13 illustrate the total number of hours of icing resulting from plume impact on buildings, etc. due to rectangular and round mechanical draft towers, respectively. Note that for rectangular mechanical draft towers (Figure D3-12) the isopleths represent the sum of the hours of icing due to downwashing and elevated plumes. Since no icing due to downwash conditions was predicted for round mechanical draft towers, the freguencies illustrated in Figure D3-13 correspond to elevated plume impacts only. It is also important to realize that the estimated hours of icing due to elevated plumes is extremely conservative. All hours characterized by sub-freezing temperature and elevated plumes extending as far as the power house structures have been included. The mean elevation at the base of the mechanical draft towers is about 1408m (4620 ft) while that of the switchyard is 10 to 20m (30 to 60 ft) lower. In addition, the cooling tower emission height is about 20m above grade. Thus, it is expected that during light wind conditions the plumes will actually pass above the switchyard structures. For this reason the values represented in Figures D3-12 and D3-13 are probably overestimates of actual icing frequencies.

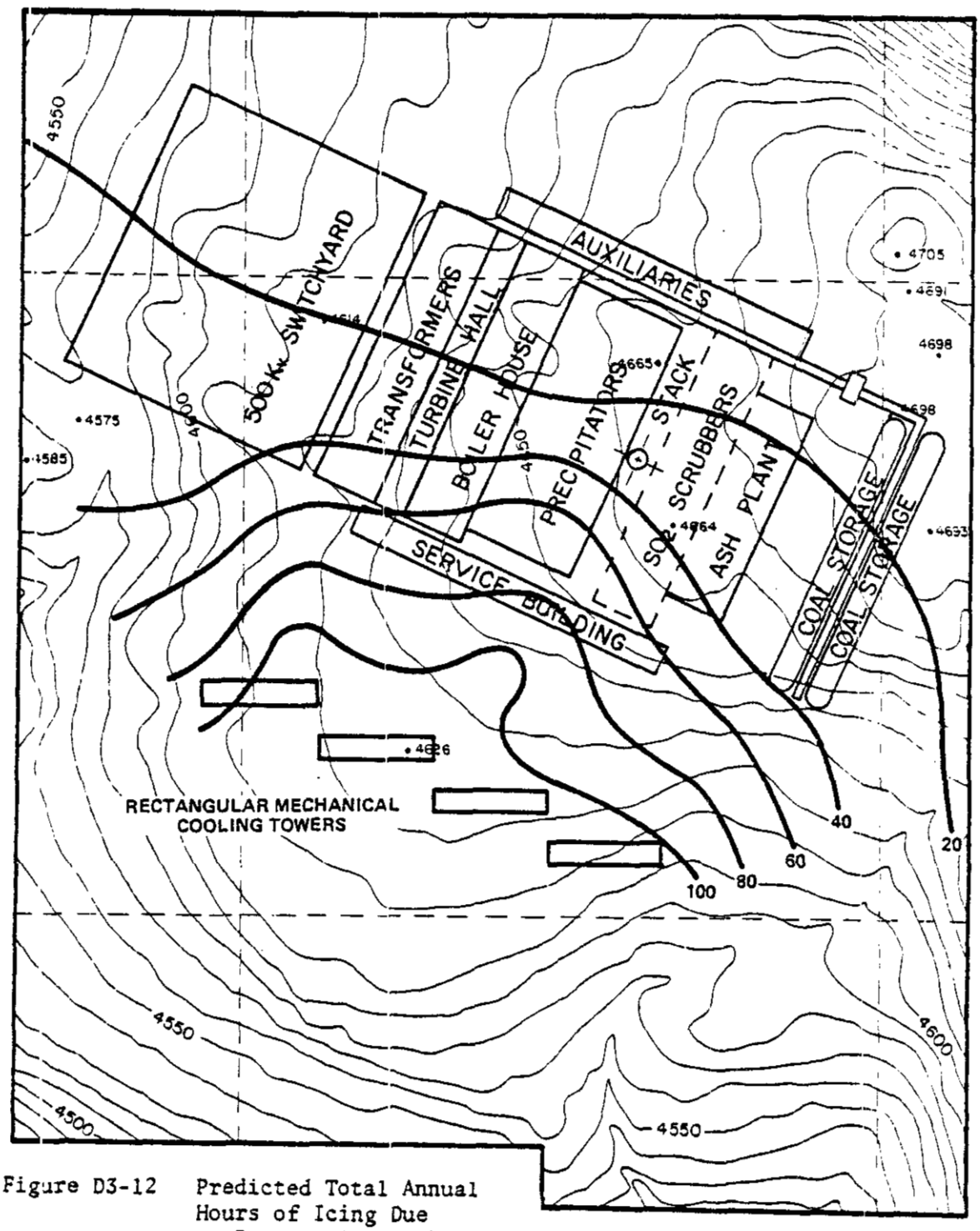

Figure D3-12 Predicted Total Annual Hours of Icing Due to Rectangular Mechanical Draft Cooling Towers

804265

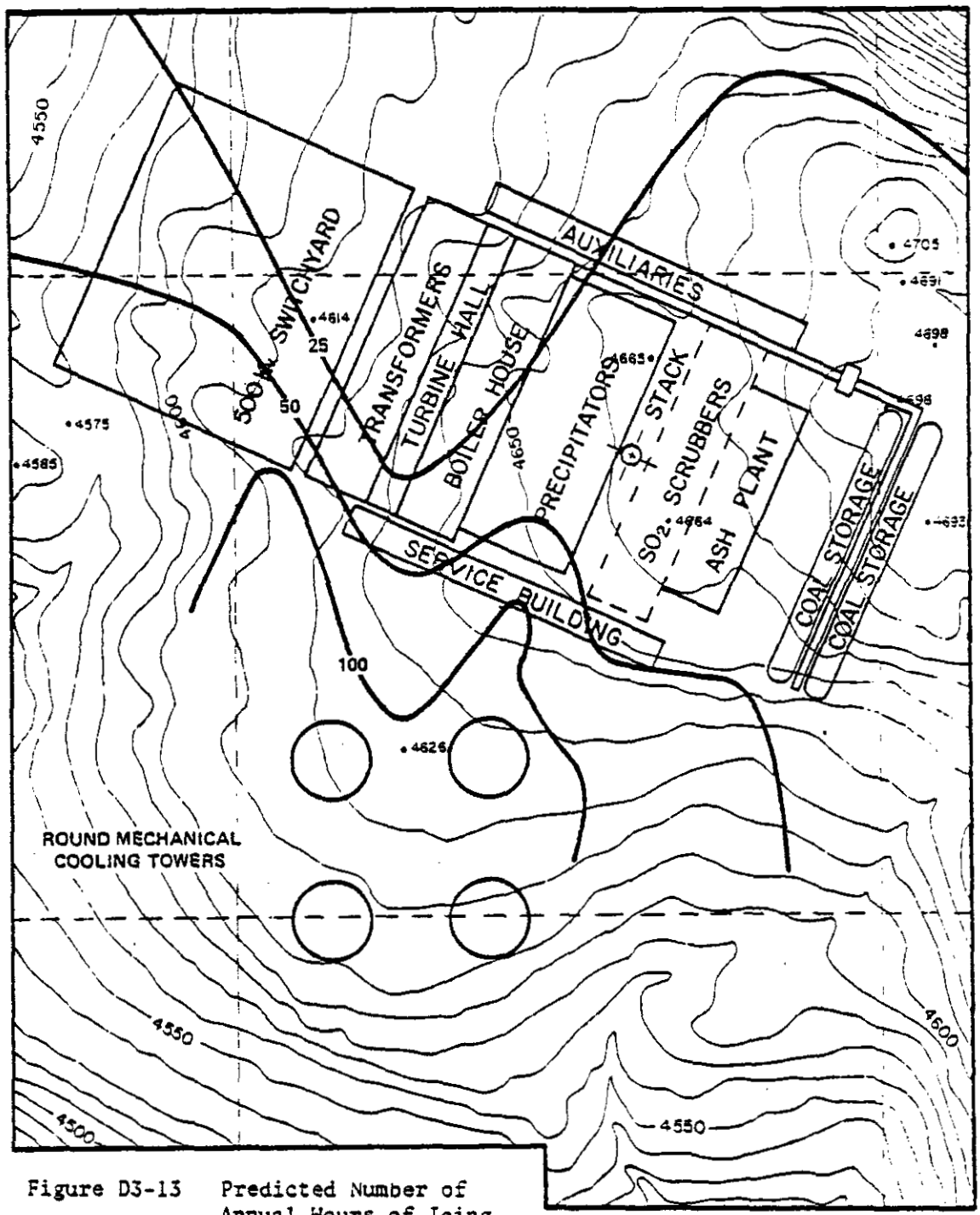

Figure D3-13 Predicted Number of Annual Hours of Icing Due to Elevated Plume Impact from Proposed Round Mechanical Draft Cooling Towers

As can be seen, rectangular mechanical draft towers are predicted to produce a maximum of 80 total hours of icing over a year. The switchyard could receive up to 40 hours of icing annually. The round mechanical draft towers will cause icing of power plant installations, including the switchyard, for as much as 100 hours. This result reflects the generally longer plume lengths expected with the round towers. The high release height of the natural draft towers eliminates the possibility that they will produce similar impacts.

Another potential problem to be considered is plume impact on elevated terrain in the region surrounding the power plant. The most significant terrain of this type is the Cornwall Hills, which are located 8 km south-southeast of the cooling towers. An examination of the annual frequencies of visible plume length leads to the conclusion that no more than five hours of ground fogging on the Cornwall Hills, due to elevated plume impact, is expected each year for any of the cooling tower designs. This is a conservative estimate, as the air flow over the Cornwall Hills is likely to prevent direct impingement in many cases.

No adverse effects due to cooling tower plumes are expected at the Hat Creek Project mine, located 8 km west-northwest of the power plant. The predicted horizontal extent of fogging and icing due to downwash does not approach this area. Elevated plumes passing over this location will be a substantial distance above the ground due to plume rise and the difference in elevation between the power plant site on the ridge and the mine in the Hat Creek Valley to the west.

Although direct plume impact (ground fogging and/or icing) is not anticipated, all tower designs are expected to produce elevated visible plumes that will pass above the Indian Reserve, located 2 km northwest of the plant site, up to 40 hours during the year.

D4.0 COOLING TOWER DRIFT

Estimated monthly, seasonal and annual salt drift deposition rates, associated with the operation of the four alternate cooling tower designs, have been calculated according to the analysis procedures outlined in Addendum B and using the meteorological data described in Addendum C. The results for an annual period and for the summer season (June, July and August), which corresponds to the highest seasonal deposition rates for the mechanical draft towers, are presented in Figures D4-1 through D4-8 for each tower configuration. The annual patterns of drift deposition, illustrated in the first four figures, reflect the dominant westerly wind directions which result in maximum drift deposition rates to the east of the towers. Although this is also true for summer, the location of maximum drift deposition rates for the other seasons are more variable, generally reflecting the predominant wind direction of the given season (see Table D4-1).

The largest drift deposition rate (51,500 kg/km^2/year or 460 lb/acre/year) is predicted for round mechanical draft towers. This relatively large deposition rate in the near field is caused by the overlapping of the patterns for individual towers as a result of their box deployment. The proposed arrangement of rectangular mechanical draft towers does not produce this effect to the same degree, but a maximum drift rate of 24,150 kg/km^2/year (216 lb/acre/year) is predicted for this design. For both mechanical draft tower systems, maximum predicted drift deposition rates are within a few hundred meters of the towers.

The two alternate natural draft tower designs produce smaller maximum drift rates, with peak values farther from the towers. In general, natural draft towers spread the drift mass over a wider area. The numerical simulations indicate that the smallest drift deposition rates will occur with the two natural draft towers (maximum = 4,700 kg/km^2/year or 42 lb/acre/year).

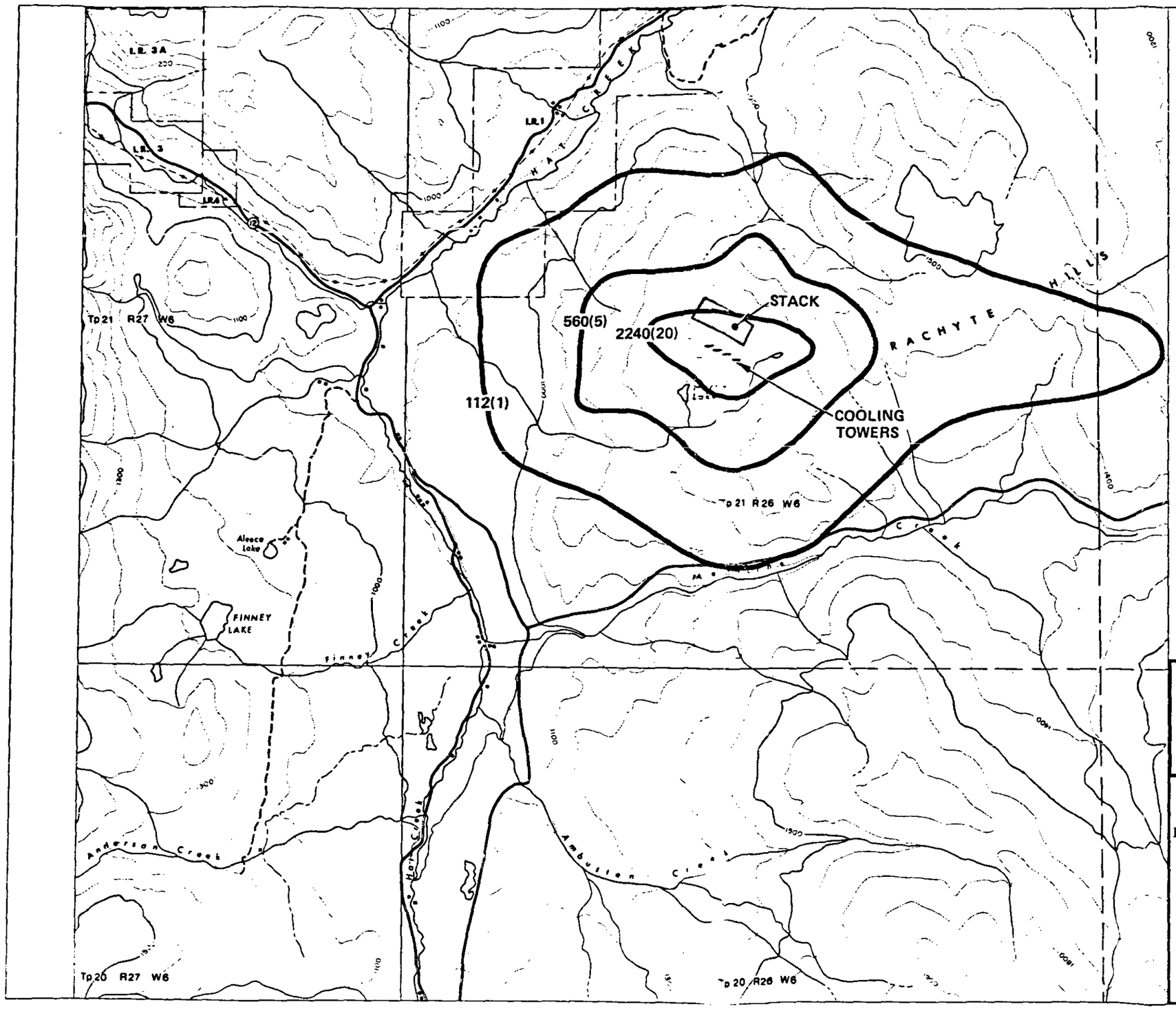

X=maximum=24,150 kg/km^2/year
(215 lb/acre/year)

SCALE - 1:50,000

0 Kilometres 1 2 3

CONTOUR INTERVAL - 100 METRES

BRITISH COLUMBIA HYDRO AND POWER AUTHORITY
HAT CREEK PROJECT

DETAILED ENVIRONMENTAL STUDIES

Figure D4-1 Predicted Annual Salt Deposition in kg/km^2/year (lb/acre/year) Due to Drift from Proposed Rectangular Mechanical Draft Cooling Towers

804267

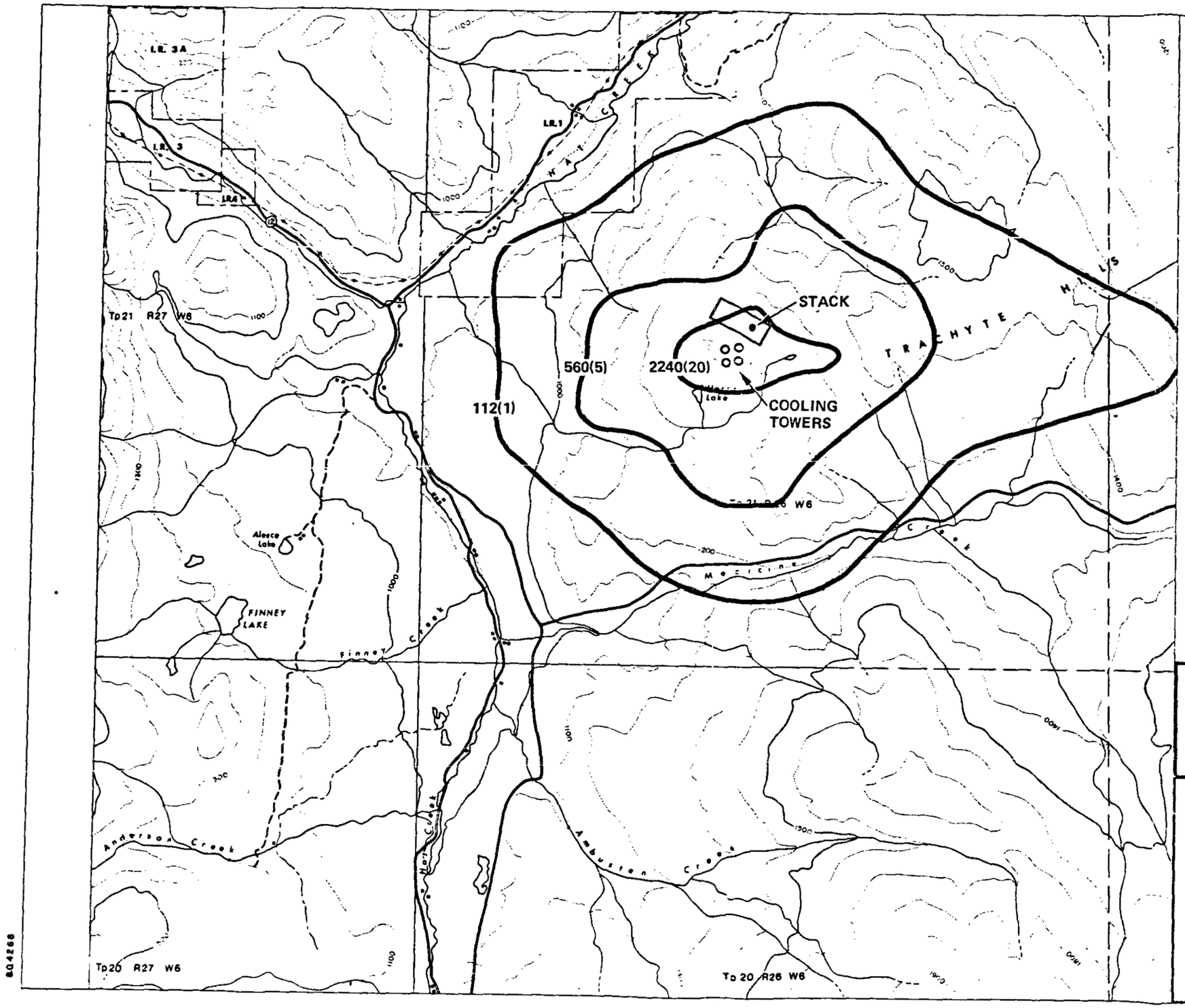

BRITISH COLUMBIA HYDRO AND POWER AUTHORITY
HAT CREEK PROJECT

DETAILED ENVIRONMENTAL STUDIES

Figure D4-2 Predicted Annual Salt Deposition in kg/km^2/year (lb/acre/year) Due to Drift from Proposed Round Mechanical Draft Cooling Towers

EQ4268

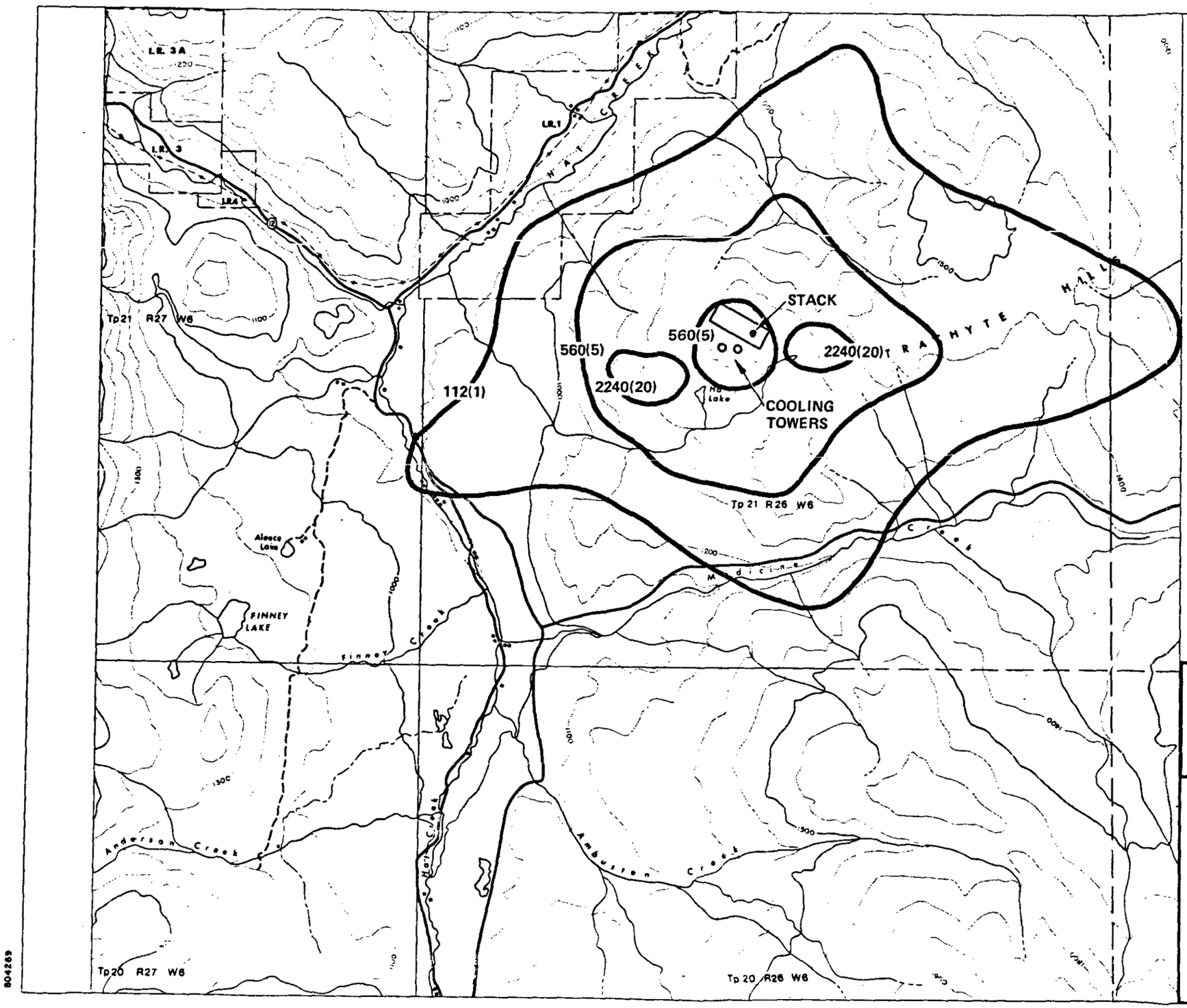

X=maximum=4700 kg/km^2/year
(42 lb/acre/year)

SCALE - 1:50,000
0 Kilometres 1 2 3
CONTOUR INTERVAL - 100 METRES

BRITISH COLUMBIA HYDRO AND POWER AUTHORITY
HAT CREEK PROJECT

DETAILED ENVIRONMENTAL STUDIES

Figure D4-3 Predicted Annual Salt Deposition in kg/km^2/year (lb/acre/year) Due to Drift from Proposed (Two) Natural Draft Cooling Towers

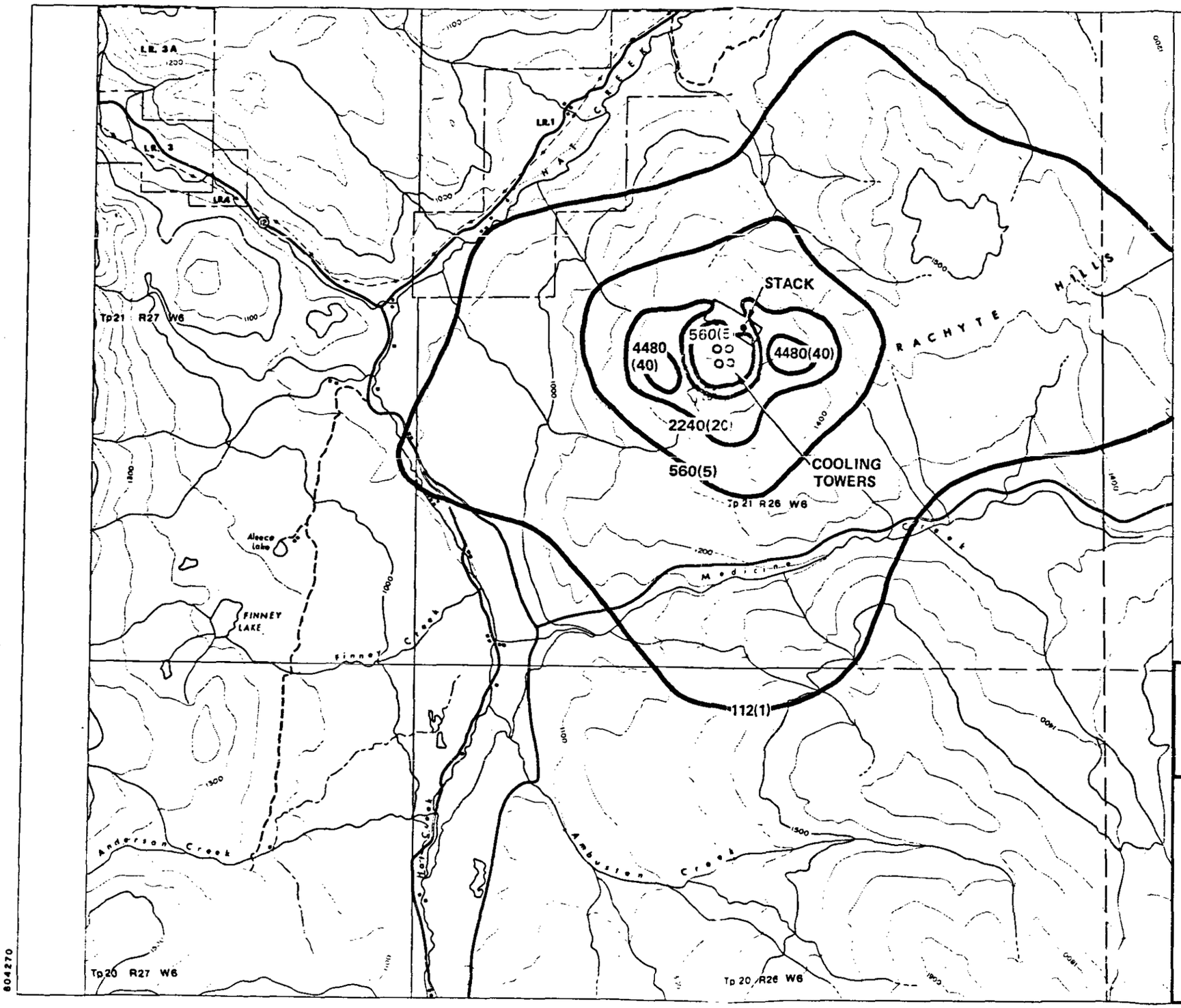

X=maximum=8736 kg/km^2/year
(78 lb/acre/year)

SCALE - 1:50,000

0 Kilometres 1 2 3

CONTOUR INTERVAL – 100 METRES

BRITISH COLUMBIA HYDRO AND POWER AUTHORITY
HAT CREEK PROJECT

DETAILED ENVIRONMENTAL STUDIES

Figure D4-4 Predicted Salt Deposition in kg/km^2/year (lb/acre/year) Due to Drift from Proposed (Four) Natural Draft Cooling Towers

804270

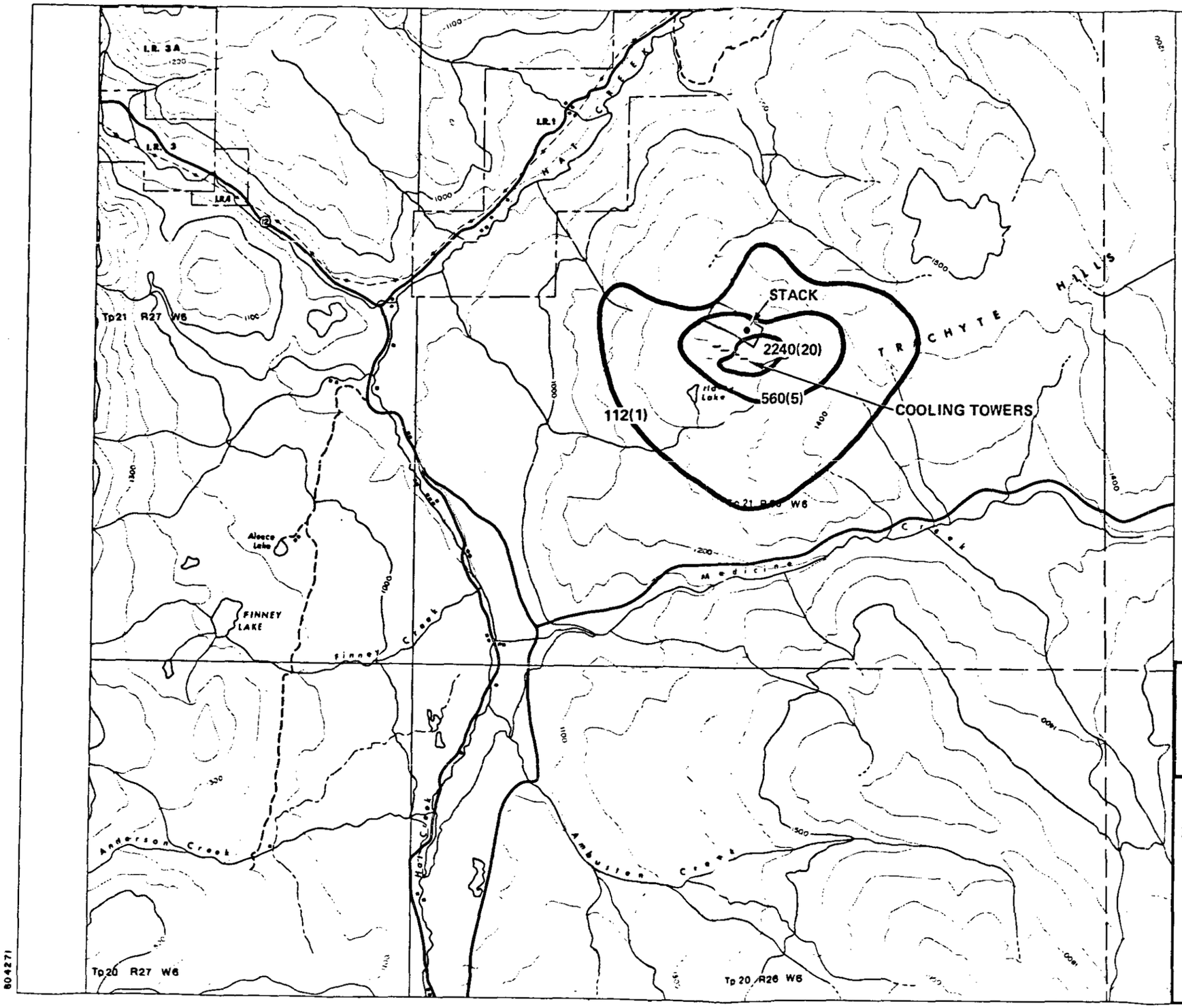

X=maximum=9632 kg/km^2/season
(86 lb/acre/season

SCALE - 1:50,000
0 Kilometres 1 2 3
CONTOUR INTERVAL - 100 METRES

BRITISH COLUMBIA HYDRO AND POWER AUTHORITY
HAT CREEK PROJECT

DETAILED ENVIRONMENTAL STUDIES

Figure D4-5 Predicted Seasonal (Summer) Salt Deposition in kg/km^2/season (lb/acre/season) Due to Drift from Proposed Rectangular Mechanical Draft Cooling Towers

804271

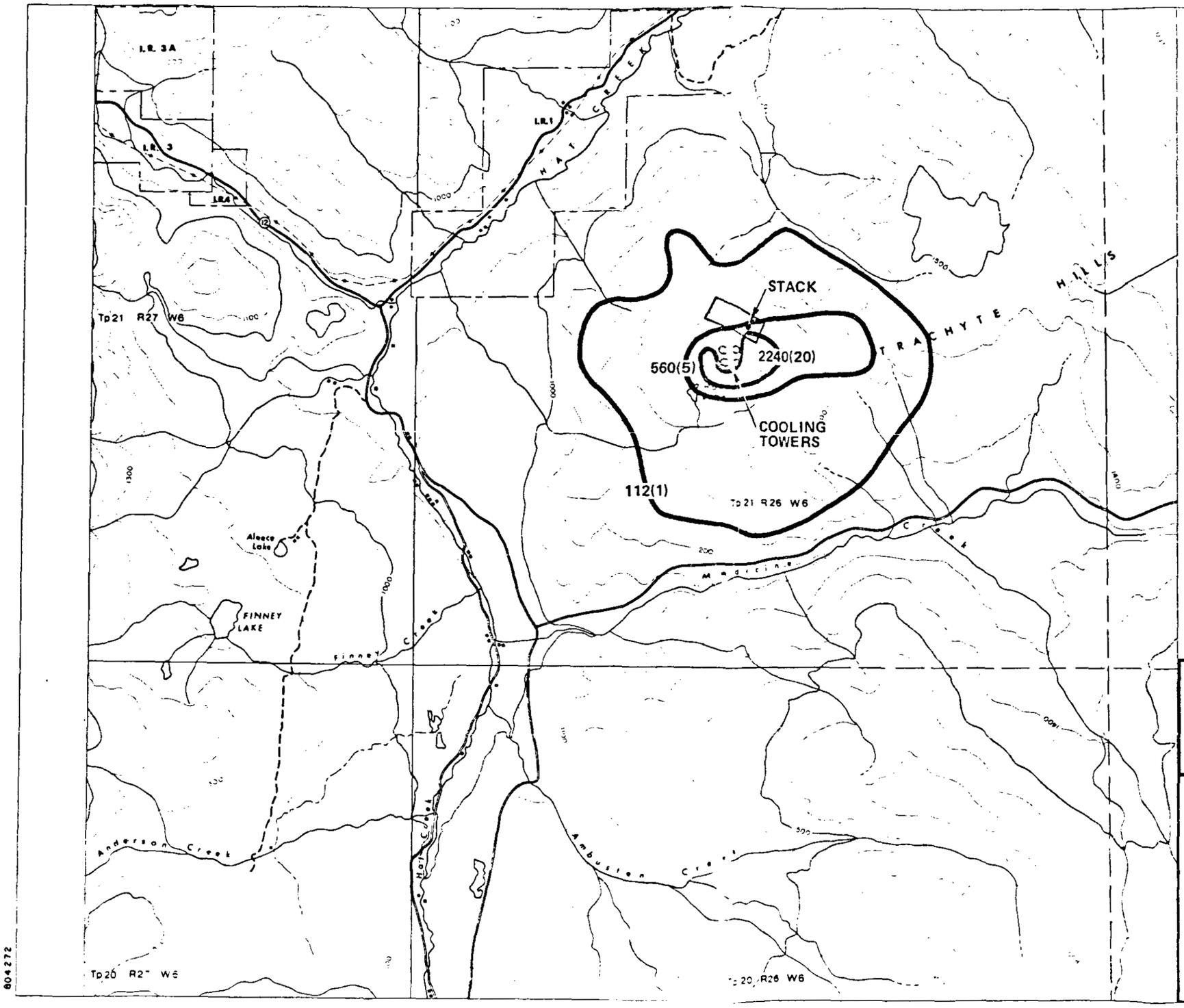

X=maximum=2280 kg/km^2/season
(190 lb/acre/season)

SCALE - 1:50,000

0 Kilometres 1 2 3

CONTOUR INTERVAL - 100 METRES

BRITISH COLUMBIA HYDRO AND POWER AUTHORITY
HAT CREEK PROJECT

DETAILED ENVIRONMENTAL STUDIES

Figure D4-6 Predicted Seasonal (Summer) Salt Deposition in kg/km^2/season (lb/acre/season) Due to Drift from Proposed Round Mechanical Draft Cooling Towers

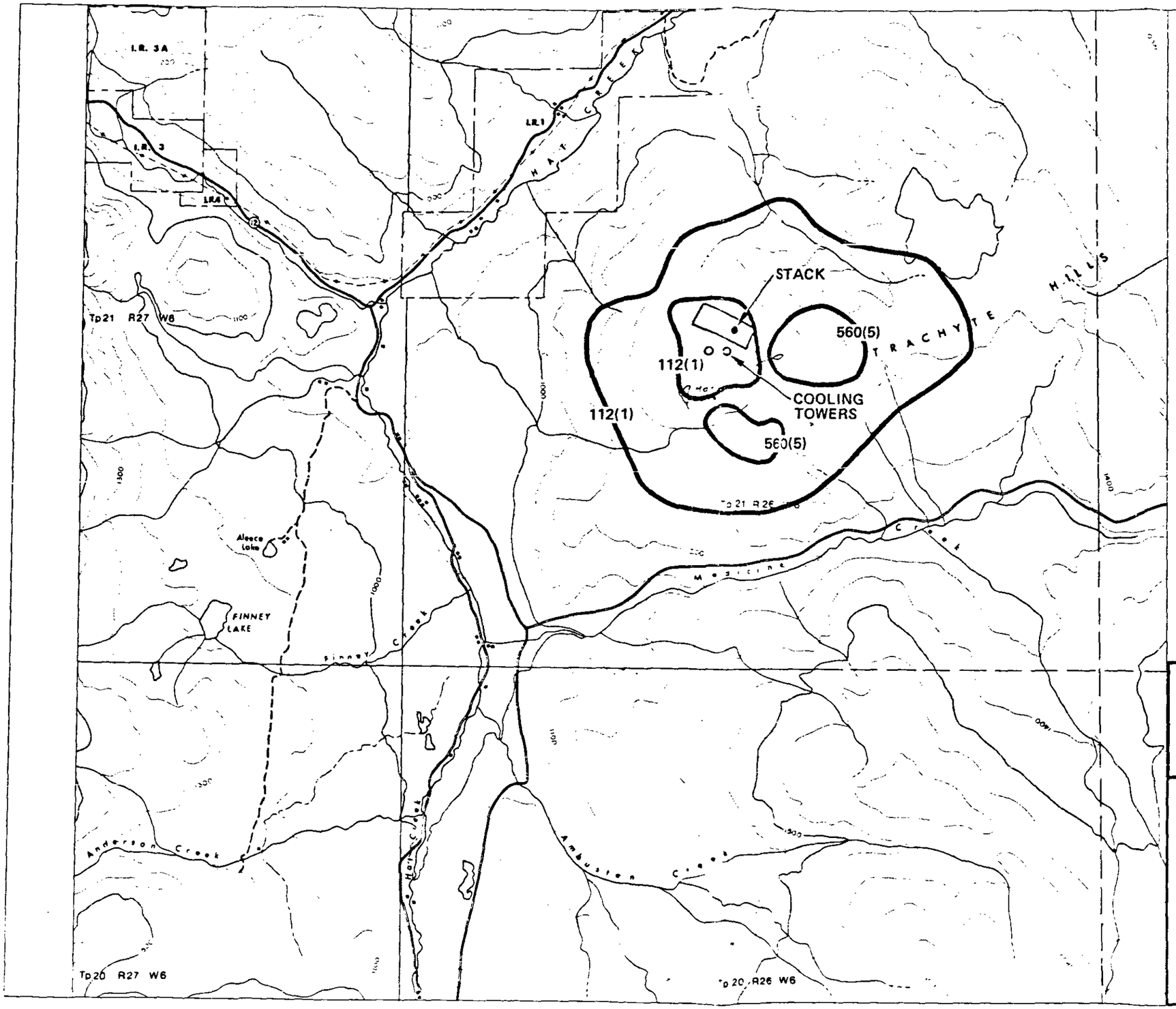

X=maximum=1792 kg/km^2/season
(16 lb/acre/season)

SCALE - 1:50,000
0 Kilometres 1 2 3
CONTOUR INTERVAL - 100 METRES

BRITISH COLUMBIA HYDRO AND POWER AUTHORITY
HAT CREEK PROJECT

DETAILED ENVIRONMENTAL STUDIES

Figure D4-7 Predicted Seasonal (Summer) Salt Deposition in kg/km^2/year (lb/acre/season) Due to Drift from Proposed (Two) Natural Draft Cooling Towers

804273

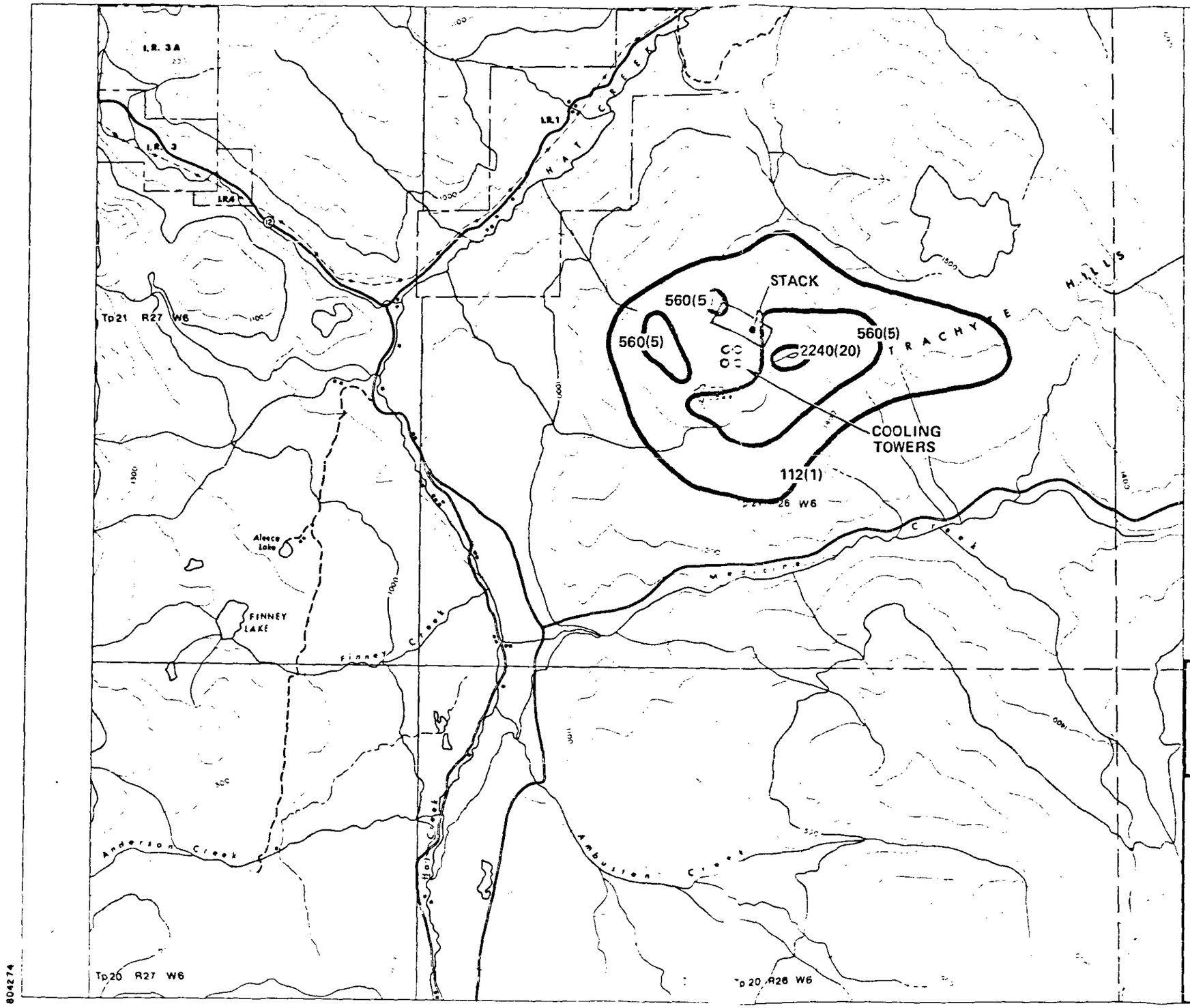

X=maximum=3248 kg/km^2/season
(29 lb/acre/season)

SCALE - 1:50,000

0 Kilometres 1 2 3

CONTOUR INTERVAL - 100 METRES

BRITISH COLUMBIA HYDRO AND POWER AUTHORITY
HAT CREEK PROJECT

DETAILED ENVIRONMENTAL STUDIES

Figure D4-8 Predicted Seasonal (Summer) Salt Deposition in kg/km^2/season (lb/acre/season) Due to Drift from Proposed (Four) Natural Draft Cooling Towers

804274

TABLE D4-1

MAXIMUM DRIFT DEPOSITION

Season	Location* (Distance (m)/Direction Relative to Towers)	Rate (kg/km^2/season)
	Rectangular Mechanical Draft Towers	
Winter	450/East	5391
Spring	225/East	3986
Summer	425/East	9660
Autumn	325/East-Northeast	4380
	Round Mechanical Draft Towers	
Winter	400/East	11,906
Spring	350/East	17,522
Summer	350/East	21,341
Autumn	400/East-Northeast	7,862
	Two Natural Draft Towers	
Winter	1,600/West-Northwest	2022
Spring	975/East	2134
Summer	1,000/East	1797
Autumn	1,100/North-Northeast	786
	Four Natural Draft Towers	
Winter	825/West-Southwest	3145
Spring	775/West-Southwest	3370
Summer	775/East	3257
Autumn	775/North-Northeast	1572

*Tabulated distances are measured from downwind edge of tower cluster.

D5.0 REFERENCES

1. Briggs, G. A. 1974. Diffusion Estimation for Small Emissions. NOAA, ATDL Contribution No. 79. Oak Ridge, Tennessee.

2. Hanna, S. R. 1974. Meteorological Effects of the Mechanical Draft Cooling Towers of the Oak Ridge Gaseous Diffusion Plant. NOAA, ATDL Contribution No. 89. Oak Ridge, Tennessee.

3. Moore, D. J. 1974. Recent Central Electricity Generating Board Research on Environmental Effects of Wet Cooling Towers. Cooling Tower Environment--1974. Available from National Technical Information Service as Document No. ER 1.11:CONF-740302. Springfield, Virginia.

ADDENDUM A

DESCRIPTION AND VALIDATION OF THE COOLING TOWER PLUME MODEL

ADDENDUM A

(A) 1.0 DESCRIPTION AND VALIDATION OF THE COOLING TOWER PLUME MODEL

ERT's numerical model for predicting the behavior of moist, buoyant plumes was employed in the investigation of atmospheric effects due to the proposed cooling towers. Input parameters to the model include physical dimensions and operating characteristics of the towers and selected ambient meteorological conditions. For a given weather situation the model computes plume centerline height, slope, radius, temperature and the mixing ratios of vapor and condensates within the plume at incremental downwind distances. To evaluate impacts over extended time periods, the model output is combined with appropriate meteorological statistics to estimate frequencies of fogging, icing, and visible plume lengths.

The theoretical basis for the COOLTOWR model is derived from techniques originally developed to predict the rise and growth of cumulus clouds. The computational scheme for depicting convective rise due to a small velocity perturbation in a quiescent atmosphere has been adapted for application to a buoyant effluent released at high velocity into a crosswind. A detailed discussion of the mathematical procedures used to simulate the complex thermodynamic and aerodynamic mechanisms governing plume behavior is presented in this Addendum.

(A)1.1 Plume Model Formulation

The mathematical equations describing the variation of the plume properties along the centerline of the plume are as follows:

Conservation of mass:

$$\frac{d}{d\ell} m_p = E \qquad \text{(A-1)}$$

Conservation of vertical momentum:

$$\frac{d}{d\ell}(m_p W_p) = \pi g b^2 (\rho_e - \rho_p) \tag{A-2}$$

Conservation of horizontal momentum:

$$\frac{d}{d\ell}(m_p U_p) = E U_e \tag{A-3}$$

Conservation of total water content:

$$\frac{d}{d\ell}(m_p r_p) = E r_e \tag{A-4}$$

Conservation of entropy:

$$\frac{d}{d\ell}(m_p s_p') = E s_e' \tag{A-5}$$

where

$$m_p = \pi b^2 V_p \rho_p \tag{A-6a}$$

is the mass flux of the plume, and

$$E = 2\pi\alpha b V_p \rho_e \tag{A-6b}$$

is the rate of entrainment of ambient air mass into the plume.

In the above,

ℓ = distance along the plume centerline from exit,

b = effective plume radius defined by

$$b^2 = 2\left[\int_o^\infty \tilde{b}\, V_p d\tilde{b}\right]^2 / \left[\int_o^\infty \tilde{b}\, V_p^2 d\tilde{b}\right]$$

where $\tilde{b}$ is the radial distance variable.

V_p = $(U_p^2 + W_p^2)^{1/2}$ = plume velocity tangential to centerline,

U_p = horizontal component of plume velocity,

W_p = vertical component of plume velocity,

ρ_p = plume density,

r_p = total plume water mixing-ratio,

s'_p = $(1 + r_p)s_p$, where s_p = plume specific entropy,

U_e = ambient wind speed,

ρ_e = ambient air density,

r_e = water vapor mixing-ratio of ambient air,

s'_e = $(1 + r_e)s_e$, where s_e = specific entropy of ambient air,

α = semi-empirical entrainment coefficient,

g = acceleration due to gravity (9.81 ms^{-2}).

Equation (A-1) states that the plume mass flux along its trajectory increases according to the rate at which ambient air is entrained into the plume. Equation (A-2) indicates that changes in the plume's vertical momentum are attributable solely to the buoyancy of the plume relative to the environment. Equation (A-3) results from equating the change in the horizontal momentum of the plume to the horizontal momentum added by the entrained ambient air. Equation (A-4) states that the total water flux of the plume along its trajectory increases according to the rate at which ambient water vapor is entrained into the plume. The effect of water droplet sedimentation ("rain-out") on the plume properties is neglected. It is assumed that the environment has no condensed water.

Simply stated, Equation (A-5) expresses the fact that thermal energy contained by the plume at any point of its trajectory is the sum of its

initial heat content and the thermal energy of the entrained ambient air. For a saturated plume with condensation of all excess vapor, the specific entropy s_p can be written as

$$s_p = s_p'/(1 + r_p) \tag{A-7}$$

where

$$r_p = r_{vs} + r_c \tag{A-8}$$

$$s_p' = s_d + r_{vs}s_{vs} + r_c s_c \tag{A-9}$$

In the above, r is the water mixing-ratio and s is the specific entropy, and the subscripts d, vs, and c denote, respectively, the dry air, saturated vapor and the condensate. For the saturated plume, the liquid-solid phase changes of the condensate are defined by the plume temperature $T(^\circ K)$ as follows:

$$\text{For } 258.16 \leq T < T_d \qquad r_c = r_\ell, \quad r_i = 0 \tag{A-10}$$

$$\text{For } 233.16 \leq T < 258.16, \qquad r_c = r_\ell + r_i \tag{A-11}$$

$$\text{For } T < 233.16, \qquad r_c = r_i, \quad r_\ell = 0 \tag{A-12}$$

Here T_d is the dew-point temperature of the plume, and the subscripts ℓ and i indicate the liquid and ice phases of the condensate. In Equation (A-11) the liquid and ice mixing ratios can be calculated as

$$r_i = \frac{(258.16 - T)}{(258.16 - 233.16)} r_c \tag{A-11a}$$

$$r_\ell = r_c - r_i \tag{A-11b}$$

Treating dry air as an ideal gas, the specific entropy s_d is defined from the first law of thermodynamics by the differential relationship:

$$ds_d = C_p d\ (\ell n\ T) - R_d d(\ell n\ P) \qquad \text{(A-13)}$$

Here, P is the pressure in the plume, R_d is the gas constant for dry air (287.04 $m^2 s^{-2}\ ^oK^{-1}$), and C_p is the specific heat at constant pressure for dry air (1004 $m^2 s^{-2}\ ^oK^{-1}$). This equation is valid for all processes, both reversible and irreversible, and it applies to the substance comprising a closed system as well as the substance undergoing a change of state as a result of flow across the boundary of an open system (see, e.g., Van Wylen[1]). Integrating Equation (A-13), for a saturated plume, we obtain

$$s_d = C_p \ell n \frac{T}{T_3} - R_d \ell n\left(\frac{P - e_s}{P_3}\right) \qquad \text{(A-14)}$$

where e_s is the saturation vapor pressure in the plume. The subscript 3 refers to the conditions of the triple point where the vapor, liquid, and solid phases coexist in equilibrium:

$$T_3 = 273.16°K$$

$$P_3 = 100 \text{ centibars (cb)}$$

$$e_3 = 0.611 \text{ centibars (cb)}$$

The specific entropy (s_{vs}) for the saturated plume vapor is given by

$$s_{vs} = s_{i3} + \frac{L_{s3}}{T_3} + C_{pv}\ \ell n \frac{T}{T_3} - R_v\ \ell n \frac{e_s}{e_3} \qquad \text{(A-15)}$$

where R_v is the gas constant for water vapor (461.5 $m^2 s^{-2}\ ^oK^{-1}$), C_{pv} is the specific heat at constant pressure for water vapor (1876.5 $m^2 s^{-2}\ ^oK^{-1}$), L_{s3} is the latent heat of sublimation at triple point (2.835 x 10^6 $m^2 s^{-2}$), and s_{i3} is an arbitrary constant.

The specific entropies of the liquid and ice phases, respectively, of the condensed vapor are given by

$$s_\ell = s_{i3} + \frac{L_f}{T_3} + C_\ell\ \ell n \frac{T}{T_3} \qquad \text{(A-16)}$$

$$s_i = s_{i3} + C_i \ln \frac{T}{T_3} \tag{A-17}$$

where C_ℓ is the specific heat of liquid (4187 $m^2 s^{-2} {}^\circ K^{-1}$) and C_i is the specific heat of ice (2000 $m^2 s^{-1} {}^\circ K^{-1}$), and L_f is the latent heat of fusion (0.334×10^6 $m^2 s^{-2}$).

In the present model, no distinction is made between the specific entropies of the liquid and the ice, and the specific entropy of the entire condensate is assumed to be that of the liquid, i.e., $s_c = s_\ell$. This approximation, while simplifying the analysis, does not introduce a significant error since, generally, the ice content is only a small fraction of the total condensate. The error may be significant for plume temperatures below -27.5°C; however, such low plume temperatures plume are not frequently expected.

The saturated vapor mixing ratio is defined by

$$r_{vs} = \frac{R_d}{R_v} \frac{e_s}{p - e_s} \tag{A-18}$$

where

$$e_s = e_3 \left(\frac{T_3}{T}\right)^{a'} \exp\left[(a' + b')\left(1 - \frac{T_3}{T}\right)\right] \tag{A-19}$$

$$a' = \frac{C_\ell - C_{pv}}{R_v} \tag{A-20}$$

$$b' = \frac{L_{s3} - L_f}{R_v T_3} = \frac{L_{v3}}{T_3} \tag{A-21}$$

Here, L_{v3} is the latent heat of vaporization (2.501×10^6 $m^2 s^{-2}$). Substituting the relations given above for r_c, s_d, s_{vs}, and s_c in Equation (A-9), and utilizing Equations (A-19) to (A-21), the relation for s'_p of the saturated plume as a function of r_p, T and p is obtained as:

$$s_p' = C_p \ln \frac{T}{T_3} - R_d \ln \frac{p - e_s}{p_3} + R_v r_{vs}\left[(a' + b')\frac{T_3}{T} - a'\right)]$$

$$+ r_p \left[s_{i3} + \frac{L_f}{T_3} + C_\ell \ln \frac{T}{T_3}\right] \qquad \text{(A-22)}$$

For an unsaturated vapor plume ($0 < e < e_s$), this expression reduces to

$$s_p' = C_p \ln \frac{T}{T_3} - R_d \ln \frac{p - e}{p_3} + r_v\left(C_{pv} \ln \frac{T}{T_3} - r_v \ln \frac{e}{e_3}\right) \qquad \text{(A-23)}$$

In the above, the pressure p in the plume, assumed to be not significantly different from that in the environment, is a known function of z. If s_p' and r_p have been computed for a certain height, Equations (A-18) to (A-22) can be solved by a successive approximation technique, such as the Newton-Raphson method (see, e.g., McCracken and Dorn[2]) to determine T at that height. The plume density is then calculated as follows:

$$\rho_p = \frac{(1 + r_p)(p - e_s)}{R_d T} \qquad \text{(A-24)}$$

We can then compute $r_c = r_p - r_{vs}$. If r_c is negative, the plume is unsaturated; T must then be recomputed by replacing Equation (A-22) with Equation (A-23) for an unsaturated plume.

The ambient wind, temperature and water vapor mixing ratio distributions, $U_e(z)$, $T_e(z)$ and $r_e(z)$ respectively, are specified at a discrete number of vertical levels as inputs to the computer program. Assuming that the ambient air has no condensed water, the ambient air density $\rho_e(z)$ is calculated as

$$\rho_e = \frac{(1 + r_e)\, p}{(R_d + R_v r_e)\, T_e} \qquad \text{(A-25)}$$

If the ambient specific humidity profile $q_e(z)$ is known, the ambient water mixing ratio can be calculated as

$$r_e = \frac{q_e}{1 - q_e} \tag{A-26}$$

Alternately, if the ambient relative humidity profile $\phi_e(z)$ is known, then,

$$r_e = \frac{\phi \quad q_{es}}{1 - \phi \quad q_{es}} \tag{A-27a}$$

where

$$q_{es} = \frac{0.622\ e_{es}}{p - 0.378\ e_{es}} \tag{A-27b}$$

$$e_{es} = 6.1078\ \exp\left(\frac{cT_e}{d + T_e}\right) \tag{A-27c}$$

In the above, for $T_e < 0°C$, $c = 21.8746$, $d = 265.49$, and for

$T_e > 0°C$, $c = 17.2694$, $d = 237.29$.

The trajectory of the plume is calculated by stepwise integration of Equations (A-1) to (A-5), starting from the plume origin at the top of the cooling tower. The known tower-exit plume properties determine the initial values of the differentiated quantities on the left hand side of the equations. The plume properties at any ℓ are determined as prognostic variables by integrating the equations through each vertical layer using a fourth-order Runge-Kutta method (see, e.g., Hildebrand).[3]

The trajectory distance increments $\Delta\ell$ are calculated for each integration step by finite-difference techniques, i.e., $\Delta\ell = (\Delta x^2 + \Delta z^2)^{1/2}$, where Δx and Δz respectively are the horizontal and vertical distance

increments. These incremental distances are determined for each integration step by the relationship:

$$\Delta x = \frac{U_p}{W_p} \cdot \Delta z \qquad \text{(A-28)}$$

For a symmetric plume, the entrainment rate (E) of ambient air, defined in Equation (A-6b), is characterized by the so-called entrainment velocity (αV_p). For a bent plume, the latter is defined by an expression similar to that given by Briggs.[4]

$$\alpha V_p = \frac{W_p}{V_p} (\beta^2 W_p^2 + \gamma^2 U_p^2)^{1/2} \qquad \text{(A-29a)}$$

The coefficients β and γ are empirically chosen, and characterize, respectively, the mixing rates associated with purely vertical plume motion and bent-over (essentially horizontal) plume. It is assumed that during the bending-over stage, the two corresponding velocities may be added vectorially. Rewriting Equation (A-29a) in terms of incremental distances,

$$\alpha = \frac{\Delta z}{\Delta \ell} \left[\frac{(\beta^2 \Delta z^2 + \gamma^2 \Delta x^2)}{\Delta \ell^2} \right]^{1/2} \qquad \text{(A-29b)}$$

Near the tower exit, where the plume is essentially vertical, this equation gives $\alpha \simeq \beta$ since $\frac{\Delta z}{\Delta \ell} \simeq 1$ and $\frac{\Delta x}{\Delta \ell} \simeq 0$. In the far field, as the plume becomes nearly horizontal, $\frac{\Delta x}{\Delta \ell} \simeq 1$ $\frac{\Delta z}{\Delta \ell} << 1$ and $\alpha \simeq \gamma \frac{dz}{dx}$ These latter expressions together with Equations (A-1), (A-6b), and the assumption that $\rho_p \simeq \rho_e$, yield the far-field relation given by Briggs.[4]

$$db = \gamma \, dz \qquad \text{(A-30)}$$

In this bent-over stage and far from the source, the plume will approach the "two-thirds law" downwind distance dependence of Briggs' buoyant plume equation.

Since very little field data exist on the far-field behavior of the plumes, we have invoked a method after Briggs[4] to define the plume trajectory and final rise far downwind under neutral stability conditions. Briggs' relation is based on observations of elevated conventional plumes and states that a characteristic downwind distance, x^*, where the entrainment rate from ambient atmospheric turbulence is of the same strength as the plume rise induced entrainment, may be estimated from the equation:

$$x^* = 34\ F_o^{0.4} \qquad \text{(A-31)}$$

where F_o is the initial buoyancy flux of the plume.

This equation should only be applied to buoyant plumes with values of F_o in excess of 55 m^4/s^3. This value of x^* implicitly assumes that the far-field entrainment coefficient is 0.6. Again, without data to the contrary, the best approximation on the value of α is obtained by assuming that the tower plumes in the far-field would have entrainment rates similar to those of conventional plumes. Final rise is estimated by Briggs by assuming a 0.6 entrainment coefficient up to a downwind distance of $3.5x^*$.

To simulate far-field plume behavior, the model operates as follows. For $x < x^*$, the entrainment coefficients, β and γ, adopted in this study have a value of 0.8. For $x^* < x < 3.5x^*$, a "bent over" entrainment coefficient of $\beta = \gamma = 0.6$ is used. At $x = 3.5x^*$, where the plume stops rising, the dispersion process is assumed to be governed completely by ambient turbulence.

The Pasquill-Turner formulation for horizontal and vertical plume growth is generally accepted for applications to the diffusion processes dominated by atmospheric turbulence. For $x > 3.5x^*$, the plume rise model has been coupled to the Pasquill-Turner formulation for predicting ground-level

pollutant concentrations. When the maximum plume rise has been achieved, the 'top-hat' plume profile generated by the numerical model is matched to fit vertical and cross-wind top-hat profiles which retain both the centerline concentration and the total cross-sectional mass flux of the original distribution. Top-hat plume widths are calculated by multiplying Gaussian plume standard deviations by a factor of 1.414. Functional forms of the horizontal and vertical standard deviations of plume distribution were derived on the basis of field studies performed at the Hat Creek site. These expressions provide estimates of σ_y and σ_z as functions of downwind distance and stability. Appropriate virtual source distances corresponding to the computed values of σ_y and σ_z are thus identified. The rates of horizontal and vertical plume growth are treated as guassian beyond the distance where plume trajectory levels off.

(A)1.2 Visible Plume Length Calculation

Figure (A)-1 shows a schematic representation of the determination of the maximum visible plume length using the psychrometric diagram. The solid line AEBD gives the variation of specific humidity of saturated air over a range of temperatures. Point A represents the initial plume conditions (T_{po}, q_{po}) at tower exit. Point C represents the average ambient air conditions (T_e, q_e). As the vapor plume rises from the tower and moves downwind, it entrains ambient air. The latter is mixed rapidly into the expanding plume by the intense convective turbulence generated due to the heat released during the condensation of vapor within the plume. At some distance downwind, the plume becomes so well mixed with the entrained ambient air that its excess temperature and moisture content over the ambient approach zero, i.e., $\Delta T = T_p - T_e = 0$ and $\Delta q = q_p - q_e = 0$. This obviously occurs at Point C. Empirical data suggest that the plume conditions approach the ambient conditions following a linear path (line AC) on the psychrometric chart. In the region where the line AC is above the curve AEBD, the vapor content of the plume is greater than saturation, and condensation of this excess vapor takes place, thus creating a visible plume. The maximum visible plume length

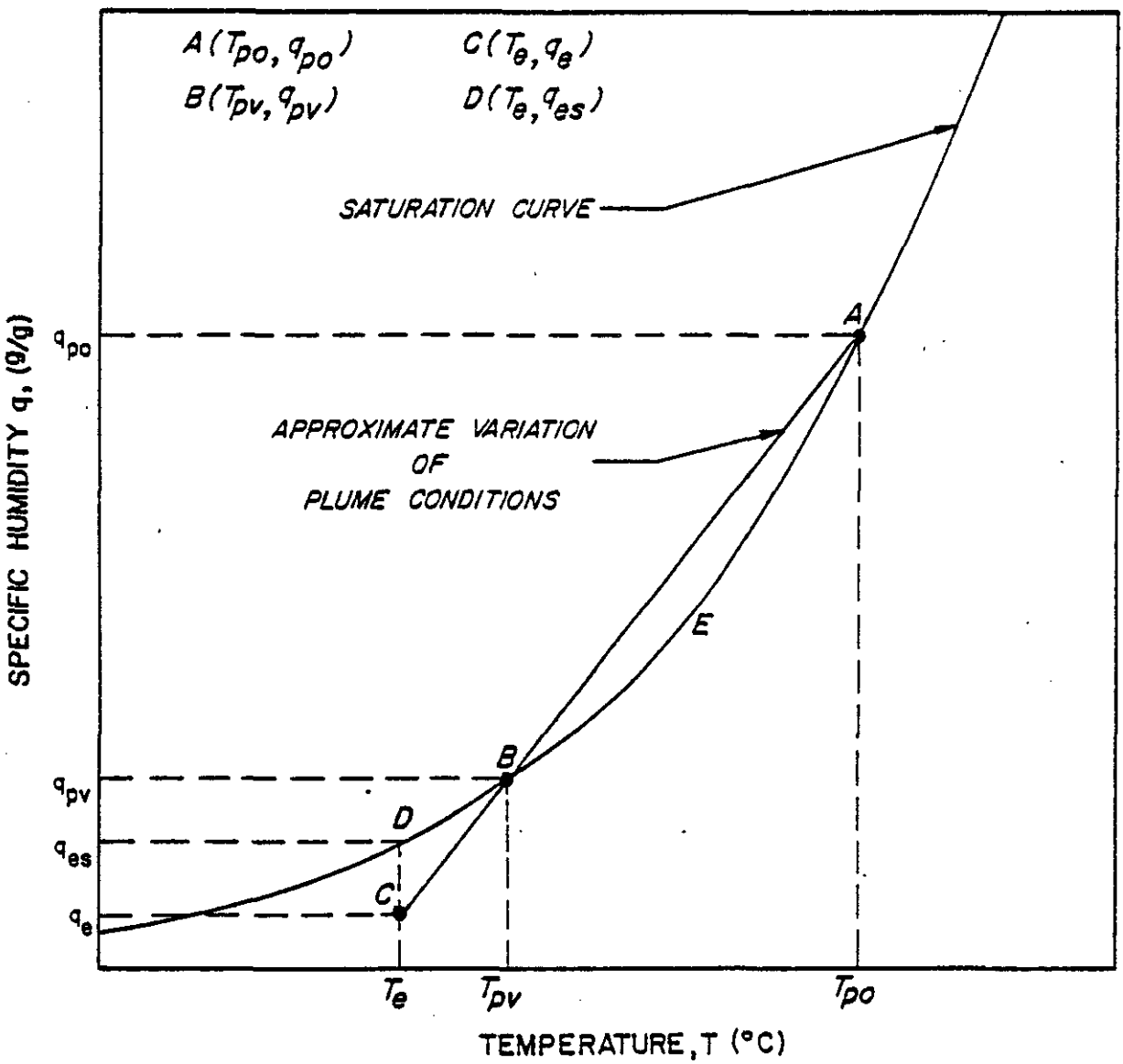

Figure (A)-1 Schematic Representation of the Determination of the Maximum Visible Plume Length on the Psychrometric Diagram

is calculated as the downwind distance at which the conditions (T_{pv}, q_{pv}) corresponding to Point B occur.

In practice the plume remains visible (due to the scattering of light) only so long as it contains droplets of condensed water of sufficient size and number to make the plume substantially opaque. Otherwise, the plume may not be visible even though it contains small amounts of the condensate. In the present model, based on the relation between horizontal visibility and the liquid water content of natural fogs given by Houghton and Radford[5], it is assumed that the plume is effectively invisible if the condensate mixing ratio ($r_c = r_\ell + r_i$) falls below 0.00001. The maximum visible plume length (x_{mvp}) is calculated directly from the model as the horizontal distance at which $r_c = 0.00001$.

(A)1.3 Calibration of Plume Rise Model

Slawson et al.[6] observed time-mean trajectories of plumes from the three natural draft cooling towers at the Tennessee Valley Authority's Paradise Steam Plant. Meyer et al.[7] presented extensive data, collected over the fall and winter of 1973-74, of the visible plume from rectangular mechanical draft cooling towers of the Potomac Electric Power Company's Benning Road generating station in Washington, D.C., where 16 tower cells serve fossil-fuel units with a total of 560 Mw capacity. These well-planned and documented observations have been used to tune ERT's existing buoyant, bent-over moist plume rise model for multiple-cell rectangular mechanical draft cooling towers. The observations of Slawson et al.[6] on natural draft cooling towers at the Paradise Steam Plant were utilized for the calibration and validation of the ERT cooling tower plume model. These observations, used as inputs to the ERT plume-rise model, are given in Table (A)-1. The ambient meteorological data shown in the table were averaged over the height of plume rise above tower top. The detailed ambient profiles, required as inputs to the model, were generated by extrapolation through these averaged quantities assuming a lapse rate, a wind shear, and a dew-point distribution appropriate to a slightly stable environment.

TABLE (A)-1

TVA PARADISE STEAM PLANT NATURAL DRAFT TOWER PLUME DATA
(Slawson, et al.)[6]

OBSERVATION	NOTATION	UNITS	(a) WINTER	(b) SUMMER
Date			02/10/71	09/07/72
Time			0653-0750	0815-0942
Plume exit velocity	V_{po}	m/s	2.5	3.6
Plume exit virtual temperature	T_{pov}	K	303.2	310.7
Plume exit specific humidity	q_{po}	g/kg	21.2	30.9
Average ambient temperature	T_e	K	262.8	292.0
Average ambient specific humidity	q_e	g/kg	0.87	12.6
Average ambient wind speed	U_e	m/s	11.6	8.0
Ambient pressure at tower height	P_o	mb	1,012.6	966.8
Maximum visible plume length	x_{max}	m	532-866	200
Buoyancy length = F_o/U_e^3	ℓ_b	m	2.3	3.7

Tower height = 132.8m

Tower exit diameter = 61.8m

The entrainment coefficients β and γ are determined by comparing the simulated and the observed plume behaviors. For the bent-over plumes, β is assumed to be equal to γ. According to Slawson et al.[6], the γ value is 0.67 for the winter and 1.23 for the summer. The plume rise and growth calculated by using these values for β and γ are shown in Figures (A)-2 and (A)-3, where they are also compared with the field observations. The predicted plume centerlines in both cases show good agreement with the observations. The predicted visible plume lengths also agree well with the observations. The predicted plume growth is slightly larger than the observed, especially in summer. This should not be surprising in view of the large entrainment of ambient air indicated by $\gamma = 1.23$. However, it is reassuring that the predictions of the lower edge of the plume are on the conservative side, since this determines whether and where the plume intercepts the ground, and the resulting ground-level fogging and icing.

The ERT plume rise model used $\beta = \gamma = 0.8$ for $x < x^*$. The corresponding predictions for the winter and summer cases are shown in Figures (A)-4 and (A)-5, respectively, where they are compared with the observations. The plume centerline predictions are not significantly different from the observed ones. The visible plume lengths also agree well with the observations. The plume growth predictions indicate that the predicted frequencies of occurrence of ground-level fogging and icing will be on the conservative side.

(A)1.4 The Multiple-Tower Option in COOLTOWR

The behavior of combined plumes from a row of identical cooling towers is simulated by a sub-model of the COOLTOWR program. Geometrical criteria are employed to determine points of intersection of individual

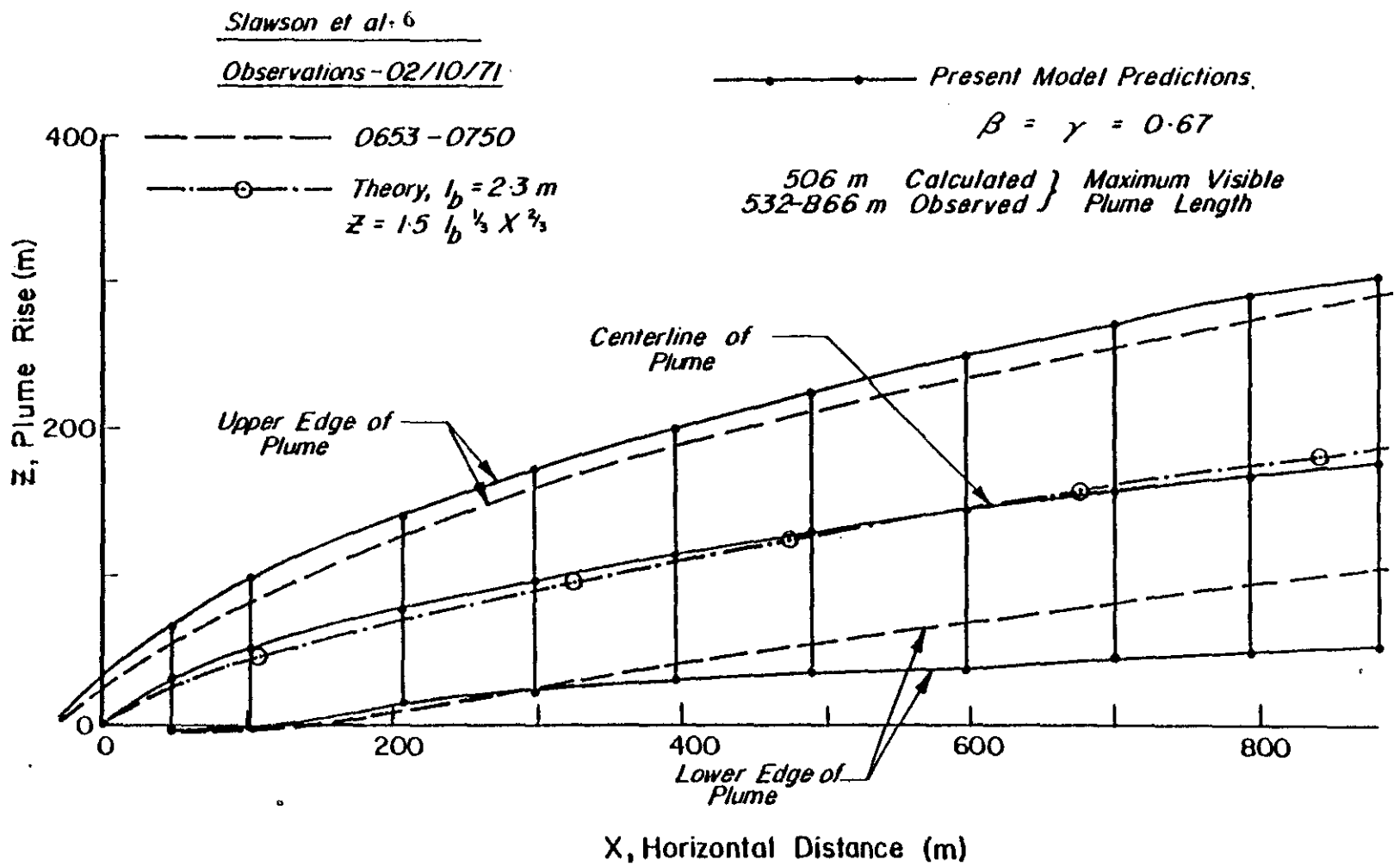

Figure (A)-2 Calculated Plume Rise and Growth (Case 1)

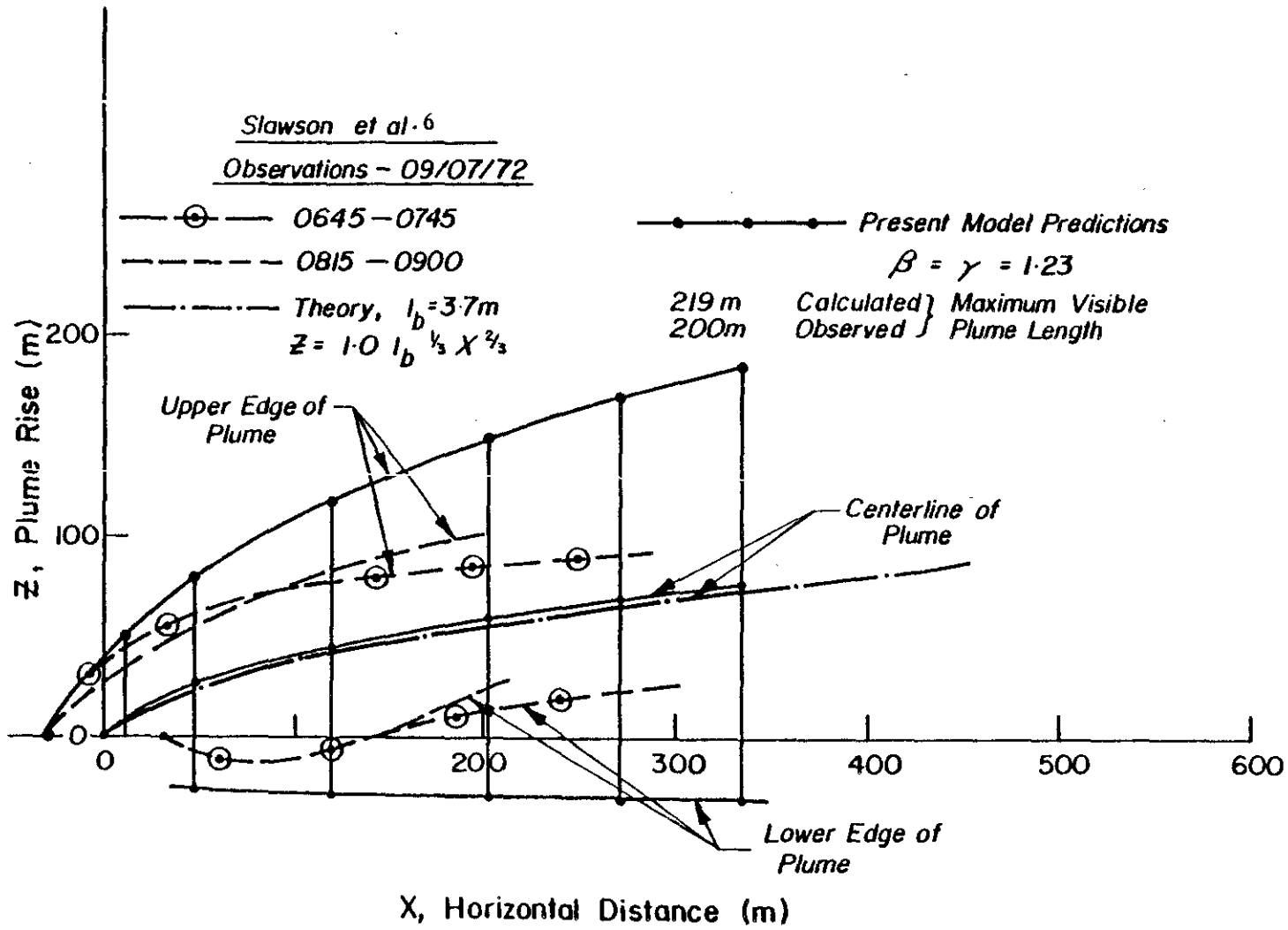

Figure (A)-3 Calculated Plume Rise and Growth (Case 2)

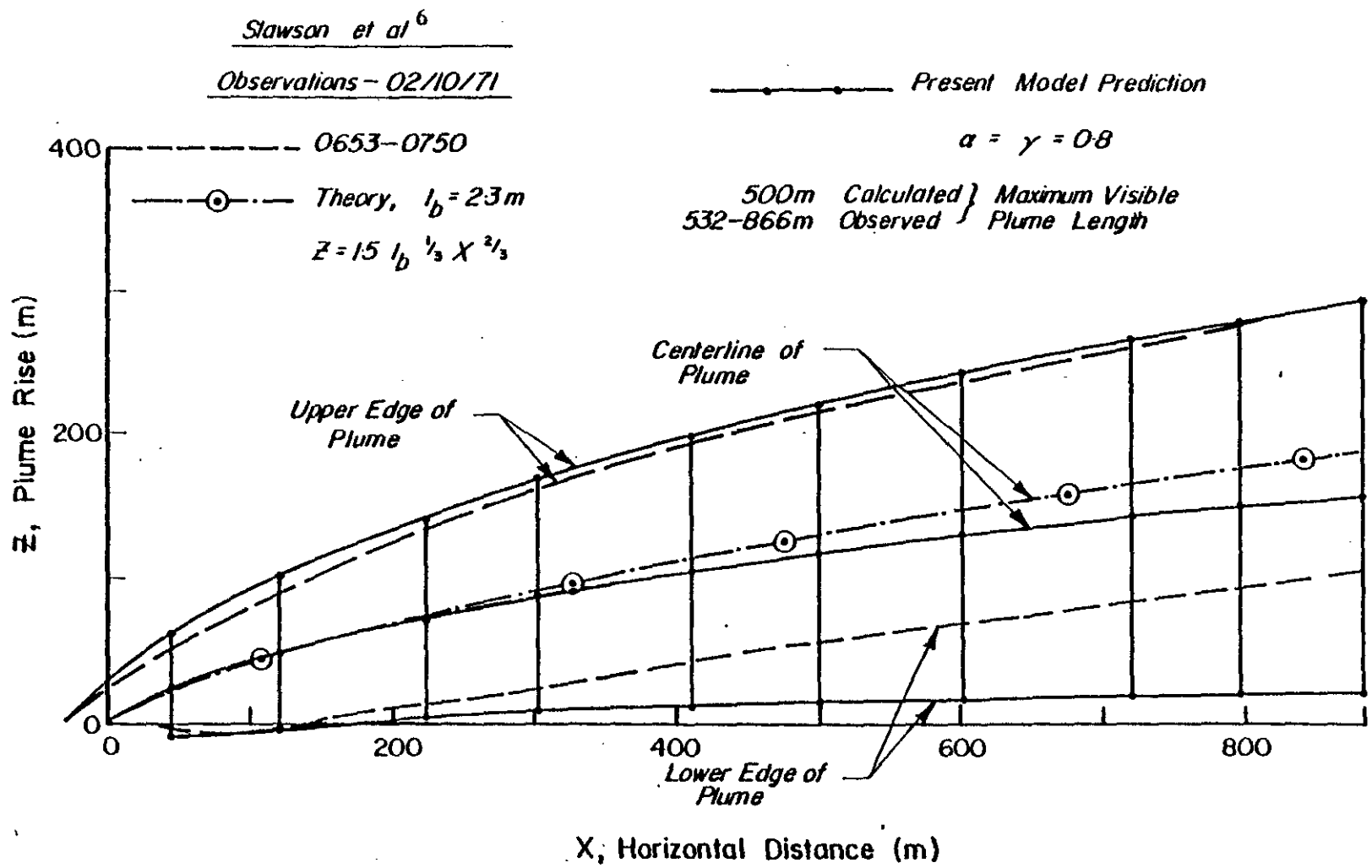

Figure (A)-4 Calculated Plume Rise and Growth (Case 3)

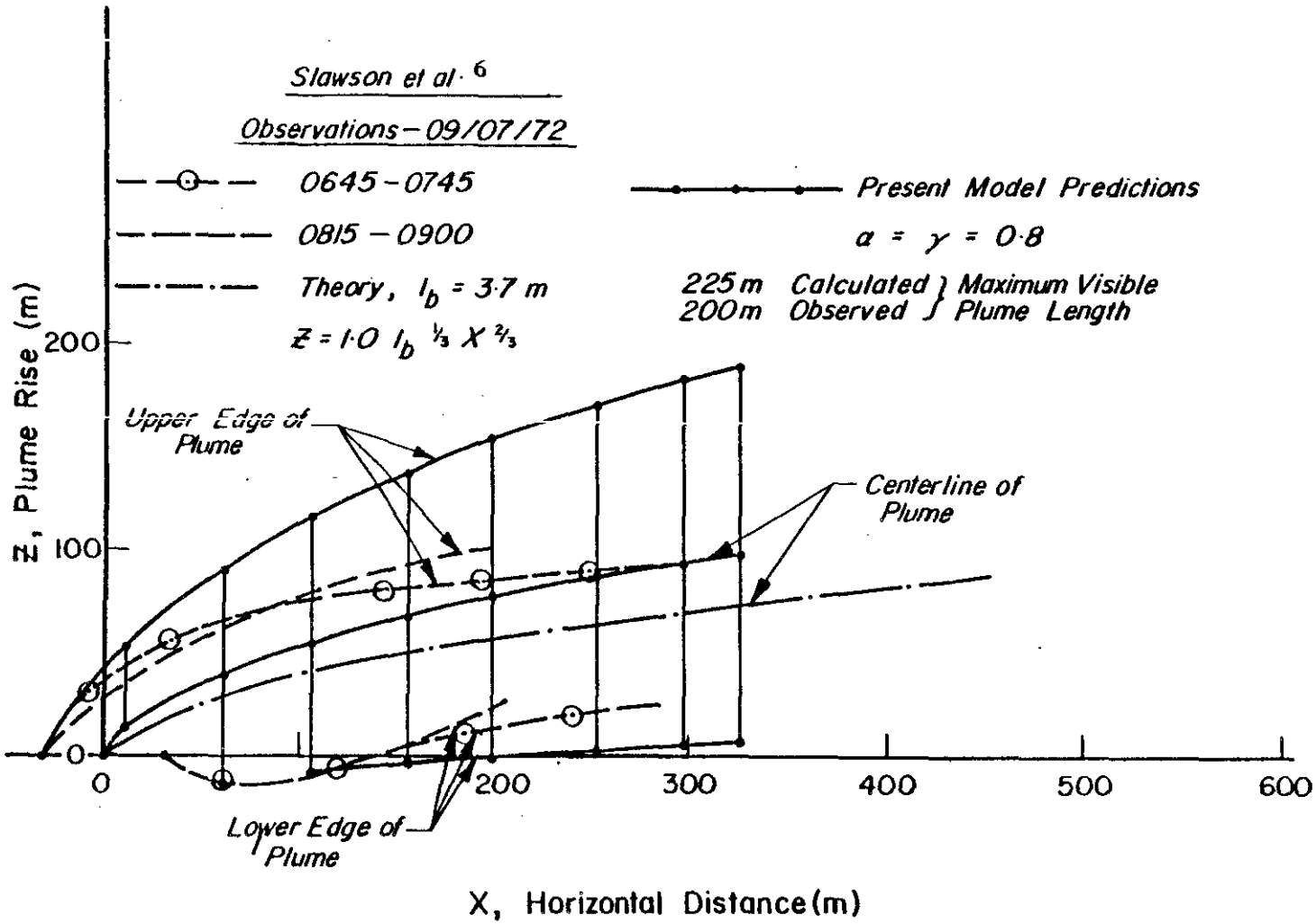

Figure (A)-5 Calculated Plume Rise and Growth (Case 4)

plumes. Then, physically realistic assumptions are used to describe alterations in plume properties (e.g., fluxes of its mass, total moisture, and momentum) resulting from the merging process.

Figure (A)-6 depicts in plan and elevation the multiple-plume geometry used in COOLTOWR. For simplicity, only two towers are shown here. The horizontal distance coordinate (X) is always measured from the tower furthest upwind. If ϕ is the angle ($\leq 90°$) of the wind relative to the line of towers and d is their center-to-center spacing, then the downwind distance coordinate measured from the second tower is $X - d\cos\phi$. In the figure, the plumes begin to overlap in the horizontal at a downwind distance $X = X_{1c}$ defined by:

$$b(X_{1c}) + b(X') = d\sin\phi \qquad \text{(A-32)}$$

where r is plume radius.

At any point in its rising phase, the half-depth of a plume is closely approximated by $b\sec\theta$, where θ is the arctangent of the centerline slope (the radius b is always normal to the trajectory). The bottom edge of the first plume must intersect the top of the second in order for merging to occur. If this condition is not satisfied at downwind distance X_{1c}, then the distance where plume interaction takes place is X_{2c}, defined by

$$Z(X_{2c}) - b(X_{2c})^* \sec\theta(X_{2c}) = \qquad \text{(A-33)}$$

$$Z(X') + b(X')^* \sec\theta(X').$$

where Z is centerline height above the ground.

At the point of merging, ($X_c = X_{1c}$ or X_{2c}), the properties of the two plumes are combined in the model as shown below. Properties of the combined plumes are indicated by asterisk superscripts, and X' always signifies $X_c - d\cos\phi$.

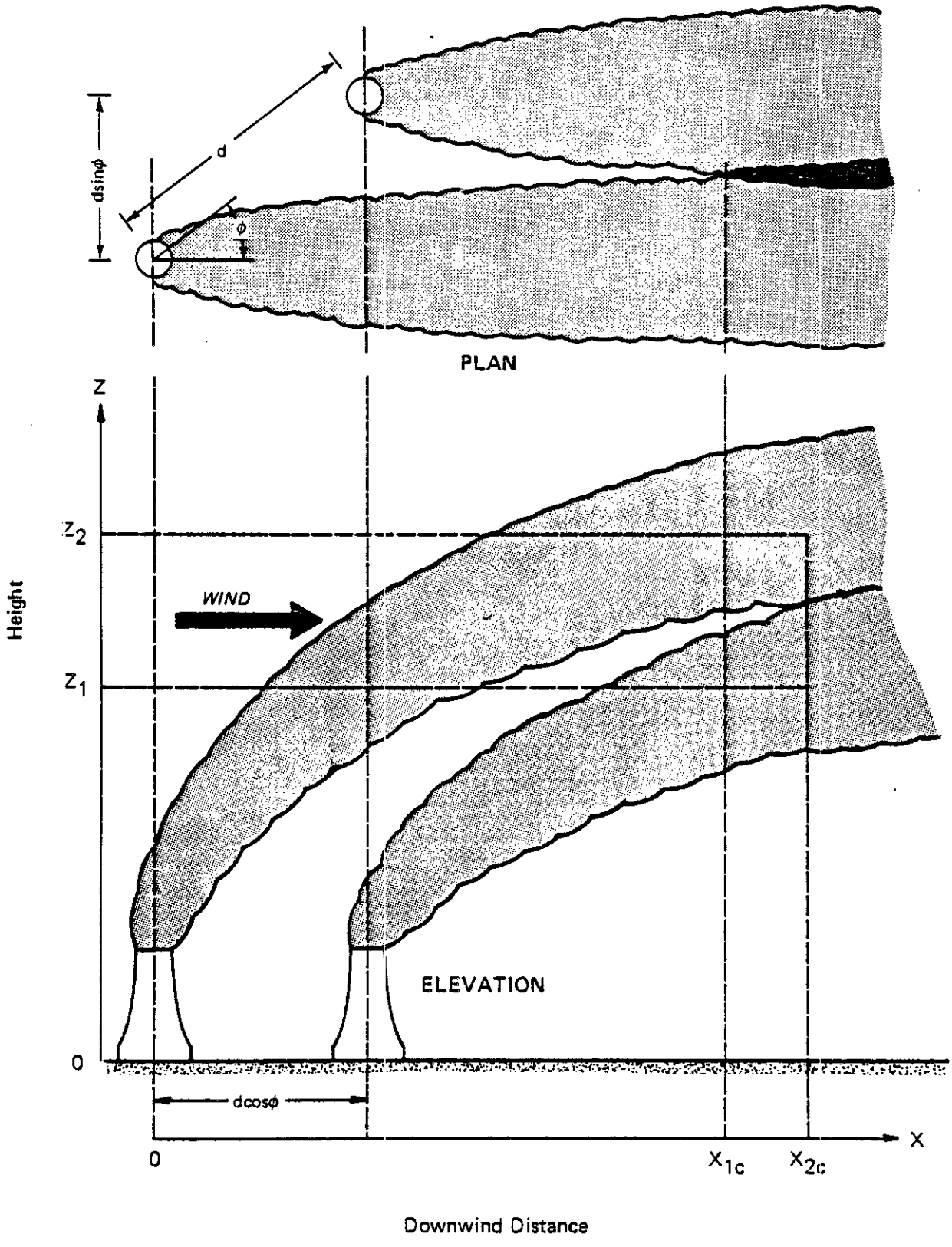

Figure (A)-6 Multiple-Tower Plume Merging Geometry for COOLTOWR Model

$$\text{radius } b^* = [b^2(X_c) + b^2(X')]^{1/2}$$

$$\text{mass flux: } m_p^* = m_p(X_c) + m_p(X') \qquad \text{(A-34)}$$

$$\text{vertical momentum flux: } [m_p w_p]^* = [m_p w_p(X_c)] + (m_p w_p(X')]$$

$$\text{horizontal momentum flux: } [m_p u_p]^* = [m_p u_p(X_c)] + [m_p u_p(X')]$$

$$\text{total moisture flux: } [m_p r_p]^* = [m_p r_p(X_c)] + [m_p r_p(X')]$$

$$\text{total entropy flux: } [m_p s_p']^* = [m_p s_p'(X_c)] + (m_p s_p'(X')]$$

The merging scheme is generalized to allow simulation of plume behavior from a row of any number of cooling towers.

(A)1.5 Entrainment During Initial Plume Rise for Multiple-Cell Towers

For round mechanical draft tower applications, the COOLTOWR model incorporates a physically realistic algorithm for dealing with the variation of the plume entrainment rate during the transition from multiple to single plume behavior. Initially, the small plumes from the individual cells rise and grow separately, until at some point they have coalesced sufficiently to be regarded thereafter as a single coherent plume. The principal advantage of the round mechanical draft design over conventional rectangular towers is that the clustered-cell geometry of the former favors more rapid merging, an effect that is independent of wind direction. The aggregate plume thus retains much of the combined buoyancy of the individual plumes. Average plume rise, therefore, is significantly enhanced in comparison with that expected from rectangular towers with equivalent heat dissipation requirements.

Individual plumes initially experience rapid mixing with ambient air due to high surface-to-volume ratios. While merging occurs quickly with the clustered-cell design, the effects of this original phase upon ultimate rise are significant. Experimental evidence indicates plume rise from round mechanical draft towers is greater than would be expected

for a single cell but less than would result from emitting the total tower effluent from an equivalent single orifice (Chan et al.)[8]. This is obviously the result of the high initial entrainment which reduces total momentum and buoyancy.

ERT's COOLTOWR model replaces the multiple plume configuration by an equivalent single plume (ESP) which conserves the total fluxes of mass, momentum, moisture and buoyancy. An important feature of the ESP model is the modification of the entrainment rate to simulate approximately the mixing of ambient air during the important transitional stage of plume development. Details of the ESP model follow.

Define X_x as the downwind distance at which all the single cell plumes may be considered entirely merged, n is the number of cells per tower (in this case, n = 13), b_o is the radius of each cell, B_o is the radius of the cooling tower, R_o is the initial radius of the ESP, B_c is the radius of a single cell plume at X_c and R_c is the radius of the ESP at X_c.

The initial fluxes of mass, momentum, moisture and buoyancy are conserved in the ESP model by the relation:

$$R_o = \sqrt{n}\, b_o \qquad \text{(A-35)}$$

At $X = X_c$, the summed cross-sectional areas of the multiple plumes and that of the ESP should be the same. This yields:

$$R_c = \sqrt{n}\, b_c \qquad \text{(A-36)}$$

where $b_c = (B_o - b_o)/(\sqrt{n} - 1)$.

At any X the entrainment of ambient air per unit length of the plume is given by the product of the local plume perimeter and the effective entrainment velocity. This suggests a means for modifying the entrainment rate in the ESP model to simulate the enhanced mixing during initial

plume rise. If we assume that the entrainment velocity is identical in both cases, the ratio of the multicell plume entrainment rate to that of the ESP is given by:

$$F_i = (B_o + b_i \; b_o)/R_i = (B_o + \frac{R_i}{\sqrt{n}} \; b_o)/R_i \qquad \text{A-37)}$$

where subscript i denotes local values. The ratio F_i changes from B_o/R_o at X = 0 to 1.0 at $X \geq X_c$.

By multiplying the local entrainment of the ESP model by F_i, we can approximately simulate the corresponding entrainment of the multiple plume configuration. This correction factor results in predicted plume rises larger than those that would be calculated for any one of the individual plumes but smaller than would result for a plume emerging initially from a single "equivalent" circular cell having the same total fluxes of mass, moisture, momentum and buoyancy. The assumptions incorporated in the multicell adaptation of COOLTOWR are considered to produce conservative estimates of plume rise and thus the extent of obscuration due to saturated plumes for the round mechanical draft design.

(A)1.6 Simulation of Downwash

During strong crosswinds, downwash of cooling tower plumes into the low pressure area of the tower wake occurs, unless the initial vertical momentum of the effluent is sufficient to carry it beyond the influence of this effect. Natural draft towers normally release plumes at heights of 400 to 500 feet. While the diameters of such towers are also large, presenting a substantial obstacle to the local wind, the exhaust height is normally sufficient to preclude impacts at the ground. COOLTOWR uses a scheme developed by Overcamp and Holt[9] to simulate downwash due to natural draft towers.

The criterion for the occurrence of downwash suggested by Overcamp and Hoult[9] for Froude number (Fr) less than 3.0 is:

$$W_o/\bar{u} < 0.45(Fr)^{2/3} \qquad \text{(A-38)}$$

where

W_o is plume exit velocity,

$\bar{u}$ is mean wind speed at plume release height, and

Fr is plume Froude number $= \dfrac{W_o}{\sqrt{B_o g \dfrac{T_o - T_e}{T_o}}}$

T_o is plume exit temperature, and

T_e is ambient air temperature

For the natural draft towers in this study, a typical Froude number is 0.6. Using an average exit velocity of 4.0 m/sec, a typical critical wind speed for the onset of downwash is 12.4 m/sec or 27.7 mph.

If the above criterion is satisfied, the effective emission height of the tower is lowered according to the following expression:

$$H' = H + 4.0 \left(\frac{W_o}{\bar{U}} - 0.45 \ (Fr)^{2/3} \right) B_o \qquad \text{(A-39)}$$

where H' is the effective emission height and H is the tower height.

The downwash criterion for round mechanical draft towers is given by Equation (A-38). A treatment similar to that for natural draft rather than conventional mechanical draft towers appears justified in view of laboratory modeling experiments (e.g., Kennedy and Fordyce).[10]

For the proposed round mechanical draft tower plume, a typical Froude number is about 2.5. Since the exit velocity W_o is known (9.6 m/sec),

the critical wind speed for the onset of downwash implied by Equation (A-38)is 11.7 m/sec or approximately 26 mph. This is consistent with results of water tank experiments conducted by Kennedy and Fordyce[10] to test recirculation and interference properties of round and rectangular mechanical draft towers. For Froude number in the vicinity of 2.5 (as defined above), the recirculation factor (fraction of plume trapped in the tower wake) began to rise significantly for velocity ratios less than about 1.0 with the round tower design.

It has been observed that rectangular mechanical draft towers frequently experience downwash which brings the plume to the ground. For this type of tower, the COOLTOWR model incorporates a modification of the procedure suggested by Briggs and found valid for rectangular mechanical draft towers by Hanna.[11] The criterion used is presented below.

$$W_o/\bar{u}' < .375(H/b_o) + 1.5 \qquad \text{(A-40)}$$

where $\bar{u}' = \bar{u} + 5.0 \cos\theta$

In the above equation for $\bar{u}'$, θ represents the angle between the wind vector and the long axis of the towers. Thus, the critical wind speed is allowed to increase from the critical wind speed defined by Briggs' equation when the wind is perpendicular to the long axis of the tower to a value 5.0 m/sec greater when the wind is parallel to the long axis of the tower. For the towers under consideration here, the critical wind speed varies from 4.7 m/sec (10.5 mph) to 9.7 m/sec (21.9 mph).

When the downwash criterion is satisfied for round and rectangular mechanical draft tower, COOLTOWR lowers the plume centerline to 5 meters (one integration step) below the ground, the plume remains there until the end of the tower's wake is reached, and then the plume is allowed to rise. The length of the tower's wake is determined from a table after Evans.[12] Although the above procedure is an artificial way to account for the effects of downwash (as are all cooling tower downwash models), COOLTOWR has been calibrated using the limited observational data available for fogging distance (e.g., Hanna).[11]

(A) 2.0 REFERENCES

1. Van Wylen. 1969. Thermodynamics. John Wiley & Sons, Inc. New York, NY.

2. McCracken, D. D. and W. S. Dorn. 1964. Numerical Methods and Computer Programming. John Wiley & Sons, Inc. New York, NY.

3. Hildebrand, F. B. 1962. Advanced Calculus for Applications. Prentice Hall, Inc. Englewood Cliffs, NJ.

4. Briggs, G. A. 1969. Plume Rise. AEC Critical Review Series. Publ. No. TID-25075. Springfield, VA.

5. Houghton, H. G. and W. H. Rodford. 1938. On the Measurement of Drop Size and Liquid Water Content in Fogs and Clouds. Pop. Phys. Ocean. Meteor. MIT. Woods Hole Oceanogr. Inst. No. 4.

6. Slawson, P. R., J. R. Coleman, and J. W. Frey. 1974. Some Observations of Cooling Tower Plume Behavior at the Paradise Steam Plant. Tennessee Valley Authority. Muscle Shoals, Alabama.

7. Meyer, J. H. 1974. Mechanical Draft Cooling Tower Visible Plume Behavior: Measurements, Models, Predictions. Applied Physics Laboratory, Reprint. Johns Hopkins University.

8. Chan, T. L. et al. 1974. Plume Recirculation and Interference in Mechanical Draft Cooling Towers. Iowa Institute of Hydraulic Research. No. 160. University of Iowa.

9. Overcamp, T. J. and D. P. Hoult. 1971. Precipitation in the Wake of Cooling Towers. Atmospheric Environment. Vol. 5. Pergamon Press.

10. Kennedy, J. R. and H. Fordyce. 1975. Plume Recirculation Interference in Mechanical Draft Cooling Towers. Cooling Tower Environment--1974. N.T.I.S. NO. ER 1.11: CONF-740302. Springfield, VA.

11. Hanna, S. R. 1974. Meteorological Effects of the Mechanical Draft Cooling Towers at the Oak Ridge Gaseous Diffusion Plant. NOAA, ATDL Contribution No. 89. Oak Ridge, Tennessee.

12. Evans, B. R. 1957. Natural Air Flow Around Buildings. Texas Engineering Experiment Station. Research Report No. 59. Texas A & M College System. College Station, Texas.

ADDENDUM B

DESCRIPTION OF THE COOLING TOWER DRIFT MODEL

ADDENDUM B

(B) 1.0 DESCRIPTION OF THE COOLING TOWER DRIFT MODEL

Drift consists of liquid droplets borne out of the cooling tower with the vapor plume. The droplets are produced mechanically by the spraying and/or splashing of the circulating water on surfaces within the tower. Breaking up the coolant into droplets increases the surface-to-volume ratio, increasing the evaporative heat transfer. As the air moves upward through the cooling tower packing, unevaporated droplets can be entrained, carried aloft out of the tower, and eventually deposited on the ground.

The drift rate of an evaporative cooling tower is normally characterized in terms of a percentage of the circulating water flow rate. Efficient eliminators reduce the total amount of drift by removing the larger droplets, thus altering the mass-size distribution of the drift.

While condensation products such as cooling tower fog are reasonably pure water, drift droplets have the chemical composition of the cooling water. Through evaporation and the addition of makeup water, dissolved solid concentrations higher than those characteristic of the source water are found in the circulating water after a few cycles through the condensers. Chemicals present in the circulating water can then be deposited by the drift over the area adjacent to the towers. Drift is carried aloft in the plume as long as its vertical motion is greater than the settling velocity of the droplets. Settling velocity is primarily determined by drop diameter. As the drift droplets fall out of the saturated plume they begin to evaporate, decrease in diameter and, therefore, decrease their fall velocity. An increase of the concentration of dissolved solids in the droplets occurs simultaneously with their evaporative shrinking.

ERT's cooling tower drift deposition model DEPOT was employed to estimate seasonal and annual deposition rates attributable to the cooling towers of the Hat Creek Project. The drift model calculates deposition rates, using information on the cooling tower plume and drift characteristics, at specified downwind distances. The depositions are assumed to be spread uniformly over a 22.5 degree sector. The final deposition estimates result from three different components, namely, the contributions of aerodynamic downwash, and of droplets less than 250 μm diameter, and of those greater than 250 μm. Each of these three contributions is calculated separately.

(B)1.1 Model Inputs

Input data to the model are the meteorological conditions, the corresponding plume parameters, and the drift emission characteristics. The meteorological conditions for the time period under consideration are classified into discrete categories of wind speed and relative humidity. Hourly observations are sorted by computer to obtain the joint frequency of occurrence of all possible combinations of wind speed and relative humidity used in the calculations. A representative wind speed and a relative humidity are selected for each group, and used in the plume rise model to obtain the behavior of plumes occurring under these conditions.

The inputs from the plume model to the drift model are the following:

$z_m = H + z_{max}$ = Maximum plume rise referred to the ground (Here H is the tower height and z_{max} is the maximum plume rise above the tower).

x_m = horizontal distance downwind of the tower at which z_{max} is reached,

t_m = travel time of the drift drops from $x = 0$ to $x = x_m$,

b_m = radius of the plume at x_m.

The spectrum of drift droplets is divided into 5 to 10 groups, depending on initial drop sizes. A representative droplet size (d) and a fraction (f) of total mass are assigned to each group to approximate the characteristics of the continuous distribution present in the drift. The deposition rates obtained from the model are highly dependent on drop size. Therefore, the greatest feasible number of groups is considered, depending upon the actual distribution and computational capabilities. The total mass drift rate (in kilograms per hour) is determined from the drift eliminator efficiency (expressed usually as a percentage of circulating water flow rate).

(B)1.2 Downwash

All particle sizes are included in the downwash calculations. Downwash occurs whenever the wind speed exceeds a specific critical value. The estimation of the critical wind speed corresponding to a particular tower design is based on the relationships given in Section (A)1.6. The calculation procedure for downwash is as follows.

The drift concentrations at specified horizontal distance increments are obtained by the so-called 'sector average' formula, Equation (B-1). This equation assumes concentrations spread over a 22.5 degree sector and evaluated at downwind distances of 2, 4, 6, 8, 10, 16, and 20 tower heights. Downwash is assumed to be negligible beyond a distance of 20 tower heights. The concentrations (χ in g m^{-3}) are given by:

$$\chi = \frac{2Q}{\sqrt{2 \cdot U_e \sigma_z L}} \exp\left(-\frac{z_e^2}{2\sigma_z^2}\right) \qquad \text{(B-1)}$$

In the above,

Q = total drift (g s^{-1})

U_e = wind speed at tower height (m s^{-1})

z_e = $H + z$ = effective plume height (m), where z is the plume rise up to the distance (x) under consideration,

L = a length unit substituted for $\sqrt{2\pi}\,\sigma_y$; this is equal to the arc length of the 22.5 degree sector at x_m.

σ_z = an artificial vertical stability factor selected to simulate large eddies formed in the wake of the tower complex. Turner stability classes (see Turner,[2]) and the corresponding σ_z values are used, as shown below.

TABLE (B)-1

TURNER STABILITY CLASSES FOR DETERMINING VERTICAL DIFFUSION COEFFICIENT (σ_z) IN DOWNWASH MODEL

Distance	2H	4H	6H	8H	10H	16H	20H
Stability Class	A	$\frac{1}{2}$(A+B)	B	B	B	C	D

Depositions (D in g m^{-2} s^{-1}) are calculated from the relationship

$$D = \chi V_d \qquad \text{(B-2)}$$

where V_d is the deposition velocity (m s^{-1}), obtained by taking a weighted average of the saturated-droplet fall velocities (V_{fs}) over the range of droplet sizes considered. The fall velocities used in this model were taken from the monograph by Hosler et al.[3]

For some situations involving mechanical draft towers, an additional downwash contribution due to recirculation is included. Information on this phenomenon is rare. The contributions for ground-level drift concentrations were estimated from diagrams given by Chan et al.[4] The recirculation effects were assumed to be negligible at distances beyond 4H.

(B)1.3 Dispersion of Small Droplets

Desposition of droplets of less than 250 μm size is calculated by the mechanisms of free fall and eddy diffusion. The calculation procedure

outline below is repeated for every combination of drop size ($d < 250$ μm), ambient relative humidity (ϕ_e), and wind speed (U_e). Additional drift parameters used are the initial fall velocity of the drops (V_{fo}), and the time (t_s) required for the droplet to evaporate enough to form a saturated solution of the dissolved salts. The time t_s is a function of the initial drop size and ambient relative humidity.

The center of gravity axis of the small drops relative to the plume (or the ground) is calculated for each downwind distance (x) starting with x_m. The effective droplet height (z_d) at x_m is calculated as

$$z_d = z_m - w_d \cdot t_m \qquad \text{(B-3)}$$

where w_d is the vertical component of the velocity of the rising droplets. For $x \leq x_m$, the latter is computed as

$$w_d = V_{fo} - k \cdot \frac{t_m}{t_s} (V_{fo} - V_{fs}) \qquad \text{(B-4)}$$

The value of the coefficient k depends on the ambient relative humidity (ϕ_e), as follows (J. M. Austin, unpublished notes):

For $\phi_e = 50\%$, $k = 0.5$
$\phi_e = 70\%$, $k = 0.25$
$\phi_e = 90\%$, $k = 0.1$

For $x > x_m$, the velocity w_d is defined as

$$w_d = V_{fs} + \frac{t_s - c t_m}{2 t_s} (V_{fo} - V_{fs}) \qquad \text{(B-5)}$$

The value of the coefficient c depends on the ambient relative humidity (ϕ_e), as follows (J. M. Austin, unpublished notes):

For $\phi_e = 50\%$, $c = 1.0$
$\phi_e = 70\%$, $c = 0.7$
$\phi_e = 90\%$, $c = 0.4$

In the above, $(t_s - ct_m)$ represents the additional time required by the droplet (upon reaching x_m) to form a saturated solution by evaporation. If the droplet is not saturated by the time it reaches x_m (i.e., $t_s > c \cdot t_m$), then the coordinates (x_s, z_s) at which it reaches saturation should be determined as follows:

$$x_s = x_m + U_e \cdot (t_s - ct_m) \tag{B-6}$$

$$z_s = z_d - w_d \cdot \frac{(x_s - x_m)}{U_e} \tag{B-7}$$

For $x > x_s$, the effective height z_e of the droplet can be determined by

$$z_e(x) = z_s - V_{fs} \cdot \frac{(x - x_s)}{U_e} \tag{B-8}$$

For $x_m < x < x_s$, the effective heights are assumed to vary linearly with distance:

$$z_e(x) = z_m - \frac{x - x_m}{x_s - x_m} \cdot (z_m - z_s) \tag{B-9}$$

If $t_s < c \cdot t_m$, $x_s = x_m$ is assumed. Thus, we can completely calculate the gravity axis of the drops as a function of distance (see Figure (B)-1).

The effective heights of the center of gravity axis of drift droplets, computed as shown above, are divided by the value of σ_z for D stability (see Turner)[2] at the various distances. Each z_e/σ_z then represents a point on the abscissa of a unit normal distribution. The difference between the two normal curve values corresponding to any two adjacent points gives the fraction of mass deposited between them (see Figure (B)-2). For example,

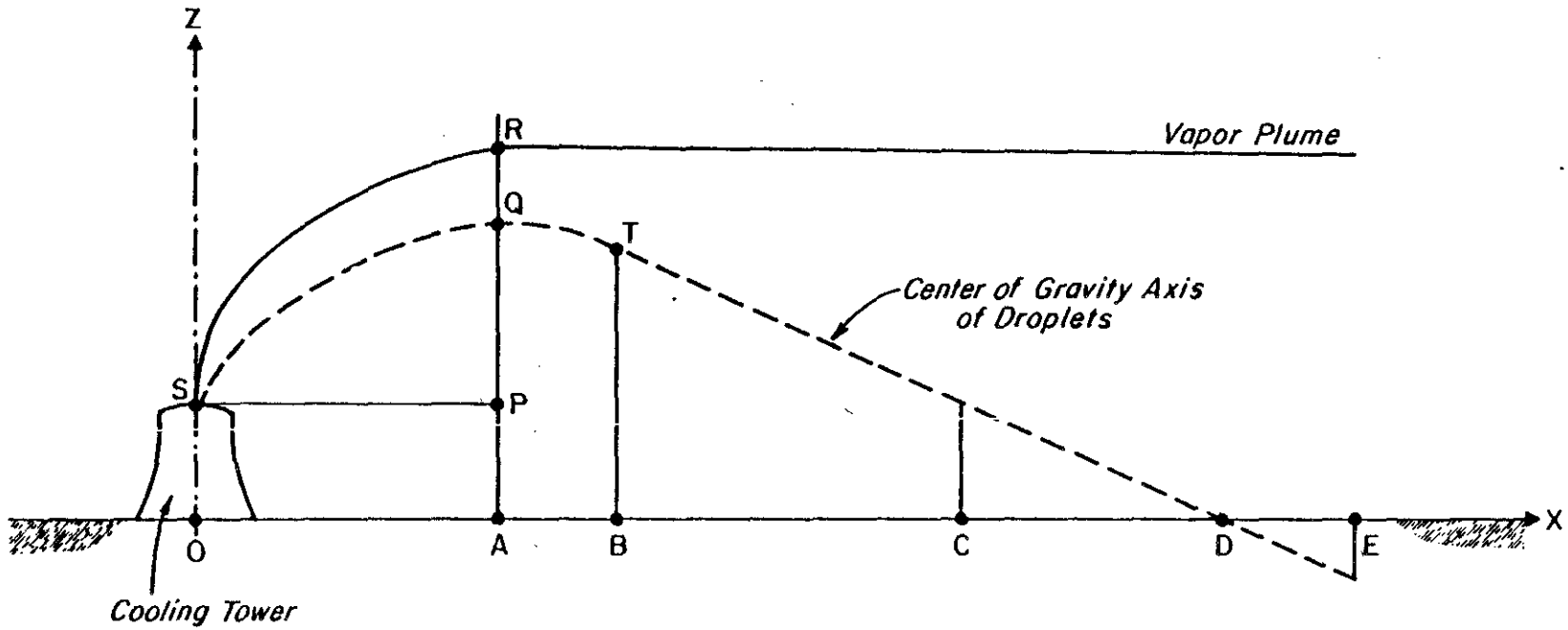

$H = OS$ $\quad Z_d = AQ$

$X_m = OA$ $\quad Z_s = BT$

$Z_{max} = PR$ $\quad X_s = OB$

$Z_m = AR$ $\quad X_i = OD$

Figure (B)-1 Schematic Representation of Drift Droplet Behavior Relative to Cooling Tower Vapor Plume Trajectory

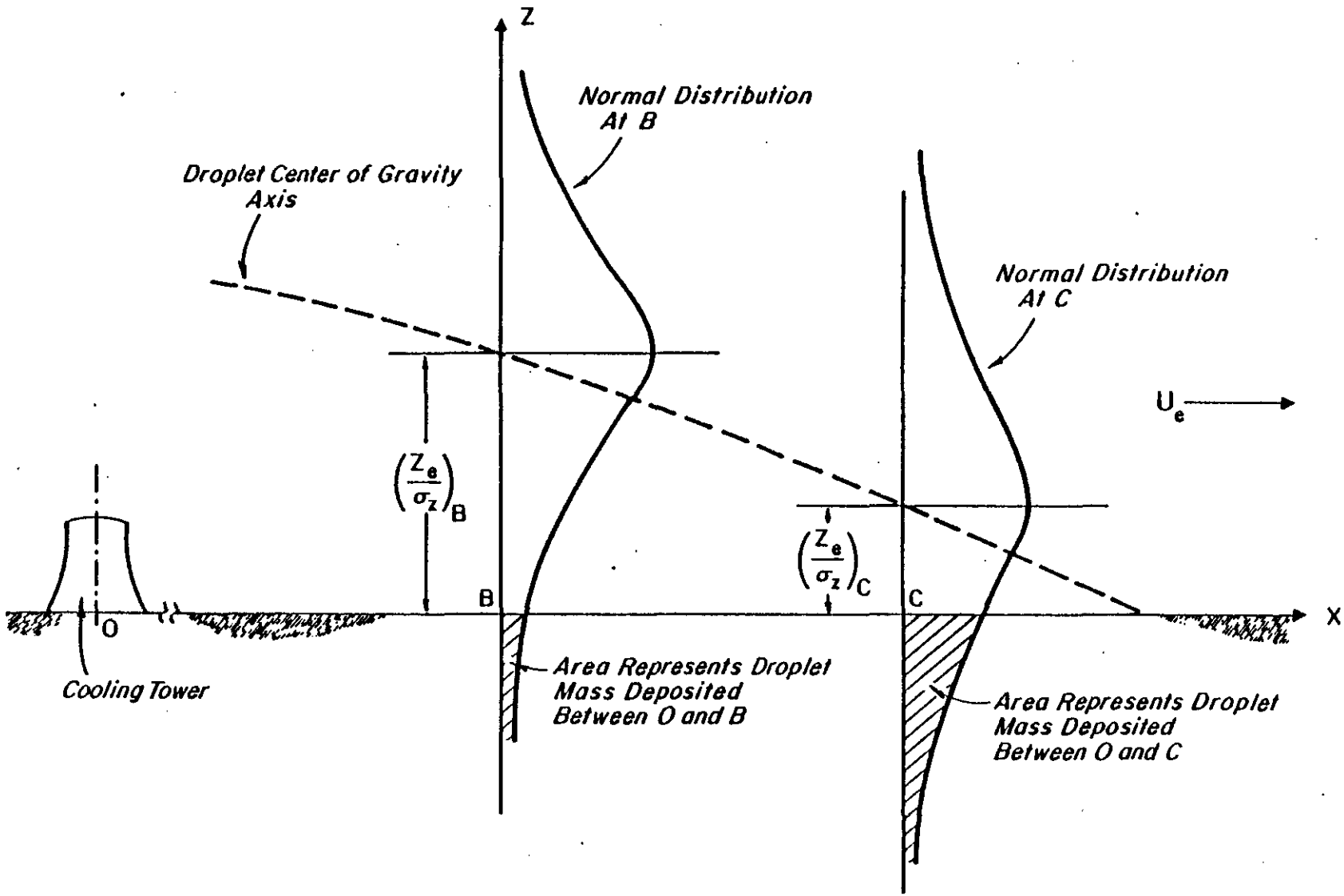

Figure (B)-2 Drift Deposition Due to the Effect of Atmosphere Eddies

$$\text{Deposition between B and C} = \left[\psi\left(\frac{z_e}{\sigma_z} \mid B\right) - \psi\left(\frac{z_e}{\sigma_z} \mid C\right)\right] \times \begin{bmatrix}\text{mass fraction of droplets under considera-}\\ \text{tion}\end{bmatrix} \times (\text{total mass}) \qquad \text{(B-10)}$$

where ψ denotes the unit normal distribution. A deposition per unit area is then obtained by dividing the deposition calculated in Equation (B-10) by the area between B and C (assuming a 22.5 degree sector downwind of the tower).

(B)-.4 Depositions of Large Drops

The larger drops ($d \geq 250$ μm) are assumed to be too large to be effectively dispersed by atmospheric turbulence. These drops fall out of the plume without the benefit of the full plume rise. The trajectories of these drops are calculated to determine the points at which they hit the ground. The following calculations are made for each combination of $d > 250$ μm, wind speed (U_e), and relative humidity (ϕ_e). The velocity (V_{dp}) of the drop relative to the plume is calculated as

$$V_{dp} = V_{fo} - U_e \frac{b_m}{x_m} \qquad \text{(B-11)}$$

The distance (x_f) at which the large drop falls out of the plume is then given by

$$x_f = U_e \frac{b_o}{V_{dp}} \qquad \text{(B-12)}$$

where b_o is the plume initial radius. The effective height (z_f) at which the drop leaves the plume is approximated by the relationship

$$z_f = H + (z_m - H)\left(\frac{x_f}{x_m}\right)^{1/2} - \left(b_o + \frac{x_f}{x_m} b_m\right) \qquad \text{(B-13)}$$

Once the drop has left the plume, it is assumed to evaporate at rates corresponding to the relative humidity, similar to the computational procedure for the smaller drops.

For $0 < t \leq t_s$, the drop is assumed to fall at a velocity of $1/2(V_{fo} + V_{fs})$. For $t > t_s$, we assumes $V_f = V_{fs}$. The total time (τ) for the drop to fall is then calculated as

$$\tau = t_s + [z_f - 0.5\ (V_{fo} + V_{fs}) \cdot t_s]/V_{fs} \qquad \text{(B-14)}$$

The point of impact on the ground (x_i) is found from

$$x_i = U_e \cdot \tau + x_f \qquad \text{(B-15)}$$

If the drop does not evaporate to a saturated solution its velocity at impact (V_{fi}) can be calculated assuming a linear decrease of velocity with height:

$$V_{fi} = V_{fo} - t_s \frac{2\ z_f}{(V_{fo} + V_{fs})}\ (V_{fo} - V_{fs}) \qquad \text{(B-16)}$$

The total time (τ) for the drop to fall under these conditions, after leaving the plume, is then

$$\tau = 2\ z_f/(V_{fi} + V_{fo}) \qquad \text{(B-17)}$$

The point of impact on the ground (x_i) is again given by Equation (B-15). The points of impact are found for every large drop, for a specified combination of relative humidity and wind speed, as illustrated in Figure (B)-3.

The mass of the drops is spread proportionately between the impact points, again assuming a 22.5 degree sector for lateral dimensions (see Figure (B)-4).

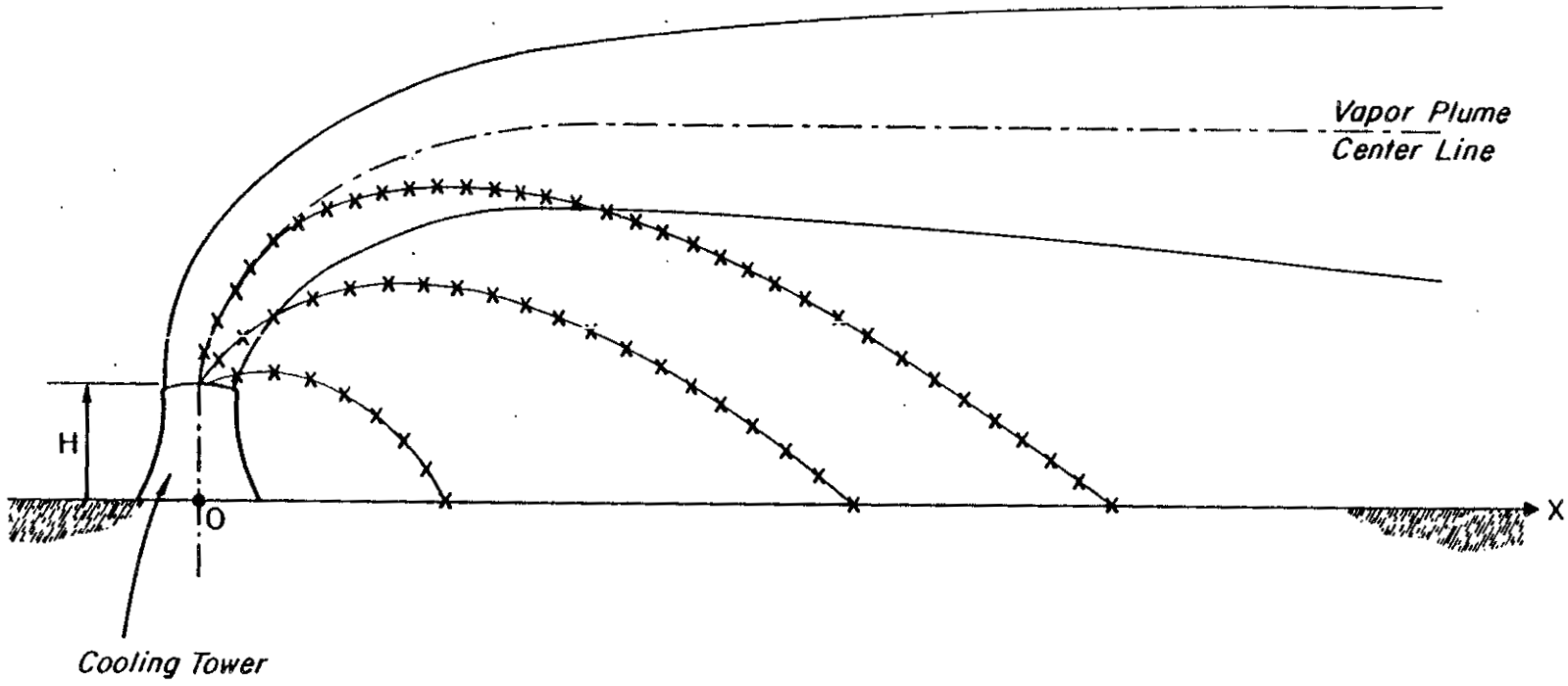

Figure (B)-3 Trajectories of Large Droplets

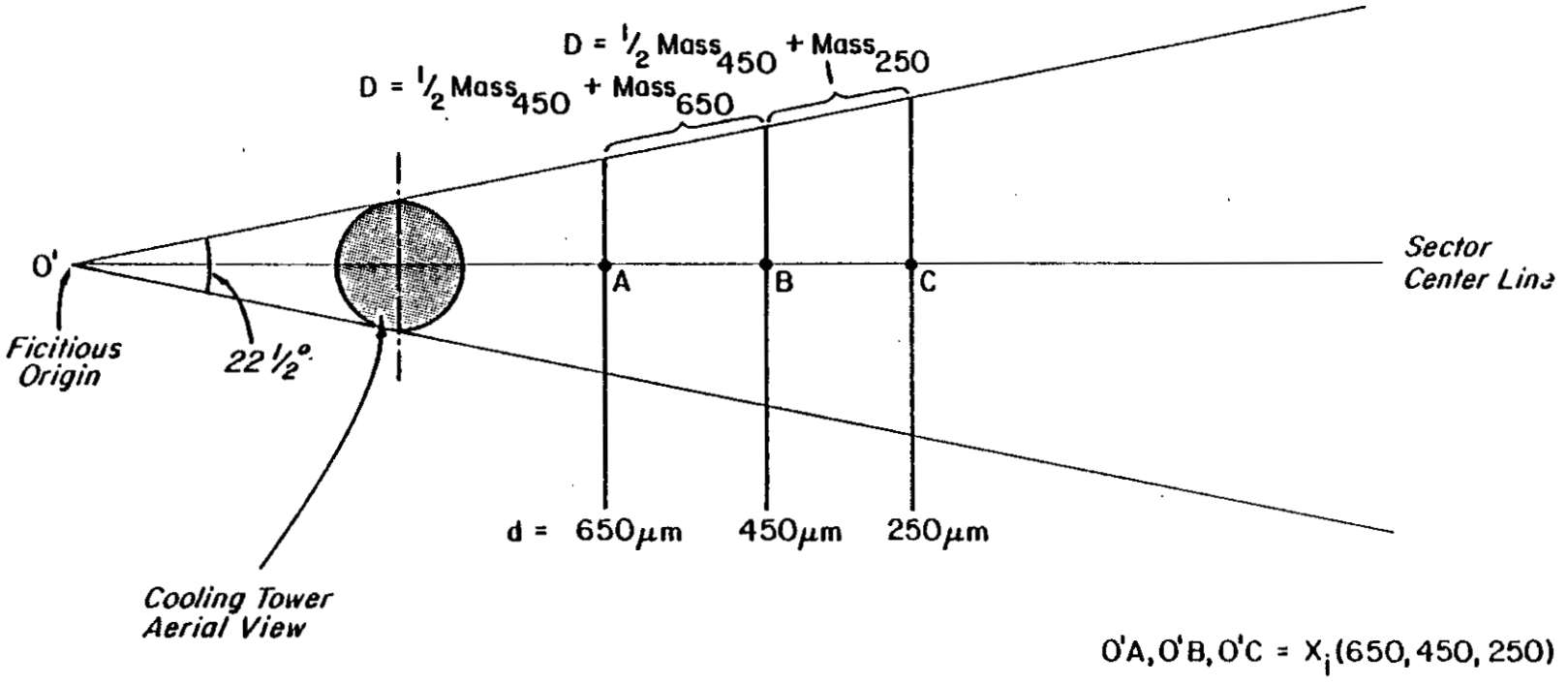

Figure (B)-4 Depositions Due to Large Drops

The deposition from the three categories of computations, namely, the downwash, the small droplets, and the large drops are combined to give the total deposition for each combination of relative humidity and wind speed.

The resulting arrays are weighted according to the frequencies of occurrence of these combinations from the observed meteorological data, thus producing final arrays of deposition for the time period under consideration.

(B)1.5 Calculation of Drift due to Multiple Towers

The combined impact of two or more cooling towers can be assessed by considering the geometry involved in the spreading and subsequent intersection of their plumes. The total drift deposition then depends upon the relative spacing of the towers and the wind direction. The combined deposition is based upon the drift calculations for one tower. Monthly, seasonal and annual deposition due to several towers can be calculated as described below.

A 22.5 degree section subtending the tower farthest upwind intersects the corresponding section of the next adjacent tower at a downwind distance from the first, given by the following equation:

$$X_1 = S \cos \sigma + (S \sin \sigma - d - P\ S \cos \sigma)/2P \qquad \text{(B-18)}$$

where:

X_1 = downwind distance (measured from the center of the upwind tower)

S = distance between the towers

σ = angle of mean wind vector with respect to the north-south axis

d = diameter of the top of the tower

P = tan $\pi/16$ (22.5 degree wind direction sector)

Similarly, the downwind distance where the plume of the first tower meets the plumes of any of the others may be calculated using Equation (B-18) by multiplying S (the distance between towers) by (n-1) to obtain the total distance between the n towers.

In general, then,

$$X_{n-1} = (n-1)\ S \cos \sigma + [(n-1)\ S \sin \sigma \quad d \quad P(n-1)\ S \cos \sigma]/2P$$

where the previous definitions apply and n = number of towers.

The total drift deposition is calculated by a weighted average of drift due to each tower. If the receptor's downwind distance is less than the distance where the first intersection of plumes occurs ($X \leq X_1$) the total drift is due to the first tower only ($D(X) = D_1(X)$. Where X is between the intersection of the first and second and the first and third plumes ($X_1 < X \leq X_2$) the total deposition calculated by;

$$D(X) = \frac{X\ D_1(X) \bullet (X - 2P\ S \cos \sigma) \cdot D_2(X)}{X + S \sin \sigma - P\ S \cos \sigma}$$

where previous definitions apply and;

$$X = 2PX + d.$$

Three plumes are involved at downwind distances between the intersections of the first and third and first and fourth plumes ($X_2 < X \leq X_3$) the equation then becomes

$$D(X) = \frac{X\ D_1(X) + (X-2\ P\ S \cos \sigma)\ D_2(X) + (X-4\ P\ S \cos \sigma)\ D_3(X)}{X + 2\ S \sin \sigma - P\ 2\ S \cos \sigma}$$

In general

$$D(X) = \frac{X\, D_1(X) + (X-2\,P\,S\cos\sigma)\, D_2(X) + \cdots + (X-(n+1)P\,S\cos\sigma)D_n(X)}{X + (n-1)\,S\sin\sigma - P\,(N-1)\,S\cos\sigma}$$

The drift deposition rates $D_2(X)$ through $D_n(X)$ can be calculated as $D_1[X-(n-1)\,S\cos\sigma]$ by interpolation, since the downwind component of distance between the towers is $(n-1)\,S\sin\sigma$. Note that at large downwind distances, $D(X)$ approaches $D_1 + D_2 + \ldots\ldots D_n$, as expected.

By repeating the above calculations at every X, and for every wind direction, the drift distribution due to all the towers can be calculated.

(B)1.6 Drift Characteristics Assumed for Model Input

A total circulating water flow rate of 40,370 ls^{-1} (640,000 USGPM) was assumed for each cooling tower system (that is, 10,090 ls^{-1} (160,000 USGPM) per tower for four-tower systems and 20,180 ls^{-1} (320,000 USGPM) for two-tower system). Makeup water for the cooling system is to be pumped to the site from the Thompson River.

On the basis of data provided by Ebasco Services Incorporated, a total dissolved solids concentration of 115 mg/liter (see Table (B)-2) has been assumed for the source water. The concentrations presented in the table are considered to be quite conservative, more representative of worst-case than annual average values. The recommended recirculation factor is 14.0. A drift mass emission rate of 1.23 g/sec/tower for the four-tower systems and 2.46 g/sec/tower for the two-tower system, corresponding to the above assumptions, was used in computing surface drift deposition rates. These values reflect the specifications of eliminators designed to limit drift to 0.008% of the circulating water flow. The spectrum of drift droplet sizes was divided according to six categories. A representative drop diameter and corresponding fraction of total drift mass was assigned to each category. The mass-size distribution assumed in the deposition calculations performed for this study is indicated in Table (B)-3.

TABLE (B)-2

SOURCE WATER PROPERTIES[1]

(Assumed for all tower designs)

Bicarbonate	(HCO_3)	57 mg/l
Sulfate	(SO_4)	13
Chloride	(Cl)	7
Nitrate	(NO_3)	0.2
Silica	(SiO_2)	4
Hardness	($CaCO_3$)	42
Calcium	(Ca)	13
Magnesium	(Mg)	2
Sodium	(Na)	13
Total organic carbon		6
Dissolved solids		109
Suspended solids		6
Total solids		115 mg/l
pH		7.5

TABLE (B)-3

ASSUMED COOLING TOWER DRIFT MASS-SIZE DISTRIBUTION[1]

Droplet Diameter (μm)	Fraction of Drift Mass
50	0.40
75	0.24
150	0.10
275	0.07
475	0.09
600	0.10

[1]Data provided by INTEG/EBASCO.

(B) 2.0 REFERENCES

1. Hanna, S. R. and S. G. Perry. 1973. Meteorological Effects of the Mechanical Draft Cooling Towers of the Oak Ridge Gaseous Diffusion Plant. NOAA, ATDL Contribution No. 86. Oak Ridge, Tenn.

2. Turner, D. B. 1970. Workbook of Atmospheric Diffusion Estimates. United States Department HEW. Public Health Service. NAPCA. Cinncinnati, Ohio.

3. Hosler, C., J. Pena and R. Pena. 1972. Determination of Salt Deposition Rates from Evaporative Cooling Towers. The Pennsylvania State University Department of Meteorology.

4. Chan, T. L. et al. 1974. Plume Recirculation and Interference in Mechanical Draft Cooling Towers. Iowa Institute of Hydraulic Research No. 160. University of Iowa.

ADDENDUM C

SELECTION OF METEOROLOGICAL DATA

ADDENDUM C

(C)1.0 SELECTION OF METEOROLOGICAL DATA

(C)1.1 Meteorological Data for Atmospheric Effects

The meteorological variables of concern in the analysis of visible plumes are wind speed and direction, temperature, relative humidity, and atmospheric stability. Analysis of local meteorological data provides a rational basis for choosing a representative subset from the vast number of possible combinations of these parameters. The COOLTOWR model is applied, using each set of the selected weather conditions to determine the corresponding visible plume length, and to determine whether and at what distances ground-level effects i.e., icing and/or fogging, will occur. Meteorological statistics appropriate to the period of interest (month, season, or year) are incorporated in the analysis to generate frequency distributions of fogging, icing, and visible plume lengths in the vicinity of the towers. The months associated with each season are as follows:

Season	Months
Winter	December, January, February
Spring	March, April, May
Summer	June, July, August
Autumn	September, October, November

Weather data used in the visible plume analysis consist of hourly surface observations recorded during the network of mechanical weather stations deployed in the vicinity of the proposed site. Station #7, the Harry Lake Station, was considered most representative of conditions at the location of the cooling towers. Whenever data were missing for this station, values from the next most representative station (as determined for each variable by correlation analyses) were substituted to develop a full annual set of meteorological parameters required for input to the

cooling tower analysis. Longer data records exist for Atmospheric Environment of Canada Weather Stations (e.g., Kamloops, Lytton, and Ashcroft). However, the distances of these stations from the Hat Creek Project area and the irregular topography which characterizes south-central British Columbia reduce the representativeness of such data sets for purposes of the present cooling tower impact analysis. Consequently, weather statistics used in this study were developed from 1975 on-site observations. It is recognized that data for a single year do not reflect the full range of meteorological situations likely to be encountered at the site. As data from the long-term meteorological monitoring program becomes available, the "representativeness" of the 1975 measurements can be more fully investigated.

Use of surface observations imposes the requirement that certain assumptions be made regarding vertical profits of temperature, winds, and humidity through the first several hundred meters above the cooling towers. Ideally, meteorological input to the plume simulation model would be derived from a data set comprised of measurements taken at various heights for more precise definition of the vertical variations of pertinent parameters. Careful consideration has been given in the selection of assumptions regarding vertical profiles to ensure that, whenever possible, such approximations lead to conservative estimates (overpredictions) of atmospheric effects associated with cooling tower plumes.

An analysis of the meteorological data was performed to define extreme values of temperature, wind speed, and relative humidity likely to occur at the Hat Creek site. The range of possible values for each parameter was subsequently divided into sub-ranges. The selection of the meteorological classes was achieved with cognizance of the sentitivity of moist plume behavior to small changes in the value of each parameter. For example, greater resolution is necessary at the upper end of the humidity spectrum than at lower levels. Similarly, temperature categories corresponding to colder temperatures must apply to smaller intervals than those for warmer conditions.

Five wind speed classes, five relative humidity classes, and five temperature classes were selected in this manner from the data. Observed frequencies of occurrence were considered in choosing representative values for each class to be used as input to the COOLTOWR model. Table (C)-1 indicates the class limits and corresponding representative values for wind speed, relative humidity, and temperature.

Any of the 16 compass directions can be expressed as one of eight possible angles between 0° and 90° relative to a row of towers. Due to the previously noted dependence of plume behavior upon wind direction, it is necessary to apply the COOLTOWR model for each combination of wind speed, relative wind direction, temperature, and relative humidity - a total of 1000 separate weather conditions. One entire set of these calculations was performed using the assumption of near-neutral atmospheric stability in the plume rise layer; another complete series of runs was made for stable stratification resulting in a total of 2000 cases. Unstable cases, which occur relatively infrequently, were not treated separately. Unstable conditions are normally characterized by low wind speeds, strong solar heating, and low surface humidities; plume rise and dispersion are enhanced in such circumstances. The decision, therefore, to assign a stability of either neutral or stable to all hours, is conservative from the standpoint of predicting visible plume length.

The categorization of atmospheric stability as either neutral or stable for each hour of the data record was accomplished from the observations of wind speed, cloud cover, and incoming solar radiation in the manner suggested by Turner[1], modified for specific application to the Harry Lake site. A stability typing scheme which incorporated the effects of the rural nature of the area and the ruggedness of the terrain was developed. Afternoon stabilities on days which were characterized by strong isolation and light to moderate wind speeds were designated as unstable. Periods

TABLE (C)-1

CLASSIFICATION OF SURFACE WIND SPEED, RELATIVE HUMIDITY, AND TEMPERATURE CATEGORIES FOR VISIBLE PLUME ANALYSIS

Wind Speed (mps)

Class	1	2	3	4*	5*
Range	≤2.0	2.1-4.2	4.3-7.0	7.1-9.6	9.7+
Representative Value	0.9	3.1	5.6	8.5	11.6

Relative Humidity (%)

Class	1	2	3	4	5
Range	0-50	51-70	71-82	83-93	94+
Representative Value	50	60	76	88	96

Temperature (°C)

Class	1	2	3	4	5
Range	≤ -12.2	-12.1to-1.0	-0.9to10.3	10.4to21.3	>21.3
Representative Value	-15.0	-6.7	4.4	15.6	26.7

*Round Mechanical Draft Towers only

To ensure a representative wind speed for which downwash will occur for the Round Mechanical Draft Towers, the following modifications were made to wind speed classes 4 and 5:

Class	4	5
Representative Value	8.9	15.6

of overcast skies and/or strong wind speeds were considered to be neutral. Finally, night and early morning hours which were characterized by clear skies and low wind speeds were classified as stable.

As stated above, certain assumptions were necessary regarding the specification of vertical temperature, wind, and humidity profiles. Since near-neutral conditions occur most frequently, a temperature lapse rate near the climatological mean (-0.5°C/100 m) was considered appropriate for these cases. A more nearly isothermal temperature structure (-0.1°C/100 m) was used in plume calculations for stable conditions. To lend conservatism to the calculations and to simulate the normal increase of stability more than about 300m (1000 feet) above the surface, the lapse rates are halved above 300 m in the model.

The profile of wind speed with height was assumed to follow a power law of the form

$$U(Z) = U_{ref} \cdot \left(\frac{z}{z_{ref}}\right)^{a} \qquad \text{(C-1)}$$

Based on Greene,[2] the value of the exponent 'a' assumed for both neutral and stable conditions is 0.14. The surface wind speed values listed in Table (C)-1 were extrapolated to tower height using Equation (C-1) to provide input wind speeds to the model. Since wind shear is generally less pronounced at higher levels than near the surface, the values of the power-law exponents are also halved above 300 m. Profiles of ambient specific humidity were generated internally by the model, using the assumption that relative humidity remains constant in the plume rise layer.

The on-site meteorological observations were processed to determine monthly and annual frequencies of occurrence for each of the 2000 conditions (i.e., 8 wind directions x 5 wind speeds x 5 relative humidities x 5 temperatures x 2 stability categories) assumed for the individual

plume model simulations. Further resolution of the data was accomplished by calculating the frequency of every condition associated with each of the 16 compass wind directions. These joint frequency distributions were generated for each month and for the entire year.

(C)1.2 Meteorological Data for Cooling Tower Drift

Meteorological data used as inputs to the deposition model include hourly values recorded at Mechanical Weather Station 7 (Harry Lake site). Missing values were supplemented by data from other stations according to correlation analyses performed for each parameter. This is the same data set used to develop statistics for the visible plume analysis.

Meteorological data were sorted by computer into six ranges of wind speed and three classes of relative humidity. Representative values were chosen for each parameter for use in the calculations. Class limits and representative values of wind speed and relative humidity chosen for use in the drift analysis are presented in Table (C)-2.

Average joint frequencies of occurrence were calculated for the 18 possible combinations of wind speed and humidity. This process was repeated for each wind direction and for each month, producing 192 separate tables of frequency data. A sample set of frequencies, corresponding to occurrences of northwest winds in March, is presented in Table (C)-3.

Five temperature classes were established on the basis of average monthly temperatures for 1975. Months with similar average temperatures were considered together. Table (C)-4 indicates these temperature classifications and the month(s) to which each category corresponds. The total number of combinations of wind speed, relative humidity, and relative humidity required 90 separate applications of the COOLTOWR

TABLE (C)-2

METEOROLOGICAL PARAMETER CLASSIFICATIONS FOR DRIFT

Relative Humidity Classes

Relative Humidity Class	Range (%)	Representative Value (%)
1	<60	50
2	60 - 80	70
3	>80	90

Wind Speed Classes

Wind Speed Class	Range (mps)	Representative Value (mps)
1	0 - 1.5	0.7
2	1.6 - 3.3	2.5
3	3.4 - 5.6	4.4
4	5.7 - 8.2	6.9
5	8.3 - 11.1	9.6
6	11.1+	13.7

TABLE (C)-3

JOINT FREQUENCIES OF OCCURRENCE FOR WIND SPEED AND RELATIVE HUMIDITIES FOR NORTHWEST WINDS IN MARCH, 1975

	Relative Humidity Class		
Wind Speed Class	1	2	3
1	0.009409	0.008065	0.004322
2	0.003763	0.000000	0.000000
3	0.002688	0.001344	0.001344
4	0.001344	0.001344	0.000000
5	0.000000	0.002688	0.001344
6	0.000000	0.000000	0.000000

*Based on data recorded at Harry Lake Mechanical Weather Station

TABLE (C)-4

TEMPERATURE CLASSIFICATIONS

Temperature Class	Months Represented	Average Temperature (°C)
1	Nov, Dec	-5.7
2	Jan, Feb. Mar, Oct	-0.7
3	Apr, Jun	7.8
4	Aug	10.2
5	May, Jul, Sep	13.7

model to define effluent behavior for each weather condition. These calculations supplied the necessary parameters related to plume trajectory and growth for input to the drift model.

(C) 2.0 REFERENCES

1. Turner, D. B. 1970. Workbook of Atmospheric Diffusion Estimates. United States Department HEW. Public Health Service. NAPCA. Cincinnati, Ohio.

2. Greene, B. R. 1968. Statistical Relationships Between the Rate of Vertical Expansion of Aerosol Clouds Released Near the Ground and Various Meteorological Predictors. GCA Technical Report No. 68-10-6. GCA Technology Division. Bedford, Massachusetts.